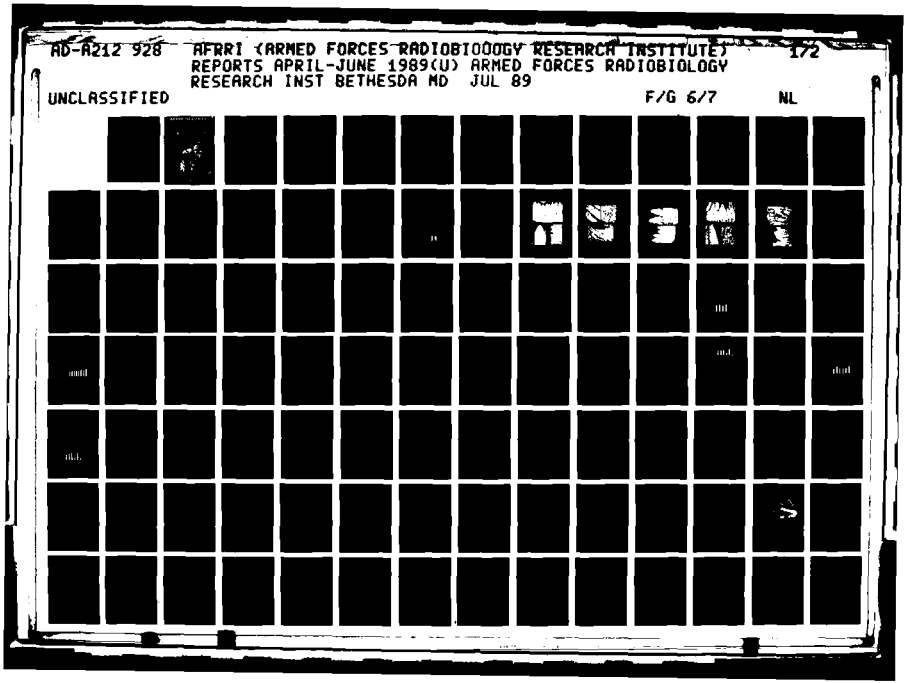
AD-A212 928 AFRRI (ARMED FORCES RADIOBIOOOGY RESEARCH INSTITUTE) 1/2
REPORTS APRIL-JUNE 1989(U) ARMED FORCES RADIOBIOLOGY
RESEARCH INST BETHESDA MD JUL 89
UNCLASSIFIED F/G 6/7 NL

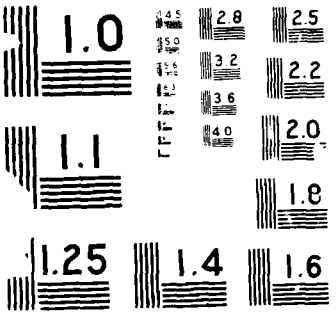
1.0
1.1
1.25
1.4
1.6
1.8
2.0
2.2
2.5
2.8
3.2
3.6
4.0
4.5
5.0
5.6
6.3

# AFRRI REPORTS



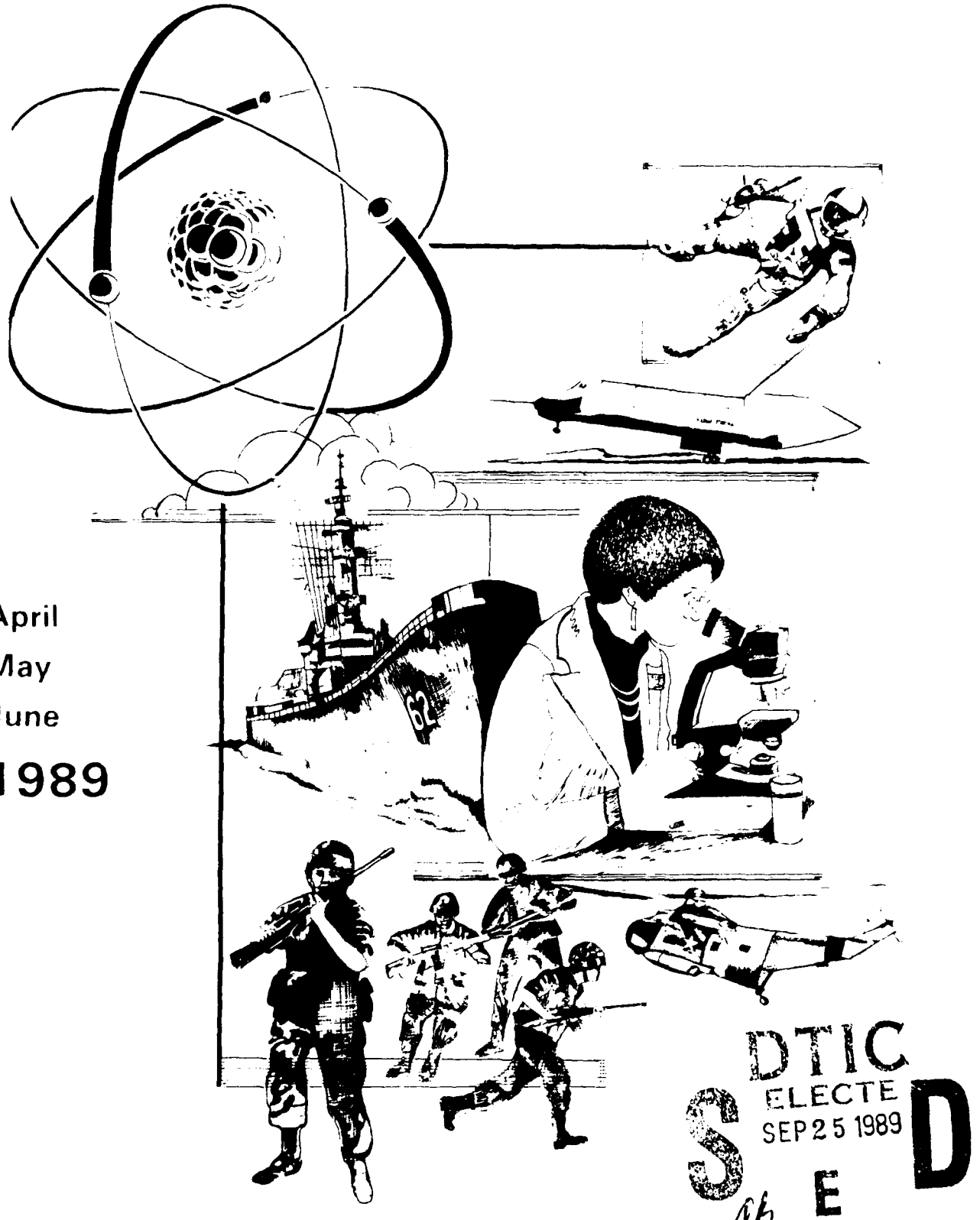

April
May
June
1989



Defense Nuclear Agency
Armed Forces Radiobiology Research Institute
Bethesda, Maryland 20814-5145

# REPORT DOCUMENTATION PAGE

| | |
|---|---|
| 1a REPORT SECURITY CLASSIFICATION<br>UNCLASSIFIED | 1b RESTRICTIVE MARKINGS |
| 2a SECURITY CLASSIFICATION AUTHORITY | 3 DISTRIBUTION / AVAILABILITY OF REPORT<br>Approved for public release; distribution unlimited. |
| 2b DECLASSIFICATION / DOWNGRADING SCHEDULE | |
| 4 PERFORMING ORGANIZATION REPORT NUMBER(S)<br>SR89-15 - SR89-25 | 5 MONITORING ORGANIZATION REPORT NUMBER(S) |
| 6a NAME OF PERFORMING ORGANIZATION<br>Armed Forces Radiobiology Research Institute<br>6b OFFICE SYMBOL (If applicable)<br>AFRRI | 7a NAME OF MONITORING ORGANIZATION |
| 6c ADDRESS (City, State, and ZIP Code)<br>Defense Nuclear Agency<br>Bethesda, Maryland 20814-5145 | 7b ADDRESS (City, State, and ZIP Code) |
| 8a NAME OF FUNDING / SPONSORING ORGANIZATION<br>Defense Nuclear Agency<br>8b OFFICE SYMBOL (If applicable)<br>DNA | 9 PROCUREMENT INSTRUMENT IDENTIFICATION NUMBER |
| 8c ADDRESS (City, State, and ZIP Code)<br>Washington, DC 20305 | 10 SOURCE OF FUNDING NUMBERS<br>PROGRAM ELEMENT NO: NWED-QAXM<br>PROJECT NO<br>TASK NO<br>WORK UNIT ACCESSION NO |
| 11 TITLE (Include Security Classification)<br>AFRRI Reports, Apr-Jun 1989 | |
| 12 PERSONAL AUTHOR(S) | |
| 13a TYPE OF REPORT<br>Reprints Technical<br>13b TIME COVERED<br>FROM _____ TO _____<br>14 DATE OF REPORT (Year, Month, Day)<br>1989 July<br>15 PAGE COUNT<br>116 | |
| 16 SUPPLEMENTARY NOTATION | |
| 17 COSATI CODES<br>FIELD / GROUP / SUB-GROUP<br>18 SUBJECT TERMS (Continue on reverse if necessary and identify by block number) | |

19 ABSTRACT (Continue on reverse if necessary and identify by block number)

This volume contains AFRRI Scientific Reports SR89-15 through SR89-25 for April-June 1989.

| | |
|---|---|
| 20 DISTRIBUTION / AVAILABILITY OF ABSTRACT<br>☐ UNCLASSIFIED/UNLIMITED ☒ SAME AS RPT ☐ DTIC USERS | 21 ABSTRACT SECURITY CLASSIFICATION<br>UNCLASSIFIED |
| 22a NAME OF RESPONSIBLE INDIVIDUAL<br>Gloria Ruggiero | 22b TELEPHONE (Include Area Code)<br>(301)295-3536<br>22c OFFICE SYMBOL<br>ISDP |

DD FORM 1473, 84 MAR 83 APR edition may be used until exhausted
All other editions are obsolete

# CONTENTS

## Scientific Reports

RADIATION RESEARCH 118, 341–352 (1989)



# Radiation Quality and Rat Motor Performance

VICTOR BOGO,* GARY H. ZEMAN,‡ AND MARY DOOLEY†

*Behavioral Sciences and †Radiation Sciences Departments, Armed Forces Radiobiology Research Institute (AFRRI), Bethesda, Maryland 20814-5145

‡Radiation Protection Department, AT&T Bell Laboratories, 600 Mountain Avenue, Murray Hill, New Jersey 07974-2070

BOGO, V., ZEMAN, G. H., AND DOOLEY, M. Radiation Quality and Rat Motor Performance, *Radiat. Res.* **118**, 341–352 (1989).

The effects of bremsstrahlung, electron, $\gamma$-, and neutron radiations were investigated on the motor performance of male Sprague–Dawley rats. Rats were irradiated at a midline tissue dose rate of 20 Gy/min ± 1 with one of the following: 18.6-MeV electrons ($N = 40$) or 18.1-MVp bremsstrahlung ($N = 57$) from a linear accelerator, $^{60}$Co 1.25-MeV $\gamma$-ray photons ($N = 48$), or reactor neutrons at 1.67 MeV tissue-kerma weighted-mean energy ($N = 43$). Radiation effects were determined by establishing median effective doses ($ED_{50}$) for rats trained on an accelerod, a shock-avoidance motor performance test. $ED_{50}$'s were based on 10-min postexposure performance. The $ED_{50}$'s were 61 Gy for electrons, 81 Gy for bremsstrahlung, 89 Gy for $\gamma$-ray photons, and 98 Gy for neutrons. In terms of relative biological effectiveness to produce early performance decrement (10 min from the start of irradiation), significant differences existed between the electrons and the other three fields and between the bremsstrahlung and neutron fields. These differences could not be explained by macroscopic dose distribution patterns in the irradiated animals. The data imply that different radiation qualities are not equally effective at disrupting performance, with high-energy electrons being the most effective and neutrons the least. © 1989 Academic Press, Inc.

## INTRODUCTION

Early performance decrement (EPD) is often produced by exposure to rapid, supralethal ionizing radiation (*1*); however, it was recently reported that EPD may occur at doses below the $LD_{50/30}$ (*2*). When EPD occurs it usually starts 10–15 min after irradiation and can last another 10–30 min. However, all radiations are not equally effective at producing EPD. For instance, $\gamma$ photons and bremsstrahlung radiation were more effective at producing EPD than neutron radiation in pigs and monkeys (*3, 4*), and electron radiation was more effective than $\gamma$ and bremsstrahlung radiation in rats (*5*). While EPD occurs in several animal models performing a variety of tasks after exposure to various radiation qualities, no comparison exists in one animal model performing the same task. This paper continues previous work (*5, 6*), and it describes the effects of bremsstrahlung, electron, $\gamma$-, and neutron radiations on rat motor performance. The objectives were to establish the median effective dose ($ED_{50}$) for rat performance after exposure to four different radiation qualities and to determine their relative biological effectiveness (RBE).



0033-7587/89 $3.00

TABLE I

LINAC Electron and Bremsstrahlung Radiation Parameters

| | *Electron* | *Bremsstrahlung* |
|---|---|---|
| Pulse width | 4.0 μs | 4.0 μs |
| Beam energy | 18.6 MeV | 18.1 MVp |
| Beam current | 0.54 amp | 0.54 amp |
| Distance | 4.4 m | 2.8 m |
| Dose/pulse | 8.3 cGy | 0.56 cGy |
| Pulse repetition rate | 4.0 $s^{-1}$ | 60.0 $s^{-1}$ |
| Dose rate | | |
| During pulse | $1.2 \times 10^6$ Gy/min | $8.4 \times 10^4$ Gy/min |
| Average | 20.0 Gy/min | 20.0 Gy/min |

## METHODS

*Subjects.* Male (Crl:CD BR VAF/Plus) rats (*Rattus norvegicus*) were used that weighed an average of 463 g ± 4 (standard error of the mean (SEM). Rats ($N = 188$) this size represented the age group of interest in our work. Rats were maintained in an AAALAC-accredited facility in keeping with the principles stated in the *Guide for the Care and Use of Laboratory Animals* prepared by the Institute of Laboratory Animal Resources, National Research Council. Rats were quarantined on arrival and screened for disease. They were maintained in plastic microisolator cages on hardwood chips changed three times/week and provided commercial rodent chow and acid water (pH 2.5 using concentrated HCl) *ad libitum*. Rat-holding rooms were maintained at 70 ± 2°F with 50% ± 10% relative humidity and at least 10 air changes/h of 100% conditioned fresh air. Rats were on a 12 h light/dark full-spectrum cycle (lights on at 0600).

*Task.* Performance was assessed with the accelerod, a shock-motivated test of motor coordination (7). Rats were trained to maintain position for as long as possible on a gradually accelerating, 5-cm-diameter rod located 15 cm above a grid shock floor. The rotational velocity of the rod increased at 1 rpm/s. In the final stages of training, a trial lasted until a rat could not maintain rod balance (in s). Shock was given only on trials that lasted less than 30 s. Training sessions lasted from 5–15 min, and it took an average of 8 training days to achieve stable performance. The average performance time prior to irradiation was 45 ± 3 s, with performance averaged over three trials/session/subject.

*Test procedure.* Once stable performance was achieved, subjects were conditioned to a sham irradiation procedure. Sham conditioning lasted 4 days for 20 min/day, simulating all aspects of the radiation-day profile. Subjects were irradiated while held in cylindrical plastic tubes (20 × 7 × 0.3 cm), with ventilation holes in the sides and one end. The open end was taped when the subject was inside. Following irradiation, each subject was tested 10 min from the start of exposure. More details about the methods can be found in Ref. (6).

*Radiations.* Rats were singly irradiated by one of the following: 18.6-MeV electrons or 18.1-MVp bremsstrahlung from a linear accelerator (LINAC), 1.25-MeV $^{60}$Co γ-ray photons, or 1.67-MeV (tissue-kerma weighted mean energy) fission neutrons from a reactor. Tissue-kerma weighted mean neutron energy is the weighted average of the neutron energy spectrum (8). Rats were unilaterally exposed, right side to the source, at a midline tissue dose rate of 20 ± 1 Gy/min (Table I). The midline tissue dose rate was determined by inserting an Exradin tissue-equivalent ionization chamber (0.5 or 0.05 $cm^3$) in the center of a 5-cm-diameter tissue-equivalent rat phantom. Ion chamber precision was 3% (9).

Electron and bremsstrahlung X-ray irradiations were done using a LINAC with parameters listed in Table I. The midline reference was a laser aligned to the center of each rat. Electron irradiations were done with rats exposed in plastic tubes placed on a wooden table. The X-ray spectrum was produced by accelerating the electron beam into a water-cooled converter consisting of four 1-mm-thick tantalum foils. A lead flattening filter (0.19 cm thick) was also interfaced 84 cm from the beam port to improve dose uniformity and to harden the beam, i.e., to remove the low-energy "tail" of the bremsstrahlung spectrum.

Each rat, in its plastic holder, was placed inside a 10-cm-thick paraffin cave to provide uniform environmental scatter. A 2-cm-thick plastic sheet was placed in front of the array to ensure electronic equilibrium (build-up).

Gamma-ray exposures were done in a 32,000-Ci $^{60}$Co facility in which $^{60}$Co ribbons were inserted in a planar source (holder) attached to a remotely controlled elevator. The source was normally stored in a water pool (1.8 × 4.9 × 10 m) located in a containment room. Gamma-ray exposures were carried out with the source at a height of 28 cm and centered on the rat, and they were terminated by lowering the source into the pool.

Neutron exposures were done with a Triga Mark F nuclear reactor, with a 15-cm-lead shield interposed between the reactor wall and the rat to attenuate most of the primary $\gamma$ rays. Rats were centered 61 cm from the tank wall and 123 cm above the floor. The tissue-equivalent ionization chambers filled with tissue-equivalent gas measured total dose, and a magnesium ionization chamber filled with argon gas separated the $\gamma$-ray component of the dose. The neutron to $\gamma$-ray dose ratio was approximately 5 at the midline of the rat dosimetry phantom. Neutron doses were the total neutron and $\gamma$-ray dose at the phantom midline. An extractor system that exceed the reactor room wall was used to remove rats after exposure. The system was an aluminum tube that extended outside the exposure room to a position in front of the core and a polyethylene carriage driven by a motorized pulley system. Rats in plastic restrainers were moved out of the exposure room 30 s after exposure.

*Depth–dose measurements.* Measurements were performed in a 5-cm-diameter cylindrical acrylic rat phantom to estimate the absorbed dose along the lateral (side-to-side), vertical (top-to-bottom), and longitudinal (nose-to-tail) axes in each of the four fields (*9*). Phantoms were equipped with removable acrylic rods fitted with small cavities in which thermoluminescent dosimeters (TLDs) or activation foils were placed. TLD measurements were averaged over several exposures to determine the dose profiles from $^{60}$Co (four test runs), electrons (eight runs), and bremsstrahlung (eight runs). Neutron depth–dose deposition was estimated from the average of indium and rhodium foil activation of three test runs.

*Analysis.* The main performance measure was EPD during the initial 10-min postirradiation test period. A modified up/down sensitivity procedure was used in the initial estimate of the $ED_{50}$ for each radiation quality starting with an arbitrary dose, e.g., 77 Gy (*10*). If the initial rat showed EPD 10 min after exposure, the next subject received 59 Gy. If no EPD occurred in the initial rat, the dose was increased (100 Gy). Once the appropriate dose range was established, more rats were tested at two dose levels above and below the estimated $ED_{50}$. EPD was defined as performance two $Z$ scores below baseline. Two $Z$ scores represent the degree of significant change in performance postirradiation at the 5% confidence level, adjusted for individual differences. The mean baseline prescore was based on 15–20 test periods, 5 min in duration. Across the radiation qualities doses ranged from 45 to 130 Gy. Probit analysis was applied to the dose ranges in each field to determine the probits, $ED_{50}$'s, and the radiation biological effectiveness of each radiation (*11*). RBE is the ratio of the absorbed dose of one radiation quality to the absorbed dose of another radiation to produce the same level of biological effect (*12*).

## RESULTS

As stated in the Introduction, this paper is a continuation of previous radiation quality work. The behavioral findings with the bremsstrahlung, electron, and $\gamma$ fields were reported elsewhere (*5, 6*). The dosimetry work was reported in an AFRRI technical report (*9*).

*$ED_{50}$.* Probit analysis of the four radiation fields assessed the effects of each radiation quality on behavior 10 min after exposure (Fig. 1) (*11*). The resulting estimated $ED_{50}$'s and their respective confidence limits for each original data field are shown in Table II in descending order of effectiveness. The analysis also indicated no significant difference in probit slopes for the four fields. Thus a pooled field was calculated and the RBEs comparing the radiation field were estimated. As shown in Fig. 2, pooling decreased the slope of the electron probit and increased the slope of the $\gamma$ probit. The findings indicated that electron radiation was significantly more effective than the other fields as shown by the following RBEs: 1.6 compared with neutron radia-

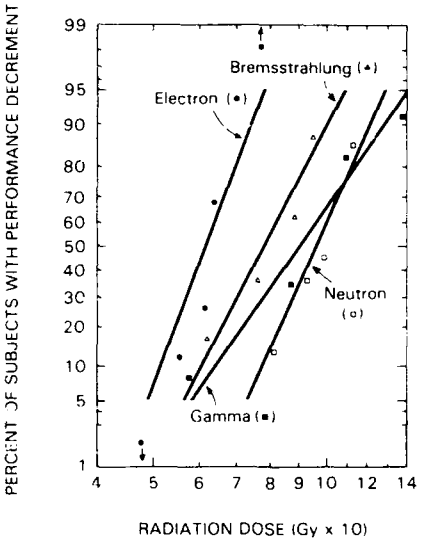


FIG. 1. Accelerod early performance decrement dose–response curves produced by bremsstrahlung, electron, $\gamma$, and neutron radiations.

tion, 1.46 compared with $\gamma$-ray photons, and 1.34 compared with bremsstrahlung X rays. Bremsstrahlung radiation was also significantly more effective than neutrons (RBE = 1.21). No significant difference existed between the $\gamma$ and neutron fields.

*Lethality.* No mortality dose–response relationship was found in any of the radiation fields, probably because the range of doses in each field was small. The average time until death for all radiation qualities was 102 h.

*Depth–dose measurements.* The depth–dose profiles for the four radiation fields in the three-exposure axes are shown in Figs. 3–5. The precision of the depth–dose measurements in the $^{60}$Co and LINAC fields was about 4%. Due to positioning problems with the extractor carriage and the small size of the activation foils, neutron measurement precision was about $\pm 10\%$.

The depth–dose distributions through the rat phantom along the radiation beam on the lateral axis (side to side) are shown in Fig. 3. These profiles indicate that the

TABLE II

$ED_{50}$ and Upper and Lower Confidence Limits for Each Radiation Quality

| *Radiation* | $ED_{50}$ *(Gy)* | *Confidence* | |
|---|---|---|---|
| | | *Lower* | *Upper* |
| Electron | 61.1 | 56.6 | 66.4 |
| Bremsstrahlung | 81.2 | 71.8 | 87.4 |
| Gamma | 89.0 | 75.9 | 97.3 |
| Neutron | 98.0 | 88.4 | 107.7 |

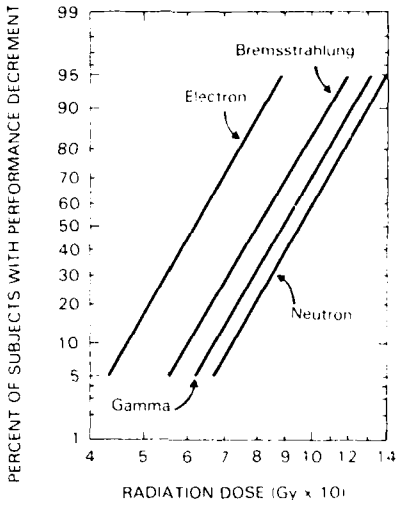


FIG. 2. Accelerod early performance decrement, pooled dose–response curves produced by bremsstrahlung, electron, $\gamma$, and neutron radiations. Electrons were significantly more effective (disrupted performance at lower radiation levels) than bremsstrahlung, $\gamma$, and neutron fields; bremsstrahlung was significantly more effective than neutrons.

neutrons are attenuated by about a factor of 2 from the entrance to the exit side of the phantom, while $^{60}$Co $\gamma$-rays are attenuated by about 35%. LINAC electrons and bremsstrahlung X rays show a fairly flat dose distribution through the phantom, although the electrons exhibited a 20% falloff in deposited energy at the exit side.

Figure 4 shows the dose variations across the vertical axis (top to bottom) of the rat phantom, and the dose distributions on the longitudinal axis (nose to tail) are shown in Fig. 5. These figures indicate that the dose distributions are uniform for all sources, with the exception of the electrons in Fig. 4. In this field, the dose was 25% greater at the underside of the phantom, i.e., the rat gastrointestinal tract.

## DISCUSSION

The present data suggest that different radiation qualities are not equally effective in producing EPD. The rank order for EPD (least to most effective) was neutron, $\gamma$-ray, bremsstrahlung, and electron radiation. High-energy electrons produced EPD at significantly lower doses than the other fields, and bremsstrahlung X rays produced EPD at significantly lower doses than neutrons. Based on traditional biological end points like cell killing, mortality, and cancer induction, these findings oppose the norm, since high-linear-energy-transfer (LET) neutron radiation is generally considered most effective, and bremsstrahlung, electron, and $\gamma$ radiation are considered equally effective (*13*). Since our findings oppose the norm, we interpret them as suggesting that radiation-induced EPD may involve biological mechanisms different than those involved in cell killing, mortality, and cancer induction.

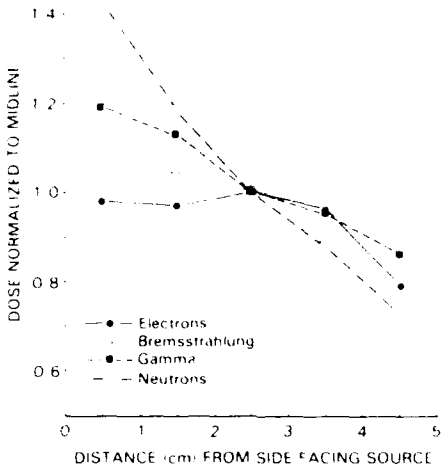


FIG. 3. Depth–dose profiles across the lateral axis (side to side) for the four radiation qualities. Dose "normalized to midline" means the proportional amount of change from 1.0 (100%), e.g., 1.4 is a 40% greater dose.

This is not the first paper to report behavioral RBE values less than one for high-LET radiations (Table III). George *et al.* (*3*) and Thorp and Young (*4*) reported that $\gamma$ rays disrupted pig and monkey performance at significantly lower doses than neutron radiation, and Young (*14*) reported that X rays were effective in monkeys at lower

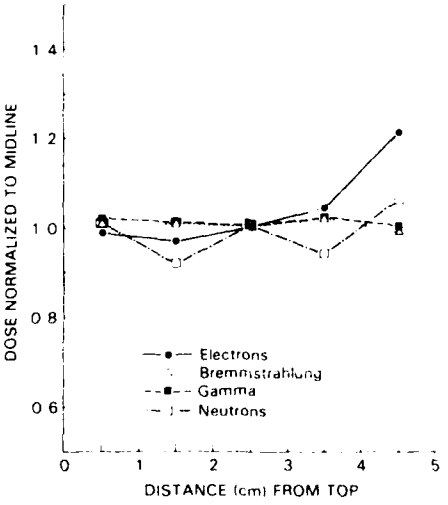


FIG. 4. Depth–dose profiles across the vertical axis (top to bottom) for the four radiation fields. See Fig. 3 for an explanation of the *y* axis.

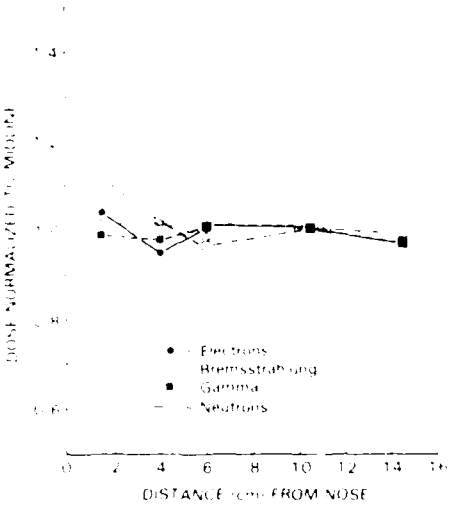


FIG. 8. Depth dose profiles across the longitudinal axis (nose to tail) for the four radiation fields. See FIG. 5 for an explanation of the y axis.

doses than were neutrons. Hunt (*15*) reported that electrons disrupted rat behavior at lower doses than $\gamma$ rays. Other recent nonbehavioral research showed that electrons were effective at lower radiation therapy doses than 10-MeV bremsstrahlung and 250-kVp X rays (*16*).

While the above behavioral work suggests that low-LET radiations are more effective at disrupting performance, this is not always so. Rabin *et al.* (*17*) reported that neutron radiation was more effective than electron and $\gamma$ rays with the conditioned taste aversion paradigm in rats and, further, that high-energy iron particles were even more effective. Conditioned taste aversion is a behavioral assay related to nausea and vomiting. Our findings are generally consistent with previous work, which is important because it establishes the accelerod rat model as a potential substitute for large, more expensive behavioral models (i.e., monkeys) used in the past. Also, the radiation quality work suggests that radiation effectiveness issues are still to be resolved.

Our data demonstrated EPD at high radiation levels, but this is not so in all animal models. Bogo *et al.* (*2*) reported that the $ED_{50}$ to produce EPD in monkeys was 7 Gy (*2*), and it has been implied that the effect level may be 3 Gy (*18*), which means the EPD effect level is near the $LD_{50/30}$ (6 Gy) (*19*) in what may be considered the best radiation model for man. Several factors may account for the difference. First, our task was insensitive, although physically demanding tasks are generally considered more radiosensitive (*20*). Another reason EPD is higher in the rat may be the time tested after exposure. In the monkey study (*2*), performance was monitored immediately after exposure while rats were tested 10 min from the start of irradiation. Unpublished research suggests that if rats are tested right after exposure, the $ED_{50}$ is much less than reported here. Another reason high doses are needed to produce rat EPD may be simply that the rat is radioresistant, which is confirmed for the rat

TABLE III

Radiation Quality RBEs in Performance Decrement Studies

| | | | Neutrons | |
|---|---|---|---|---|
| | $^{60}$Co γ rays | X rays | AFRRI | NRL |
| Primary energy | 1.8 MeV | 1.8 MeV p | 1.67 MeV | d(3.4–7)+Be |
| Lineal energy ($\bar{y}_D$) (keV/μm) | 1.90 | 2.08 | 7.10 | 8.10 |
| Behavioral RBE | | | | |
| Pig (Ref. [28]) | | | 0.23 | |
| Rat | | | | |
| Present | 1.46 | 1.10 | 0.91 | |
| Ref. [15] | 1.65 | | | |
| Monkey | | | | |
| Ref. [4] | — | — | 0.68 | |
| Ref. [34] | — | — | — | 0.86 |

Naval Research Laboratory cyclotron mean neutron energy was 1.5 MeV [14].

$\bar{y}_D$ for the AFRRI 15-cm-Pb-shielded neutrons is from Ref. [39]. Since no lineal energy data were available for the other radiations, representative $\bar{y}_D$ values for these fields are from Ref. [31]. Values are similar to primary energies: electrons = 1.5 MeV, X rays = 4.2 MV p, and neutrons = d(35)+Be.

The reference radiation for the rat studies was $^{60}$Co ($\bar{y}_D$ = 2.43 keV/μm) [39]; for the swine [3] and one of the monkey studies [4] it was an AFRRI reactor γ-ray high-energy spectrum; for the other monkey study it was 1.8-MV p bremsstrahlung X rays from a LINAC [14].

$ED_{50/30}$ is higher than that of the monkey, i.e., 7.5 and 6.0 Gy, respectively [19]. In the past, the search for the mechanism of effect of EPD was done with models that demonstrate the effect. However, another approach might be to study models that are more resistant, i.e., the rat, or that do not demonstrate EPD, i.e., the dog [6] and the mouse (unpublished research).

In previous radiation quality research on EPD at AFRRI, reasons for the inequalities in radiation effectiveness were suggested, but no dosimetric or theoretical explanation could explain the differences [6]. Physical factors possibly involved in the differing sensitivities to the four radiations include the accuracy of the dose measurement, the different macroscopic depth–dose distribution, electron dose perturbations at interfaces, dose rate or pulse timing effects, and different radiation quality or LET.

Dosimetry accuracy is a concern in radiation quality studies for a number of dosimetric techniques are used to measure the energy deposited by different radiations. For high-energy electrons and X rays, high dose rates in the beam pulses (Table I) required the determination and application of ionization saturation corrections to each chamber reading [21]. Other complications in LINAC dosimetry were differing stopping powers of electrons and bremsstrahlung X rays compared to $^{60}$Co, and the ionization-chamber-specific corrections needed due to wall effects and displacement of phantom material in the chamber [22]. Proper handling of these variables is assured at AFRRI by collaborating with the National Institute of Standards and Technology (formerly the National Bureau of Standards) in routine ionization chamber calibration and Fricke dosimetry studies [23], in which a ±5% accuracy was maintained for the nonreactor radiations for over a decade. Since no reference exists for neutron radiation, a ±5–10% standardization is achieved at AFRRI by adherence to

specific protocols (*24*) and intercomparisons between different techniques and laboratories (*8*, *24*).

Further efforts to understand the differences in behavioral sensitivity to radiation quality were measurements of the macroscopic depth–dose distribution (Figs. 3–5). Figure 5 shows that dose deposited over the length of the rat is uniform, i.e., ±10%, but this is not true of the distributions in Figs. 3 and 4. Figure 3 shows that neutrons fell off markedly over the width of the rats, suggesting that neutrons were less effective due to nonuniformity on the exit side. However, several things argue against this point. First, high-LET neutrons are normally less penetrating, yet they are more effective in producing biological effects like emesis, mortality, and cancer than low-LET radiations. Second, the deposited doses were measured at the rat midline. Thus, while the number of neutrons deposited on the exit side was less, it was greater on the entrance side. Finally, Young (*14*) conducted a study comparing the effects of bremsstrahlung X rays and neutron radiation on monkey performance in which the depth–dose gradient was constant. In that study, the $ED_{50}$ for X rays was significantly lower than with neutron radiation. This evidence suggests that the neutron falloff in deposited dose in our study is probably not the reason neutron radiation was less effective in producing EPD.

As further shown in Fig. 3, electron dose deposition decreased across the lateral axis about 20%, and it increased the same on the vertical axis (top to bottom) as shown in Fig. 4. The increase in Fig. 4 was attributed to electron scattering from the wood platform below the plastic holder (*9*). However, it is difficult to say if a 20% regional nonuniformity would alter radiation effectiveness. For instance, we reported a nonuniformity in the bremsstrahlung field, i.e., a 20% drop was noted midhead (*6*). A beam flattener corrected the falloff and the effectiveness of the X rays was tested in the uniform field. The new $ED_{50}$ did not differ from the original. Thus, while correcting nonuniformity is justified, it is questionable whether the 20% regional variations noted here can account for the overall differences in radiation effectiveness.

The enhanced effectiveness of electrons for EPD may be due to dose inhomogeneities of high-energy electrons where anatomical structures interface. Electron dose distributions at interfaces display cold spots (less dose) in denser material and hot spots (higher dose) in less dense material (*26*). For 10- to 30-MeV electrons the size of the effects can be 15–30% at simple air–water interfaces and half as much at bone–water interfaces, which can extend over areas of one to several millimeters. The magnitude of these inhomogeneities is amplified at complex anatomical structures, like small bones. This feature may be a factor in influencing the effect of charged-particle irradiation on tissues surrounded by bone, i.e., the spinal cord and the brain, as well as regions of low tissue density, i.e., the lung. The charged-particle dose distribution in appropriate phantoms is required to define the potential role of localized dose inhomogeneities. The state of the art in electron beam dosimetry has advanced so that realistic calculations may now be possible (*27*).

Another reason that the different radiations were not equally effective on behavior may be dose rate. George *et al.* (*28*) used reactor γ rays to show an 80-Gy drop (100 to 20 Gy) in the $ED_{50}$ of pig performance for dose rates of 5 to 20 Gy/min. Another study reported that two split 44-Gy electron doses created a 1–10 min time course for repair and development of immunity to degradation from the second dose in

motor performance (*29*). Bruner (*18*) stated that EPD increased from 7 to 81% at $\gamma$ dose rates of 0.3 to 1.8 Gy/min in monkeys given a total dose of 10 Gy. These studies suggest that a complex dose-time dose-rate relationship exists for the behavioral effects of radiation. In our studies, the pulsed nature of LINAC irradiations (Table I) is different from the continuous exposure with the $^{60}$Co source or the reactor, with the electron beam having a fifteenfold lower pulse rate than the bremsstrahlung X rays. Not only is the LINAC dose delivery partitioned into microsecond pulses at rates of several/s, but each pulse is divided into a structure of radiofrequency wave packets. Thus the LINAC radiation time scales are such as to possibly implicate several levels of physicochemical mechanisms in the dose-time dose-rate relationships.

The physical mechanisms which might be implicated when a biological effect decreases with increasing LET can be elucidated by considering the characteristics of certain solid-state dosimeters. In many physical systems the response to neutron radiation is known to be less than the response to equivalent $\gamma$-ray doses. For example, in liquid ionization chambers (*30*), it is the initial recombination of closely spaced ionizations produced by high-LET radiations which causes neutron-induced ionization currents to be much lower than those produced by equal doses of $\gamma$ rays. In photographic film (*31*), two physical effects cause a reduced sensitivity for high-LET radiations compared to low-LET radiations as follows: (a) the dense ionizations along a high-LET particle track are far in excess of those needed to produce maximal density, and much of the deposited energy is wasted ("overkill effect"); (b) the cascade of secondary electrons produced by X and $\gamma$ rays causes low-LET amplification of the number of photographic grains produced by each incident photon. Finally, in TLDs the response/Gy is reduced when the range of particulate radiation is less than the diameter of the TLD grains; this site-size-specific effect has been attributed to an insensitive outer layer of the TLD grain (*32*). The existence of these physical effects suggests that the behavioral effects of ionizing radiation may have explicable causative mechanisms on a solid-state physics or physicochemical level, i.e., ionic or radical interaction with neurons or membranes, rather than within the traditional microbiological or biochemical theories.

The current data may also have implications for the manned space program, since the relative comparisons suggest that high-energy electrons (common in space) (*33*) disrupt behavior at lower doses than other radiations, regardless of the doses needed to produce EPD. This concern may be greater now than before, since future probes will be deeper in space for longer durations, or the spacecraft will use geostationary orbits with less atmospheric shielding (*34, 35*). Also, while massive radiation is not normal in space, fairly high levels have been reported from large solar proton events (*33*). For instance, in August 1972, a large event occurred that would have given space personnel 2.9 Gy/h over 15 h for a total skin dose of 44 Gy in a normal orbit. Although this event was the worst reported, the study of solar activity is new and the worst case may be unknown. Other space radiations may also affect the behavioral ability of personnel, such as high $Z$ and high-energy (HZE) particles that can create microscopic lesions in tissue. Recent work showed that $^{56}$Fe can induce a conditioned taste aversion (a variant of nausea (*36*)) and disrupt motor performance at very low doses compared to $\gamma$ photons or high-energy electrons (*37, 38*). If this is true, a study of the effects of space radiation, especially HZE particles and proton radiation, is needed before astronauts are a regular part of that environment.

## ACKNOWLEDGMENTS

The authors thank C. A. Boward and G. G. Kessell for their technical assistance in training and testing the subjects, W. F. Jackson for statistical analysis, and R. W. Young for helping to formulate the research. This research was supported by the Armed Forces Radiobiology Research Institute, Defense Nuclear Agency (DNA), under Research Work Unit MJ B4096. Views presented in this paper are those of the authors; no endorsement by DNA has been given or should be inferred.

RECEIVED: August 19, 1988; ACCEPTED: January 6, 1989

## REFERENCES

1. V. Bogo, Early behavioral toxicity produced by acute ionizing radiation. *Comments on Toxicology* **2**, 265–276, 1988.
2. V. Bogo, C. G. Franz, and R. W. Young, Effects of radiation on monkey visual discrimination performance. In *Radiation Research* (E. M. Fielden, J. F. Fowler, J. H. Hendry, and D. Scott, Eds.), Vol. 1, p. 259. Taylor & Francis, London, 1987. [Abstract]
3. R. F. George, R. L. Chapel, D. M. Verrelli, and E. L. Barron, The relative effectiveness of fission neutrons for miniature pig performance decrement. *Radiat. Res.* **48**, 332–345 (1971).
4. J. W. Thorp and R. W. Young, *Neutron Effectiveness for Causing Incapacitation in Monkeys*. Scientific Report SR72-5, Armed Forces Radiobiology Research Institute, Bethesda, MD, 1972.
5. V. Bogo, Comparative effects of bremsstrahlung, gamma, and electron radiation on rat motor performance. In *Proceedings of the 9th Symposium of Psychol. in the Department of Defense*, pp. 68–72. United States Air Force Academy, 1984.
6. V. Bogo, Effects of bremsstrahlung and electron radiation on rat motor performance. *Radiat. Res.* **100**, 313–320 (1984).
7. V. Bogo, L. A. Hill, and R. W. Young, Comparison of accelerod and rotarod sensitivity in detecting ethanol- and acrylamide-induced performance decrement in rats: Review of experimental considerations of rotating rod systems. *Neurotoxicology* **2**, 765–787 (1981).
8. G. H. Zeman, M. Dooley, D. M. Eagleson, L. J. Goodman, R. B. Schwartz, C. M. Eisenhauer, and J. C. McDonald, Intercomparison of neutron dosimetry techniques at the AFRRI TRIGA reactor. *Radiat. Prot. Dosim.* **23**, 317–320 (1988).
9. M. A. Dooley, D. E. Eagleson, and G. H. Zeman, *Rat Phantom Depth Dose Studies in Electron, X-ray, Gamma-ray, and Reactor Radiation Fields*. Technical Report 86-5, Armed Forces Radiobiology Research Institute, Bethesda, MD, 1986.
10. W. J. Dixon and F. J. Massey, Jr., *Introduction to Statistical Analysis*. McGraw-Hill, New York, 1969.
11. D. J. Finney, Quantal responses and the tolerance to distribution. In *Statistical Methods in Biological Assay*, pp. 349–369. Macmillan Co., New York, 1978.
12. ICRU, *Quantitative Concepts and Dosimetry in Radiobiology*. Report 30, International Commission on Radiation Units and Measurements, Washington, DC, 1979.
13. ICRU, *Radiation Dosimetry: Electron Beams with Energies between 1 and 50 MeV*. Report 35, International Commission on Radiation Units and Measurements, Bethesda, MD, 1984.
14. R. W. Young, *Prediction of the Relative Toxicity of Environmental Toxins as a Function of Behavioral and Non-Behavioral Ends Points*. University Microfilm International, Ann Arbor, MI, 1979.
15. W. A. Hunt, Comparative effects of exposure to high-energy electrons and gamma radiation on active avoidance behaviour. *Int. J. Radiat. Biol.* **44**, 257–260 (1983).
16. H. J. Amols, B. Faqui sen, and D. Cagna, Radiobiological effectiveness (RBE) of megavoltage X-ray and electron beams in radiotherapy. *Radiat. Res.* **105**, 58–67 (1986).
17. B. M. Rabin, W. A. Hunt, and J. A. Joseph, An assessment of the behavioral toxicity of high-energy iron particles compared to other qualities of radiation, in press.
18. V. Bruner, Immediate dose-rate effects of $^{60}$Co on performance and blood pressure in monkeys. *Radiat. Res.* **70**, 378–390 (1977).
19. A. P. Casarett, *Radiation Biology*. Prentice-Hall, Englewood Cliffs, NJ, 1968.
20. G. A. Mickley, V. Bogo, and B. West, Behavioral and neurophysiological changes associated with exposure to ionizing radiation. In *Textbook of Military Medicine* (R. I. Walker, T. J. Cerveny, and J. A. Van Duesen, Eds.), Vol. 1, Part 2. U.S. Army, Washington D.C., in press.

32. ICRU. *Use, Dosimetry of Pulsed Radiation.* Report 34. International Commission on Radiation Units and Measurements. Bethesda, MD. 1982.

33. Task Group 21 of the American Association of Physicists in Medicine. A protocol for the determination of absorbed dose from high energy photon and electron beams. *Med. Phys.* **10,** 741–771 (1983).

34. C. G. Soares, E. L. Bright, and M. Eisenhut. *Dosimetry in High Energy Electron Beams.* National Bureau of Standards Special Publication 280-4. U.S. Department of Commerce. Washington, DC. 1987.

35. L. J. Goodman. *Practical Guide to Ionization Chamber Dosimetry at the HFRR Reactor.* Contract Report CR 85-1. Armed Forces Radiobiology Research Institute. Bethesda, MD. 1985.

36. ICRU. *In Vivo Dosimetry. Neutron Dosimetry Comparison.* Report 27. International Commission on Radiation Units and Measurements. Bethesda, MD. 1977.

37. W. Poblete and K. H. Mangold. Electron dose distribution in inhomogeneous media. In *High Energy Physics and Electronics* (N. Kramer, N. Suntharalingam, and G. F. Zinninger, Eds.). Wiley. New York. 1976.

38. K. R. Shortt, C. K. Ross, A. F. Bielajew, and D. W. O. Rogers. Electron beam dose distributions near standard inhomogeneities. *Phys. Med. Biol.* **31,** 235–249 (1986).

39. R. F. George, R. F. Chappell, and E. E. Barron. *The Dependence of Mental Pig Performance Decrement upon Gamma Ray Dose Rate.* Scientific Report SR 72-20. Armed Forces Radiobiology Research Institute. Bethesda, MD. 1972.

40. R. F. Chappell and P. A. Berardo. Increased brain radioresistance after supralethal irradiation. *Med. Phys.* **1,** 148–151 (1974).

41. J. C. H. Chu, W. H. Grant III, and P. R. Almond. A liquid ionisation chamber for neutron dosimetry. *Phys. Med. Biol.* **26,** 1133–1148 (1980).

42. K. Becker. *Solid State Dosimetry.* CRC Press. Cleveland. 1973.

43. *ICRU. Microdosimetry. Report 36.* International Commission on Radiation Units and Measurements. Bethesda, MD. 1983.

44. I. I. Kovalev. U.S.S.R. space biology and medicine: Radiation protection during space flight. *Aviat. Space Environ. Med.* **54,** S16–S23 (1983).

45. V. Bogo. Radiation: Behavioral implications in space. *Toxicology* **49,** 299–307 (1988).

46. G. V. Mickley, V. Bogo, M. R. Landauer, and P. C. Mele. Current trends in behavioral radiobiology. In *Terrestrial Space Radiation and Its Biological Effects* (P. D. McCormack, C. E. Swenberg and H. Bücker, Eds.). Plenum. New York. in press.

47. B. M. Rabin and W. A. Hunt. Mechanisms of radiation-induced conditioned taste aversion learning. *Neurosci. Biobehav. Rev.* **10,** 55–65 (1986).

48. W. A. Hunt, B. M. Rabin, J. A. Joseph, T. K. Dalton, W. R. Murray, Jr., and S. A. Stevens. Effects of iron particles on behavior and brain function: Initial studies. In *Terrestrial Space Radiation and Its Biological Effects* (P. D. McCormack, C. E. Swenberg and H. Bücker, Eds.). Plenum. New York. in press.

49. J. Joseph, W. A. Hunt, B. M. Rabin, and T. K. Dalton. Correlative motor behavioral and striatal dopaminergic alterations induced by $^{56}$Fe. In *Terrestrial Space Radiation and Its Biological Effects* (P. D. McCormack, C. E. Swenberg and H. Bücker, Eds.). Plenum. New York. in press.

50. H. M. Gerstenberg and J. J. Coyne. Calculated microdosimetry spectra and their use to indicate neutron source quality. *Radiat. Prot. Dosim.* In *Radiation Research* (E. M. Fielden, J. F. Fowler, J. H. Hendry, and D. Scott, Eds.). Vol. 1, p. 86. Taylor & Francis. London. 1987. [Abstract]

RADIATION RESEARCH 117, 419–432 (1989)

# Gamma Radiation Affects Active Electrolyte Transport by Rabbit Ileum

## II. Correlation of Alanine and Theophylline Response with Morphology

PAMELA J. GUNTER-SMITH

*Physiology Department, Armed Forces Radiobiology Research Institute, Bethesda, Maryland 20814-5145*

GUNTER-SMITH, P. J. Gamma Radiation Affects Active Electrolyte Transport by Rabbit Ileum. II. Correlation of Alanine and Theophylline Response with Morphology. *Radiat. Res.* **117**, 419–432 (1989).

The response of ileal segments isolated from rabbits to an actively transported amino acid and a secretagogue was evaluated following exposure to 10 Gy whole-body $\gamma$ irradiation. The ability of ileal segments to respond to the actively transported amino acid, alanine, was not significantly diminished until 96 h postexposure. Decreased responsiveness to the secretagogue, theophylline, occurred earlier at 72 h. These effects did not appear to be accounted for by decreased food intake of irradiated animals alone. Examination of intestinal morphological changes with respect to these changes in electrolyte transport revealed that decreased amino acid transport coincides with loss of intestinal villi. Although a morphological correlate of decreased secretory response was not as striking as that for absorption, the theophylline response appeared to decline concomitant with the appearance of increased mitotic activity in the intestinal crypts. The results of this study indicate that, following a dose of 10 Gy, the inability of these tissues to respond to amino acids is due to a loss of mature villus absorptive cells subsequent to denudation of the intestinal mucosa. There appeared to be little impairment of cell membrane transport processes for alanine. In contrast, the decreased secretory response could not be correlated with the disappearance of any one cell type and perhaps results from increased proliferation in the crypts at the expense of differentiation. 

## INTRODUCTION

Although effects of ionizing radiation on the gastrointestinal tract have been well documented (reviewed in (*1, 2*)), recent studies continue to provide new insight into the mechanisms underlying postirradiation dysfunction. Many studies have focused on the effects of radiation on nutrient absorption (*3–8*). There is, however, essentially little information concerning the effect of radiation on the other mode of transport in these tissues, electrolyte secretion. Not only are cellular transport processes underlying secretion different from those associated with absorption, absorptive and secretory cells appear to be localized to distinct regions of the intestinal mucosa, villus and crypt, respectively (*9–11*). Recent observations from this laboratory (*12*) indicated that active transcellular electrolyte secretion is stimulated 24 h following radiation exposure, which may contribute to fluid and electrolyte loss. Thus information con-



0033-7587/89 $3.00

cerning the effect of radiation on secretory as well as absorptive processes is important to an understanding of intestinal dysfunction postirradiation.

To examine the role of membrane transport processes in postirradiation intestinal dysfunction in greater detail, this study assesses in rabbit ileum the effect of radiation on two well-characterized active transport processes. Both absorption, stimulated by amino acids, and secretion, stimulated by theophylline, are evaluated. These data are correlated with changes in morphology to examine the relation between functional and morphological damage induced by exposure to ionizing radiation. In addition, since absorption and secretion are localized to different areas, the results are discussed with respect to regional effects of radiation. The results show that both absorption and secretion are inhibited by radiation exposure with different time courses. Further, in some cases, this loss of function can be attributed to the demise of a population of intestinal cells.

## METHODS

Male New Zealand White rabbits (Hazelton Dutchland, Denver, PA) weighing 2–3 kg were screened for evidence of disease prior to use. They were individually housed in stainless steel cages and maintained in rooms at 21°C, 50% RH, 12 h light/12 h dark (no twilight). They were allowed access to commercial chow and tap water *ad libitum* except for "fasted" animals from which food was withheld. All procedures used for animal irradiation and assessment of transepithelial transport have been reported previously (*12*). Briefly, the terminal ileum was isolated from euthanatized New Zealand White rabbits (80 mg/kg iv, pentobarbital sodium) that were either exposed to *10 Gy whole-body $^{60}Co$ radiation, sham irradiated, or fasted.* These tissues are referred to as irradiated, control, and fasted, respectively. The following times were selected for isolation of tissues from the animal: 24, 48, 72, or 96 h postirradiation or postfast.

For the assessment of transepithelial electrical parameters, the tissues were mounted in chambers and bathed with a standard Ringer's solution (*12*). Transepithelial potential (PD), resistance ($R_t$), and short-circuit current ($I_{sc}$, which represents the sum of all active transcellular ion movements across the tissue) were monitored as previously described (*12*). After steady-state baseline values were achieved (generally 80–100 min), the response of the intestinal segments to an actively transported amino acid was determined by the addition of alanine from stock solutions to the luminal bath (final concentration, 10 m*M*). Subsequently, alanine was removed allowing the reestablishment of baseline values and then replaced by Ringer's containing the secretagogue theophylline (*10 m*M*). The response of irradiated and fasted segments was always compared to that of a control animal from the same "batch" of animals to minimize differences arising from different groups of animals. All results are expressed as the mean ± SEM. Significant differences from control were determined at the 0.05 level using the Student's *t* test.

Additional segments of tissue isolated from the same animals used in transport studies were prepared for morphological examination. Sections were stained with hematoxylin and eosin and examined for qualitative changes in morphology postirradiation.

## RESULTS

*Transport studies.* The results of a typical experiment are shown in Fig. 1 in which the response of ileal segments isolated from an irradiated animal 24 h postexposure is compared to that from a control animal. Although the baseline $I_{sc}$ was elevated 24 h postirradiation, the response of the tissue to both alanine and theophylline was essentially identical to control. Previous studies from this laboratory (*12*) have shown that the elevated basal $I_{sc}$ postirradiation reflects a stimulation of cellular secretory processes (blood to lumen) that are similar to those elicited by secretagogues such as theophylline (*13*). This differs from the ionic basis of the increase in $I_{sc}$ following alanine addition, which reflects increased transcellular absorptive processes (*9*).

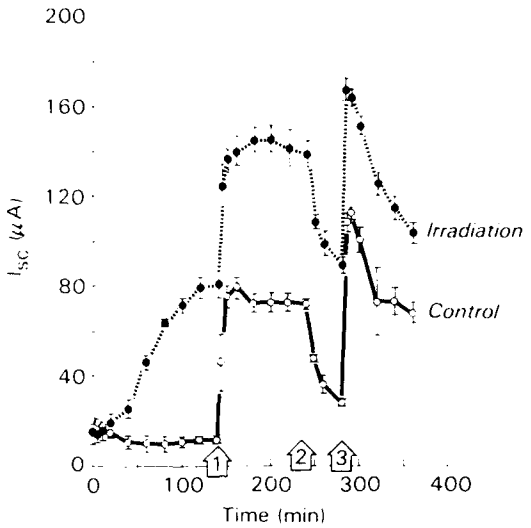


FIG. 1. $I_{sc}$ of ileal segments from a control and an irradiated animal (10 Gy) with respect to time after mounting in chambers. Each point is the mean of values for four segments from the same animal. Arrows labeled 1, 2, and 3 indicate alanine addition, alanine removal, and theophylline addition, respectively.

The time course of differences in the response of irradiated segments (10 Gy) to alanine or theophylline with respect to controls is shown in Fig. 2. There were no significant differences observed in the response to alanine until 96 h postexposure by which time the response was greatly diminished. Significant declines in the response of irradiated segments to theophylline were observed to occur earlier at 72 h postirradiation.

Since food intake of irradiated animals initially decreases following exposure, the effect of fasting on the response to alanine and theophylline was evaluated in control

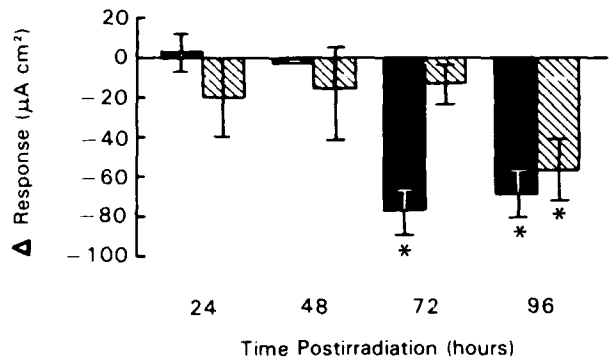


FIG. 2. Response of irradiated tissues to alanine (hatched bars) and theophylline (filled bars) compared to controls with respect to time postirradiation. ΔResponse = $\Delta I_{sc}$ (irradiated) − $\Delta I_{sc}$ (control); $n$ = 4 irradiated and 4 control tissues for each bar; * indicates significant difference.

TABLE I

The Effect of Fasting on the Response to Alanine and Theophylline

| | *24 h* | *48 h* | *72 h* | *96 h* |
|---|---|---|---|---|
| Alanine | 6.6 ± 15.4 | 54.8 ± 11.3 | 17.7 ± 12.5 | 22.3 ± 11.9 |
| *P* | NS | < 0.03 | NS | NS |
| Theophylline | 11.2 ± 14.4 | 28.0 ± 5.7 | 42.9 ± 20.6 | 44.8 ± 26.2 |
| *P* | NS | < 0.03 | NS | NS |

*Note.* Data are expressed as the mean of $\Delta I_{sc}$ (fasted) − $\Delta I_{sc}$ (control) for four experiments. NS = nonsignificant.

animals. As shown in Table I, the response of "fasted" animals to both alanine and theophylline was decreased compared to nonfasted controls at 48 h postfast. Differences in the response were not significant at the other times studied including those at which significant effects of radiation were noted. Direct comparison of the fasting with the irradiated data (Table I and Fig. 2), however, did not show significant differences between these two groups at 72 or 96 h.

*Morphology.* The morphology of ileal segments isolated from tissues used in the transport studies above was examined in an attempt to further define the factors underlying the changes in transport properties following radiation exposure. Figure 3 shows the typical appearance of an ileal segment from a control animal. Long finger-like projections, villi, protrude into the lumen with numerous crypts at their base (Fig. 3A). Cells lining the villi are columnar epithelial cells; their brush borders (composed of microvilli on the individual cells) are clearly visible in Fig. 3B. A smaller population of mucus-secreting goblet cells is also present. In contrast to the villus area, the crypt area (shown in Fig. 3C) has at least five main cell types (*14*). Three of these are easily identified in the field: Paneth cells located at the base of the crypt, goblet cells, and a proliferative cell in which a mitotic figure is visible. Argentaffine and undifferentiated crypt cells are not easily identified in this section.

The effects of radiation on the morphology of rabbit ileum was similar to that observed in this and other species for a dose that is considered "threshold" for gut injury (*15*). The severity of the damage was quantitatively less than that associated with pure gut death and a proliferative burst was observed in the crypts at the later times. The time course of the changes in morphology is detailed in Figs. 4–7. At 24 h postexposure little change in the gross morphology of the tissue is visible (Fig. 4A). There is no obvious blunting of the villi and the brush border membranes are still prevalent (Fig. 4B). There is no major disruption of the crypt epithelium, although discrete areas of cell death are visible (Fig. 4C). While the radiosensitive cells cannot be identified in the figure, the Paneth cell population appears virtually unaffected. Interestingly, mitotic figures are not frequently seen at this time, suggesting that, while major alterations in morphology have not occurred, mitosis has been interrupted. Blunting of the villi is observed by 48 h postirradiation, and a greater proportion of the villus appears occupied by goblet cells compared to control (Figs. 5A, 5B). Cell death in the crypts appears comparable to that at 24 h. However, at this time mitotic

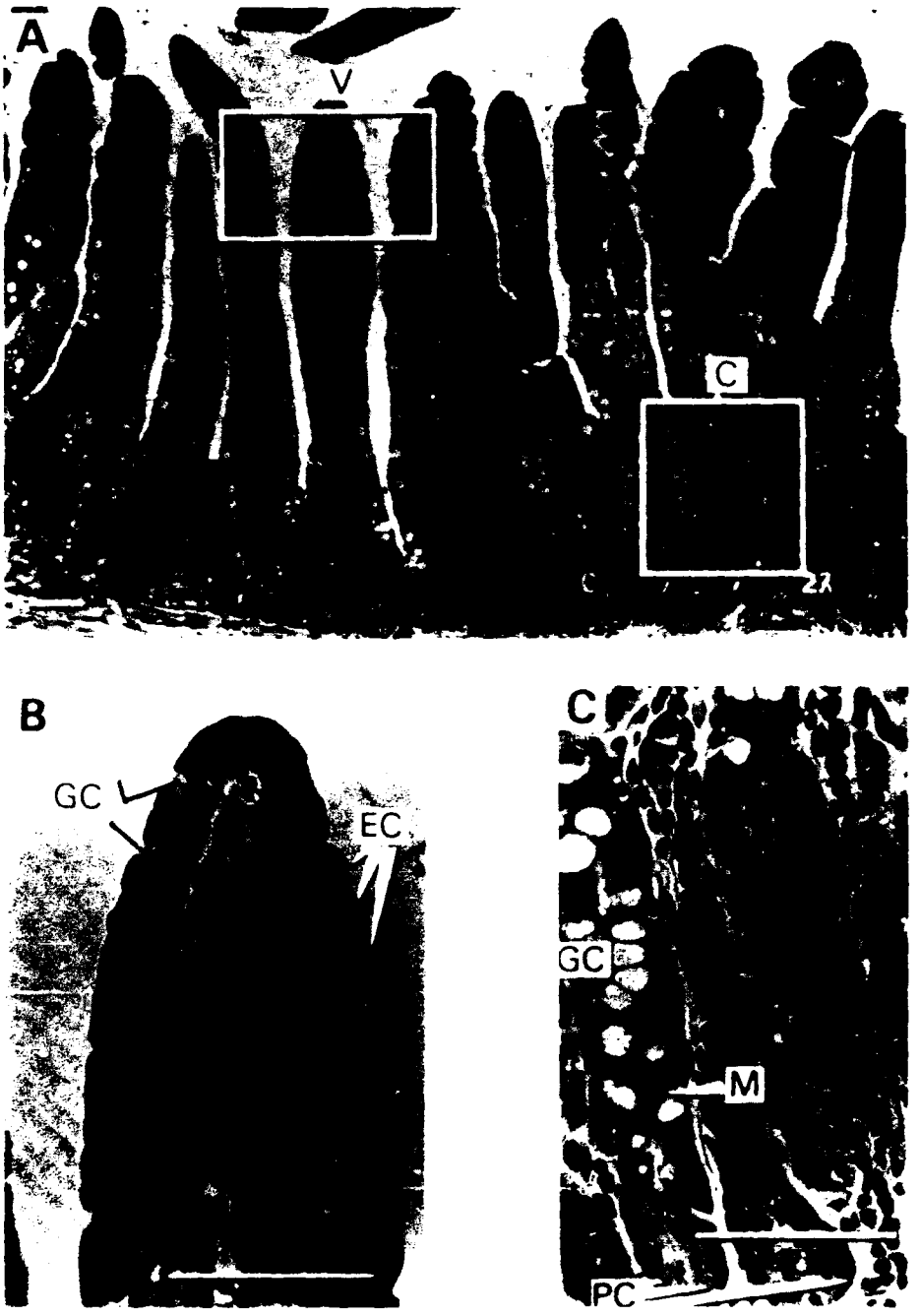


FIG. 3. (A) Morphology of ileal segment from a control animal. Villus (V) and crypt (C) regions are designated. Boxes indicate regions from which higher magnifications ((B) and (C)) were taken. (B) Higher magnification of villus showing goblet (GC) and epithelial cells (EC). (C) Higher magnification of crypt showing goblet (GC) and Paneth cells (PC). A mitotic figure is shown at M. The scale shown is 200 $\mu$m.


FIG. 4. (A) Gross morphology of ileal segment 24 h postirradiation. Higher magnification of villus and crypt regions is shown in (B) and (C), respectively. Arrows indicate cell damage. Scale shown is 200 $\mu$m.

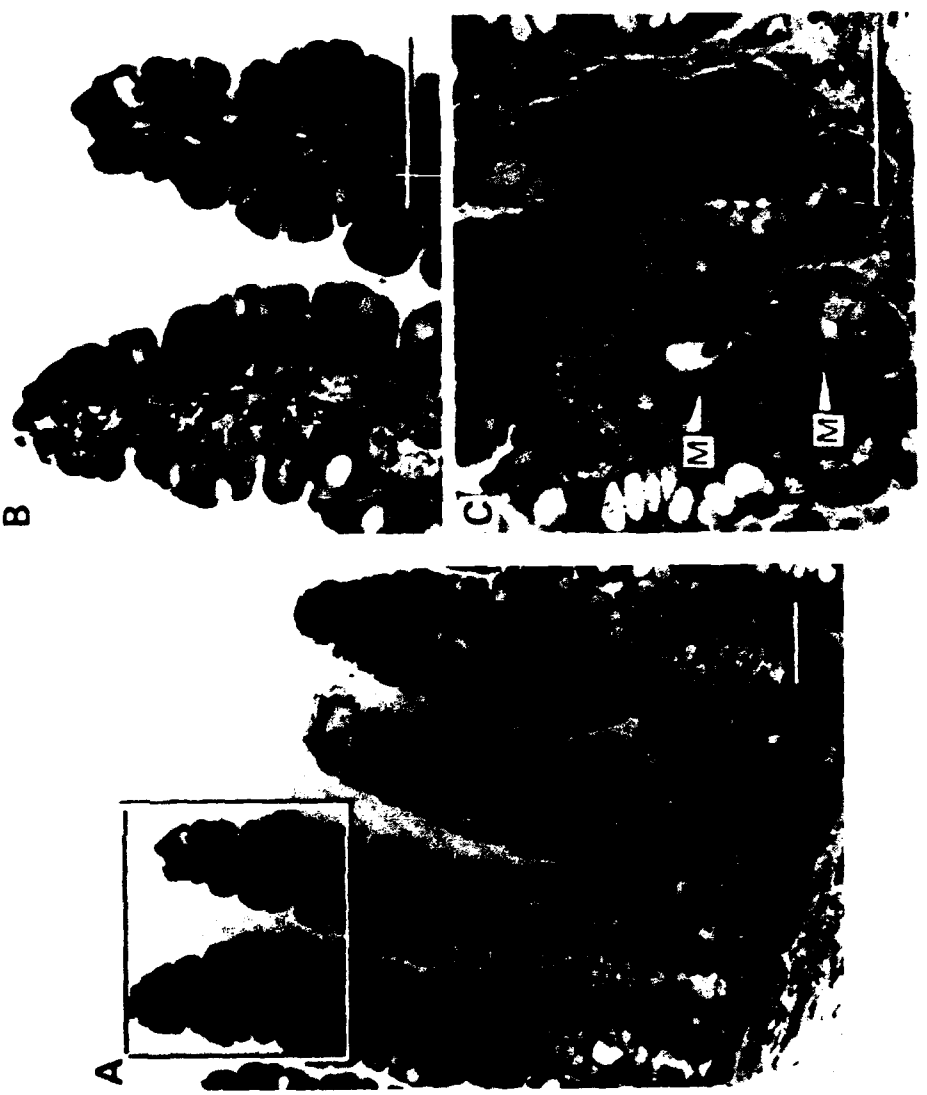


FIG. 5. (A) Gross morphology of ileal segment 48 h postirradiation. Higher magnification of villus region shown in (B) is from boxed area of (A). Higher magnification of the crypt regions shown in (C) is from a different area of the same section. M designates mitotic figures. Scale is 200 μm.

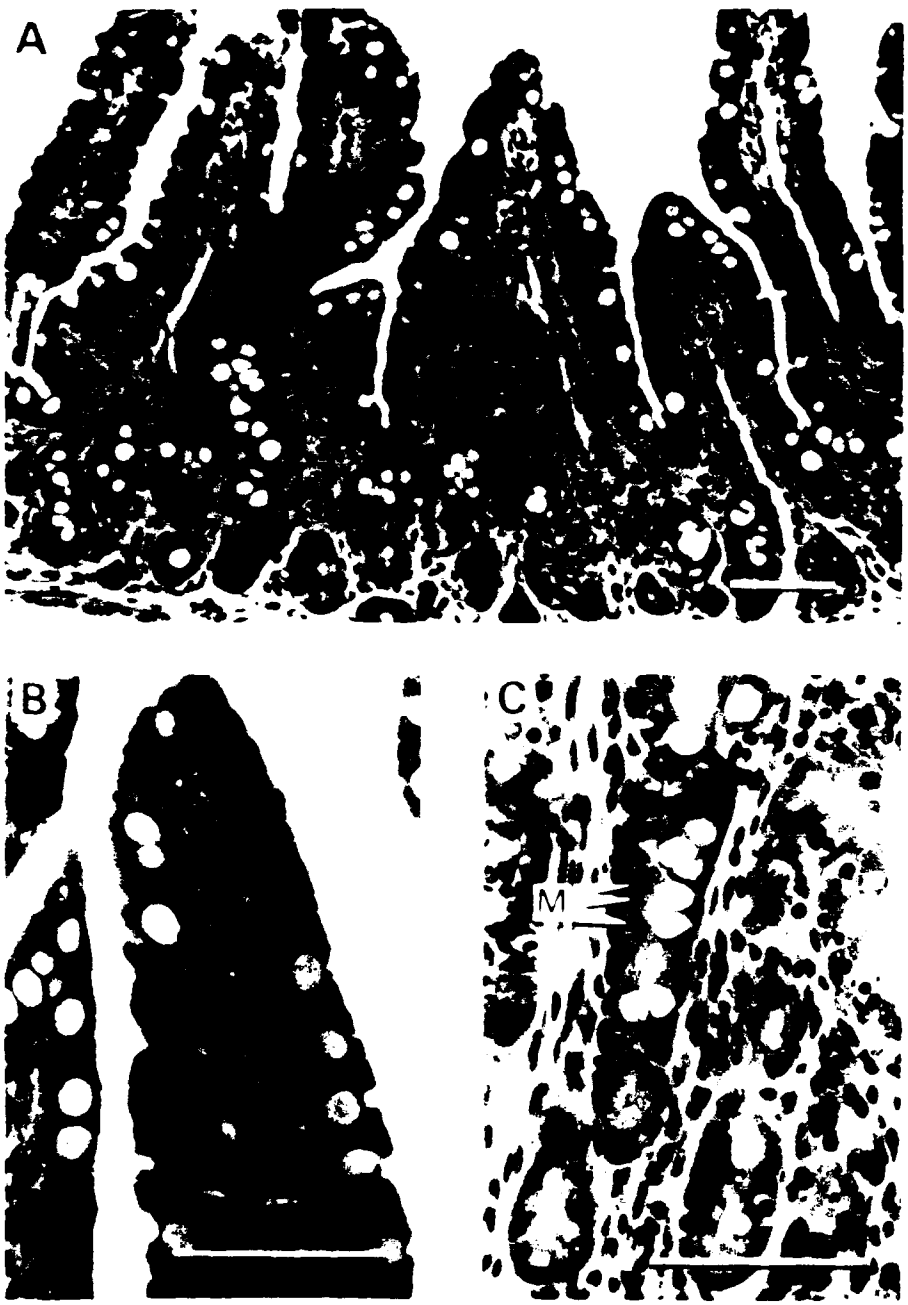


FIG. 6. (A) Gross morphology of ileal segment 72 h postirradiation. Higher magnification of villus and crypt regions in (B) and (C) is taken from different sections but from the same animal. A mitotic figure is shown at M. Scale is 200 μm.

FIG. 7. Intestinal morphology 36 h postirradiation. Higher magnification of crypt epithelium shown in *B* is from a different section from the same animal. M designates mitotic figures. Scale is 200 μm.

figures are observed once again (Fig. 5C). Similar changes in morphology are observed 72 h postirradiation (Figs. 6A, 6B); blunting of the villi appears to have increased. The number of mitotic figures appearing in the crypt area also seems to have increased in Fig. 6C. By 96 h postirradiation, blunting of villi has progressed until they are virtually absent (Fig. 7A). Where not denuded, the villus remnants are covered with cuboidal rather than columnar cells (Fig. 7B). The overall depth of the crypt epithelium has increased. Mitotic figures are numerous and observed even in the neck region of the crypt. This was not seen at earlier times. Thus the entire mucosa appears to be undergoing a proliferative burst at this time, perhaps in an attempt to repopulate the mucosa with viable cells.

## DISCUSSION

In an earlier study (*12*), changes in basal transcellular electrolyte transport processes of rabbit ileum were described with respect to dose and time after radiation exposure. The results indicated that a stimulation of electrolyte secretory processes occurred 18–24 h postirradiation that was suggested to contribute to fluid and electrolyte loss associated with the gastrointestinal syndrome. In the present study, changes in the physiological function of the intestinal mucosa with radiation have been explored in greater detail and correlated with morphological changes. The response of *ileal segments from irradiated animals was determined for* both an actively transported amino acid, alanine, and a secretagogue, theophylline. Since the responses of the tissue to these agents have been previously attributed to different cell populations (*9–11*), evaluation of these processes allows differential examination of functional damage to these two regions of the intestinal mucosa.

Increases in $I_{sc}$ following the addition of actively transported amino acids and sugars to the luminal solution have previously been shown to reflect increased transcellular Na absorption (*9*). Na absorption is stimulated because the influx of sugars and amino acids into the cell is energetically coupled to Na entry. In addition, overall fluid absorption is increased in the process due to the resulting osmotic driving force. Previous studies have provided compelling evidence that only the columnar epithelial cells lining the intestinal villi acquire transport processes required to absorb sugar and amino acids at some time during migration along the villus (*16*). Thus the assessment of the response to alanine following radiation exposure specifically probes one facet of the functional integrity of the villus epithelium.

A significant effect of radiation on the response of ileal segments to alanine was not observed until 96 h postexposure by which time the response was virtually absent. Morphological examination of the tissue indicated that this decline in the response to alanine coincided with the disappearance of the intestinal villi. Since the electrical resistance of the tissue was previously shown to be maintained at this time (*12*), the $I_{sc}$ still appears to assess transport accurately in these tissues. Thus decreased amino acid transport can be attributed to a loss of absorptive villus cells, rather than to an effect of radiation on the underlying cellular transport mechanisms.

Previous studies of the effect of radiation on nutrient absorption by rat intestine postirradiation (*3–7*) reported decreased intestinal absorption at 72 h consistent with the results of the present study. In some cases (*3–6*), an initial increase was observed

at 20 h that was not seen in the present study. Reduced nutrient transport postirradiation was attributed to an impairment of underlying cellular transport processes. However, in support of the conclusions drawn in the present study, reduced transport often coincided with severe morphological damage to the intestinal mucosa (*5, 6*). Likewise, Kwock *et al.* (*17*) observed that decreased Na-dependent amino acid transport in lymphoid cells immediately preceded decreased cell viability. Additional support for the notion that decreased nutrient transport does not result from impaired cellular transport processes is found in more recent studies in which the effects of radiation on transport can be clearly distinguished from cell killing and effects on proliferation. Cheeseman *et al.* (*18*) observed no change in leucine transport in enterocytes isolated from rats 3 days after 6 Gy; glucose transport was actually enhanced in these cells. This latter effect was suggested to be compensatory subsequent to a loss of absorptive surface area. Additionally, Moran *et al.* (*18*) observed no change in basal Na-coupled sugar transport following irradiation of cultured renal epithelial cells. They observed, however, an inability of irradiated cells (~5 Gy) to up-regulate the number of glucose transporters when given an appropriate stimulus that was attributed to an effect of radiation on gene expression.

In addition to studying nutrient absorption, this study also examines intestinal secretory processes postirradiation. Assuming (as is generally accepted) that these processes reside in cells of the crypt epithelium (*9–11*), evaluation of the response of the tissue to a secretagogue such as theophylline will assess the functional integrity (in terms of transport) of this region. Theophylline was observed to increase $I_{sc}$ of control as well as irradiated intestinal segments at early times postexposure (< 72 h). The increase in $I_{sc}$ elicited by theophylline is related to a stimulation of anion secretory processes (*13*). As is true for osmotic fluid absorption resulting from alanine transport, this secretory process stimulates the secretion of fluid into the intestinal lumen. Indeed, it is the stimulation of cellular secretory processes that is responsible for fluid and electrolyte loss associated with a large number of diarrheal diseases (*19*).

Decreased responsiveness of ileal segments to secretagogues was observed 72 h postirradiation. Examination of the morphology of the intestinal mucosa at this time revealed blunting of the villi and increased mitotic activity in the crypts. By 96 h postirradiation, mitotic figures were observed even at the neck of the crypts, but a major loss of cellularity in the crypt epithelium during this time was not apparent. Thus, as described previously for the small intestine of other species (*20–22*), rabbit ileum apparently undergoes a proliferative burst in an attempt to repopulate the intestinal mucosa. Evaluation of transport data with respect to the morphology of the crypt epithelium would suggest that, in contrast to absorption, secretion is diminished in spite of a maintenance of cellularity in the crypt epithelium. Since substantial blunting of the villi does occur 72 h postirradiation, this result could be interpreted as indicating that some villus cell population that is secretory is lost by this time. Since amino acid transport (clearly a villus cell function) was not diminished at 72 h but was diminished at 96 h, this would require a preferential decline in secretory processes and/or enhancement of absorptive processes in these cells. Given the evidence suggesting that secretion is localized to the crypts (cf. (*9–11*)) and that increased mitosis is observed at 72 h, a more attractive explanation for the data is that the

inability of the tissue to respond to a secretagogue is related to decreased differentiation of the crypt cell population.

These results complement our earlier observations (*12*) of changes in basal active electrolyte transport postirradiation. A secretory response was observed which peaked between 18 and 24 h postirradiation and subsequently declined. The basis of this time course was unexplained. It now appears reasonable to suggest that as for secretion stimulated *in vitro* by theophylline, the basal secretory response postirradiation declines due to population of the intestinal crypts with less differentiated cells undergoing mitosis.

In interpreting the results of this study with respect to the effect of radiation on intestinal function, two important caveats require consideration. The first is that the experimental conditions employed may not precisely reflect the environment of the irradiated intestine *in vivo*. This is a consequence of the requirements for measuring active transcellular intestinal transport which must be done *in vitro* using a well-defined media bathing the tissue. Thus the tissue is not exposed to various substances normally present in the lumen (e.g., bile and pancreatic enzymes) or blood that may contribute to alterations in intestinal transport postirradiation. This concern is tempered, however, by the fact that the tissues used in this study were isolated from the animal immediately before transport was assessed and therefore exposed to these *in vivo* factors from the time of exposure to the time of measurement. Prolonged effects and/or damage from such agents would still be observed in these studies, and although short-lived effects would not be observed, they are less likely to be factors in the response.

The second caveat is that the changes observed may not reflect direct radiation damage to the intestinal mucosa, but secondary effects of agents such as those discussed above or other factors resulting from radiation exposure. One of these is the possible influence of decreased food intake observed in irradiated animals which was evaluated in this study by comparing the response of fasted animals to alanine and theophylline to that of their matched controls in a separate series of experiments. Diminished alanine and theophylline responses of segments from fasted animals were significant at 48 h but not at later times when significant effects were observed between irradiated animals and controls. Although the magnitude of the differences in the response for irradiated animals was nearly twice that of fasted animals, a direct comparison of the data from these two groups did not reveal statistically significant differences between fasting and irradiation at 72 or 96 h. While this may be related to the degree of variance associated with the physiological response of the two groups to these conditions, it prevents concluding unequivocally that decreased food intake is not a factor in the radiation response. However, considering that irradiated animals are not totally fasted and have resumed eating by 72 h postexposure, the direct comparison of fasting and irradiated data may overestimate the role of fasting in the response of irradiated tissues. This taken together with previous studies of starving rats (*23, 24*) indicating less severe morphological changes than those observed in this study in irradiated rabbits makes it difficult to reconcile the results from irradiated animals as only secondary to decreased food intake.

In summary, the response of the intestinal mucosa to an actively transported amino acid and a secretagogue was used to assess differential effects of radiation on

villus and crypt epithelia, respectively. These results taken together with the morphological changes observed suggest that secretory processes decline at 72 h perhaps due to increased proliferation in the crypts at the expense of differentiation. Nutrient absorption was observed to decline later at 96 h and was related to the loss of mature villus cells which normally occupy the intestinal villus.

## ACKNOWLEDGMENTS

The author thanks I. Heman-Ackah for preparation of tissues for light microscopy; T. Wilczynski for technical assistance in transport studies; and Dr. J. Nold for helpful discussions concerning the morphological studies. This work was supported by the Armed Forces Radiobiology Research Institute, Defense Nuclear Agency, under research work unit MJ00107. The views presented in this paper are those of the author; no endorsement by the Defense Nuclear Agency has been given or should be inferred. Research was conducted according to the principles enunciated in the "Guide for the Care and Use of Laboratory Animals" prepared by the Institute of Laboratory Animal Resources, National Research Council.

RECEIVED: February 9, 1988; REVISED: September 15, 1988

## REFERENCES

1. V. P. BOND, T. M. FLIEDNER, and J. O. ARCHAMBEAU, *Mammalian Radiation Lethality*. Academic Press, New York, 1965.
2. P. J. GUNTER-SMITH, Effect of ionizing radiation on gastrointestinal physiology. In *Military Radiobiology* (J. J. Conklin and R. I. Walker, Eds.), pp. 135–151. Academic Press, Orlando, FL, 1987.
3. M. F. SULLIVAN, Absorption of the gastro-intestinal tract of the rat after X-irradiation. *Am. J. Physiol* **201,** 1013–1017 (1961).
4. A. D. PERRIS, Intestinal transport and metabolism following whole-body irradiation. *Radiat. Res.* **29,** 597–602 (1968).
5. A. BECCIOLINI, G. B. GERBER, and J. DEROO, In vivo absorption of carbohydrates in rats with gastrointestinal radiation syndrome. *Acta Radiol. Ther. Phys. Biol.* **16,** 87–96 (1977).
6. M. MOHIUDDIN, K. TAMURA, and P. DEMARE, Changes in absorption of glucose and proline following irradiation to the exteriorized ileum. *Radiat. Res.* **74,** 186–190 (1975).
7. A. B. R. THOMSON, C. I. CHESSEMAN, and K. WALKER, Effect of abdominal irradiation on the kinetic parameters of intestinal uptake of glucose, galactose, leucine, and gly-leucine in the rat. *J. Lab. Clin. Med.* **102,** 813–827 (1983).
8. C. I. CHESSEMAN, A. B. R. THOMSON, and K. WALKER, The effects of abdominal irradiation on intestinal transport in the rat as assessed with isolated epithelial cells. *Radiat. Res.* **101,** 131–143 (1985).
9. S. G. SCHULTZ, R. A. FRIZZELL, and H. N. NELLANS, Ion transport by mammalian small intestine. *Annu. Rev. Physiol.* **36,** 51–91 (1974).
10. M. FIELD, Intracellular mediators of secretion in the small intestine. In *Mechanisms of Intestinal Secretion* (H. J. Binder, Ed.), pp. 83–91. Alan R. Liss, New York, 1979.
11. R. A. FRIZZELL and S. G. SCHULTZ, Models of electrolyte absorption and secretion by gastrointestinal epithelia. In *International Review of Physiology (Gastrointestinal Physiology III)* (R. K. Crane, Ed.), Vol. 19, pp. 205–225. Univ. Park Press, Baltimore, 1979.
12. P. J. GUNTER-SMITH, Ionizing radiation affects active electrolyte transport by rabbit ileum: Basal Na and Cl transport. *Am. J. Physiol.* **250** (*Gastrointest. Liver Physiol.* 13), G540–G545 (1986).
13. M. FIELD, Ion transport in rabbit ileal mucosa. II. Effects of cyclic 3′,5″-AMP. *Am. J. Physiol.* **221,** 992–997 (1971).
14. J. S. TRIER, Morphology of the epithelium of the small intestine. In *Handbook of Physiology* (C. F. Code, Ed.), Sect. 6, Vol. III, pp. 1125–1175. Am. Physiol. Soc., Washington, 1968.
15. J. MAISIN, J. R. MAISIN, and A. DUNJIC, The gastrointestinal tract. In *Pathology of Irradiation* (C. C. Berdjis, Ed.), pp. 296–344. Williams & Wilkins, Baltimore, 1971.

16. W. B. KINTER and L. H. WILSON, Autoradiographic study of sugar and amino acid absorption by everted sacs of hamster intestine. *J. Cell Biol.* **25,** 19–39 (1965).

17. I. KWOCK, P.-S. LIN, and L. CIBOROWSKI, Differences in the effect of ionizing radiation on $Na^+$-dependent amino acid transport in Human T (Molt-4) and Human B (RPMI 1788) Lymphoid cells. *Radiat. Res.* **80,** 512–533 (1979).

18. A. MORAN, L. DAVIS, and M. HAGAN, Effect of radiation on the regulation of sodium-dependent glucose transport in LLC-PK epithelial cell line: Possible model for gene expression. *Radiat. Res.* **105,** 201–210 (1986).

19. H. J. BINDER, Net fluid and electrolyte secretion. In *Mechanisms of Intestinal Secretion* (H. J. Binder, Ed.), pp. 1–16. Alan R. Liss, New York, 1979.

20. S. LESHER and J. BATMAN, Recovery of reproductive activity and the maintenance of structural integrity of the intestinal epithelium of the mouse after single dose whole-body 60-Co gamma ray exposure. In *Effect of Radiation on Cellular Proliferation and Differentiation. Proceedings of a Symposium on the Effects of Radiation on Cellular Proliferation and Differentiation*, pp. 507–513. IAEA, Vienna, 1968.

21. H. C. YAU and A. B. CAIRNIE, Cell-survival characteristics of intestinal stem cells and crypts of Co-irradiated mice. *Radiat. Res.* **80,** 92–107 (1979).

22. W. R. HANSON, D. L. HENNINGER, R. J. M. FRY, and A. R. SALESE, The response of small intestinal stem cell in the mouse to drugs and irradiation treatment. In *Cell Proliferation of the Gastrointestinal Tract* (D. R. Appleton, J. P. Sunter, and A. J. Watson, Eds.), pp. 198–212. Pitman Medical, Marshfield, 1980.

23. M. STEINER, H. R. BOURGES, L. S. FREEDMAN, and S. J. GRAY, Effect of starvation on the tissue composition of the small intestine in the rat. *Am. J. Physiol.* **215,** 75–77 (1968).

24. F. S. DEBNAM and R. J. LEVIN, Effect of semistarvation on the kinetics of active and passive sugar absorption across the small intestine in vivo. *J. Physiol.* **252,** 681–700 (1975).

From: TERRESTRIAL SPACE RADIATION AND ITS BIOLOGICAL EFFECTS
Edited by: Percival D. McCormack, Charles E. Swenberg,
and Horst Bücker
(Plenum Publishing Corporation, 1988)

# EFFECTS OF IRON PARTICLES ON BEHAVIOR AND BRAIN FUNCTION: INITIAL STUDIES

Walter A. Hunt, Bernard M. Rabin, James A. Joseph,
Thomas K. Dalton, Warren E. Murray, Jr., and Sherrie A. Stevens

Behavioral Sciences Department
Armed Forces Radiobiology Research Institute
Bethesda, MD 20814-5145

## INTRODUCTION

Successful operations in space depend in part on the performance capabilities of astronauts and little is known about potential consequences of exposure to ionizing radiation on behavior and the brain during manned space flights. This possible threat has not been given much attention, since all manned mission have been located in low equitorial orbit and radiation there has not been considered hazardous. Future missions in space will probably involve polar orbits, long-term space travel beyond the Earth, and extended periods during which astronauts are operating outside their space craft. Since exposure to radiation increases under these conditions because of the absence of the Earth's normally protective transpolar magnetosphere, astronauts may be placed at considerable additional risk. An understanding of this risk may be vital to the survival and effective performance of future missions in space. Therefore, it is desirable to understand the medical and operational risks to personnel, including an assessment of possible behavioral and neurobiological deficits.

Radiation hazards outside the protection of the Earth's magnetic shield arise from solar flares and intragalactic cosmic rays. Intragalactic cosmic rays are composed of protons, alpha particles, and particles with high charge and

energy (HZE), such as iron. Although the hazards of exposure to cosmic rays are often minimized, they can destroy existing cells. Unless their effects can somehow be reduced, the effects on the various organs of the body, including the brain, by their continuous bombardment by radiation during long space flights could be disastrous. In some instances, it has been suggested that the effects of cosmic rays on space travelers could result in symptomatology resembling those of Alzheimer's or Parkinson's disease or advancing age, including significant cognitive and/or motor impairments. Such impairments could jeopardize the successful completion of a mission and have long-term consequences on the health of astronauts. Presently, little research has been done to address these issues.

Considerable advances have been over the last 20 years in the study of behavior and their neurobiological correlates. Specific paradigms are being used to inv tigate the effects of ionizing radiation on behavior (Mickley et al., 1988), as well as neurochemical and neurophysiological endpoints that underlie behavior under study. By combining these analyses with very sensitive behavioral assessments that can measure specific aspects of cognitive or motor performance following HZE irradiation, more information can be obtained concerning important biochemical and behavioral relationships that will eventually aid in predicting and controlling possible performance deficits occurring during manned space flight.

## AFRRI RESEARCH IN SPACE BEHAVIORAL NEURORADIOBIOLOGY

### General Considerations and Design

In order to gain some insight into the possible behavioral and neurological risks of irradiation in space, investigators at the AFRRI initiated a broad research effort using a variety of approaches. More specifically, the general research program is designed to gain information on possible alterations in behavior and the brain after exposure to heavy particles, such as those that might be encountered during space travel. The objectives are to describe and characterize radiation-induced behavioral deficits, determine their underlying causes, and develop approaches to minimize such deficits.

In May, 1987, the research group spent 3 weeks at the Lawrence Berkeley Laboratory (LBL) in Berkeley, CA, assessing the effects of 600 MeV

$^{56}$Fe particles delivered by their Bevalac after doses of 50, 100, or 500 rads on several behavioral and neurochemical endpoints (Table 1). These measurements were performed at various times after irradiation (Table 2) in an effort to obtain preliminary information on the potential hazards of space travel outside the protective shield of the Earth's magnetosphere. The effects of the three different doses of radiation were studied in rats at five different times after irradiation (3 days to 6 months). Although all of the data have not been fully analyzed (6-month groups), several important observations were made. Presented here are the results of studies examining the induction of a conditioned taste aversion by $^{56}$Fe particles and the actions of these particles on sodium channels in synaptosomal membranes. Motor responses of animals exposed to $^{56}$Fe particles and the mechanisms in the brain underlying them can be found in the paper of Joseph et al. (1988) in this volume.

In the basic experimental design of these experiments, several assumptions were made. First of all, in spite of the complexities of the radiation environment in space, it is presumed that conditions in space can be simulated on Earth under controlled conditions. Biological experiments in space are very expensive, yield too little information when sensitive systems have not yet been identified, and are generally impractical. Secondly, since little is known about what space radiation might do to behavior and the brain, effects found with other qualities of radiation are presumed likely to be found after exposures to space radiation. This approach provides a starting point for the design of appropriate experiments. Finally, since long-term, low-level irradiations are impractical with the sources available, the effect of a single dose over time is assumed to provide useful insights into how space radiation might affect the behavior and the brain. This assumption may be especially useful when studying the brain, since the brain does not significantly repair itself after damage.

The irradiations were performed at the Lawrence Berkeley Laboratory (LBL) with the remainder of the experiments completed at the AFRRI. Male Sprague-Dawley rats were irradiated by 600 MeV $^{56}$Fe particles delivered by the LBL Bevalac. Iron particles were chosen because of their high LET and the difficulty to shield against them. Doses of 50, 100, and 500 rads were used to reflect the maximum exposures expected. Measurements were made at five time intervals after irradiation ranging from 3 days to 6 months in order to look for acute and delayed effects.

TABLE 1

EXPERIMENTAL MEASURES

| | |
|---|---|
| BEHAVIORAL ENDPOINTS | |
| Taste Aversion Learning | (Index of Nausea & Emesis) |
| Motor Tasks: | |
| Inclined Screen | (Muscle Tone & Stamina) |
| Wide Rod | (Motor Coordination) |
| Narrow Rod | (Motor Coordination) |
| Wire Suspension | (Upper Body Strength) |
| NEUROCHEMICAL ENDPOINTS | |
| Sodium Channels | (Basic Neuronal Process) |
| Dopamine Release | (Motor Function) |
| Catecholamines and Turnover | (Brain Damage & Rate of Information Transfer) |

TABLE 2

GENERAL EXPERIMENTAL DESIGN
FOR MAY 1987 EXPERIMENTS

ANIMAL MODEL

Male Sprague-Dawley Rats

RADIATION SOURCE

600 MeV/nucleon Iron Particles (LBL Bevalac)

DOSES

50, 100, 500 Rads

DOSE RATE

100 Rads/min

TIMES AFTER IRRADIATION

3 Days, 8 Days, 14 Days, & 6 Months

General Methods

Five behavioral and three neurochemical endpoints were assessed in these experiments (Table 1). These endpoints were chosen because of their sensitivity to other qualities of radiation. The behavioral endpoints include the conditioned taste aversion (CTA), an index of nausea and vomiting, and several motor tasks, measures of muscle tone, stamina, coordination, and upper body strength. The neurochemical endpoints include the movement of sodium ions through channels, a basic neuronal process; dopamine release, a regulator of motor activity; and catecholamine levels and turnover, a rough estimate of brain damage and the rate of information transfer in the brain.

Male Sprague-Dawley Crl:CD(SD)BR rats (Charles River Breeding Laboratories, Kingston, NY) weighing 200-300 g were used in these experiments. Rats were quarantined on arrival and screened for evidence of disease by serology and histopathology before being released from quarantine. The rats were housed individually in polycarbonate isolator cages (Lab Products, Maywood, NJ) on autoclaved hardwood contact bedding ('Beta Chip' Northeastern Products Corp., Warrensburg, NY) and were provided commercial rodent chow ('Wayne Rodent Blok' Continental Grain Co., Chicago IL) and acidified water (pH 2.5 using HCl) ad libitum. Animal holding rooms were kept at 21 $\pm$ 1$^{o}$ C with 50 $\pm$ 10% relative humidity on a 12-hr light:dark lighting cycle with no twilight.

The rats were irradiated with high-energy $^{56}$Fe particles (600 MeV) in the Bevalac at the LBL. The animals were irradiated in well-ventilated Plexiglas holders with one of three doses, including 50, 100, and 500 rads, at a dose-rate of 40-140 rad/min. Dosimetric support was provided by personnel at the Bevalac. Animals irradiated with other radiation sources were exposed to a single dose of 50, 100, or 500 rads of gamma photons from a $^{60}$Co source at a rate of 40 rads/min or high-energy electrons (18.6 MeV) from a linear accelerator. Radiation dosimetry was performed using paired 50-ml ion chambers. Delivered dose was expressed as a ratio of the dose measured in a tissue-equivalent plastic phantom enclosed in a restraining tube, to that measured free in air.

General Observations after $^{56}$Fe Irradiation

Although not a specific part of the experimental design, any unusual

reactions by the animals were noted. Based on subjective observations, the animals appeared normal after irradiation with $^{56}Fe$ particles. However, after exposure to 500 rads, several changes were observed. The exposed rats progressively lost weight, totaling about 20% of body weight over a 14-day period. In addition, they experienced a reduction in muscle tone, a hind limb tremor, and hypothermia (animals cool to the touch) 3 days after irradiation, effects that had disappeared by 8 days after irradiation.

## CONDITIONED TASTE AVERSION LEARNING AFTER IRRADIATION

### Characteristics of the Conditioned Taste Aversion

Animals have developed over the course of evolution mechanisms to help prevent accidental poisoning, the best-known one being the emetic response. Emesis can occur as a result of consuming presumably tainted food that is then expelled from the stomach. In addition to emesis, animals are also capable of avoiding potentially toxic substances after a single ingestion of quantities less toxic than those required to induce vomiting. This is done through a process called the conditioned taste aversion (CTA). A CTA develops when the animal associates the taste of novel tasting food with a physiological response, possibly illness, and then subsequently avoids further ingestion of that food. In a laboratory setting, a CTA is typically induced by pairing a normally preferred but novel tasting fluid with exposure to a toxin. The animal will then avoid drinking the fluid when presented again.

The conditioned taste aversion (CTA) paradigm in the rat can be used as a model system to study the mechanisms by which exposure to non-lethal levels of ionizing radiation can produce changes in the behavior of an organism (Rabin and Hunt, 1986). Because the functional effects of emesis and taste aversion learning are similar, in the sense that they limit the intake and/or absorption of toxic substances, a number of investigators have argued that the CTA paradigm represents a model system for the study of radiation-induced nausea and emesis (Garcia et al., 1985; Rabin and Hunt, 1986). Therefore, the CTA provides an index of the probability that nausea and emesis will occur.

The CTA paradigm offers a number of advantages over emesis models. The paradigm can be used with rats, inexpensive and easily used animals. They are small enough that more uniform fields of radiation can be obtained with particle accelerators than with larger animals. Because a CTA can be easily induced in a relative large number of animals, a great deal of information can be accumulated quickly as well as the characterization of any responses. Since the mechanisms underlying the CTA and emesis appear to be similar, this approach will allow for the formulation of more specific hypotheses that could be applied eventually to emesis models.

The CTA induced by ionizing radiation has been extensively studied and a clearer idea of how it develops has been emerging. The most important discovery is the involvement of a specific nucleus in the brain stem, the area postrema. The area postrema has been demonstrated to play an critical role in the development of CTAs induced by a broad range of unrelated toxins. This part of the brain is sufficiently important that if the area postrema is lesioned, the development of a CTA is blocked. These toxins include not only ionizing radiation (Ossenkopp, 1983; Rabin et al., 1983), but also lithium chloride (Ritter et al., 1980; Rabin et al., 1983), copper sulfate (Rabin et al., 1985), aluminum chloride (Rabin and Hunt, unpublished observation), paraquat (Dey et al., 1987), angiotensin II (Rabin et al., 1986), amphetamine (Rabin et al., 1987), WR-2721 (Rabin et al., 1986), and cisplatin (Rabin and Hunt, unpublished observation). In addition, other evidence indicates that the area postrema is also required for the development of emesis (Wang et al. 1958; Brizzee, 1970; Harding et al., 1985; Rabin et al., 1986). Not all toxic drugs induce CTAs through the area postrema. For example, ethanol- and morphine-induced CTAs are not blocked by lesions of the area postrema (Hunt et al., 1987; Rabin and Hunt, unpublished observation).

Since many unrelated toxins induce CTAs through the area postrema, it has been suggested that a common mechanism may underlie all these effects (Rabin and Hunt, 1986). Also, since toxins are generally foreign substances, specific receptors for each possible toxin are not likely to have evolved. Consequently, an intermediary mechanism in the induction of CTAs and emesis involving one or more secondary mediators has been postulated (Hunt et al., 1965; Rabin and Hunt, 1986). If these mediators interact with receptors in the area postrema, they may then activate the neural circuits that evoke CTAs.

Induction of a CTA after Exposure to $^{56}Fe$ Particles

Research was initiated to determine whether high-energy iron particles could induce a CTA similar to other qualities of ionizing radiation, such as gamma photons. The first experiments were designed to find the doses of $^{56}Fe$ particles that would induce a CTA and compare the sensitivity of the animals to those irradiated with gamma photons or high-energy electrons.

Conditioned taste aversions were produced by first placing the rats on a 23.5-hr water deprivation schedule for 5 days during which water was available for only 30 min daily during the early light phase of the diurnal cycle. On the conditioning day (day 6), the rats were presented with a solution of 10% sucrose, after which the intake of the fluid was recorded. Immediately following the drinking period, rats were irradiated with the doses stated above. On the following day (test day), 10% sucrose was presented again and the consumption during a 30-min period was recorded. A CTA existed when the amount of fluid consumed on the test day was significantly less than that consumed on the conditioning day.

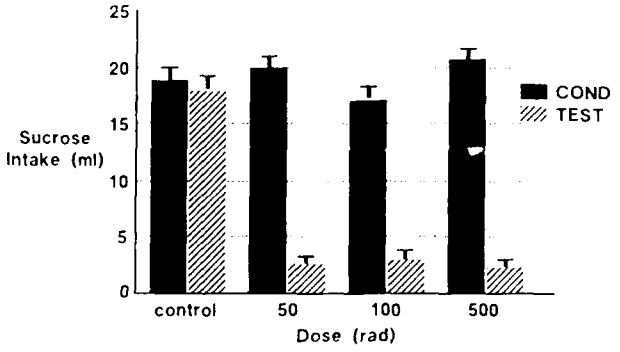


Fig. 1. Conditioned taste aversions after different doses of $^{56}Fe$ ions. Sucrose intake was significantly reduced after all doses studied. The maximum effect of the radiation is presumed to be < 50 rads.

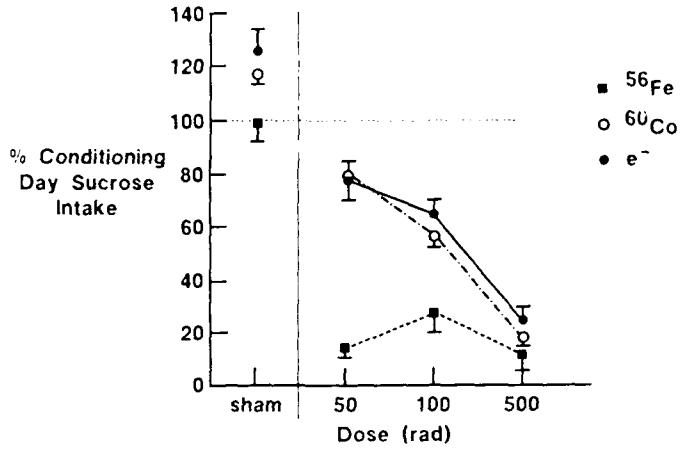


Fig. 2. Conditioned taste aversions after different doses of $^{56}Fe$ ions, gamma photons ($^{60}Co$), and high-energy electrons (LINAC). $^{56}Fe$ ions were at least 10 times more effective in inducing a CTA than do gamma photons or electrons.

Exposure to all doses of high-energy $^{56}Fe$ particles tested resulted in significant dose-dependent reductions in sucrose intake, indicating the development of a CTA. In fact, maximum reductions were found after all 3 doses of radiation (Fig. 1). For comparison, when rats were exposed to these same doses of gamma photons or high-energy electrons, dose-dependent decreases in sucrose intake were observed, indicating the development of a CTA (Fig. 2). However, $^{56}Fe$ particles were considerably more effective than the other two qualities of radiation. A maximal CTA was observed only after exposure to 500 rads of photons or electrons. A further characterization of the dose-response effects of $^{56}Fe$ particles compared to other qualities of radiation is currently in progress.

## CEREBRAL SODIUM CHANNELS AFTER IRRADIATION

### Characteristics of Sodium Channels in the Brain

The generation and propagation of electrical impulses or action potentials in neurons is initiated by the rapid inward flow of sodium ions across the

neuronal plasma membrane (Hodgkin and Huxley, 1952). In the resting state a neuron maintains a resting membrane potential that results from the unequal distribution of sodium, potassium, and chloride ions across the membrane (Koester, 1981a,b). When neurons are electrically excited, sodium ions flow inward on their concentration gradient until the membrane potential is reversed (Koester, 1981c). The movement of potassium ions out of the neuron proceeds until the neuron has repolarized and the neuron is again in the resting state.

Sodium ions enter the neuron through pores in the membrane called channels. These channels are specific to sodium and traverse the neuronal plasma membrane. They are glycoproteins containing multiple subunits (Catterall, 1982) and have an absolute requirement for lipids for normal functioning (Tamkin et al., 1984). At least three functional sites within sodium channels have been identified based on the actions of specific neurotoxins (Catterall, 1980). Site I, located on the external surface of the neuronal membrane, binds tetrodotoxin and saxitoxin, drugs that block the generation of action potentials. Site II, located in the lipid core of the membrane, binds batrachotoxin and veratridine, lipid-soluble drugs that activate sodium channels. And site III, located on the membrane surface but with projections down to site II, binds scorpion and sea anemone toxins that enhance the actions of toxins on site II but have no intrinsic activity of their own. Neurochemically, the functioning of the sodium channel can be studied with a synaptosomal (pinch-off nerve endings) preparation (Krueger and Blaustein, 1980; Tamkin and Catterall, 1981). The rate of uptake of $^{22}Na$ can be measured after exposure to the neurotoxins batrachotoxin or veratridine, thereby assessing what would occur under normal physiological conditions.

Sodium Channel Function after Exposure to $^{56}Fe$ Particles

The rate of $^{22}Na$ uptake was determined in synaptosomes from the cerebral cortex as detailed previously (Mullin et al., 1986). A crude mitochondrial preparation containing synaptosomes was prepared from a cortical homogenate. The final pellet was resuspended in ice-cold incubation buffer (8-10 ml/brain) containing 5.4 mM KCl, 0.8 mM $MgSO_4$, 5.5 mM glucose, 130 mM choline chloride, and 50 mM N-2-hydroxyethyl-piperazine-N'-2-ethanesulfonic acid (HEPES), with the pH adjusted to 7.4 with Tris base. The uptake of $^{22}Na$ was measured as follows. Aliquots (50 $\mu$l) of the synaptosomal suspension were incubated for 2 min at 36$^{o}$ C. The neurotoxin

veratridine was then added, and the incubation was continued for an additional 10 min. The samples were then diluted with 300 $\mu$l of uptake solution containing 5.4 mM KCl, 0.8 mM $MgSO_4$, 5.5 mM glucose, 128 mM choline chloride, 5 mM ouabain, 2 mM NaCl, 1.3 $\mu$Ci $^{22}Na$, 100 $\mu$M veratridine, and 50 mM HEPES (pH adjusted to 7.4 with Tris). After a 5-sec incubation, uptake was terminated by adding 3 ml of ice-cold wash solution containing 163 mM choline chloride, 0.8 mM $MgSO_4$, 1.7 mM $CaCl_2$, 1 mg/ml of bovine serum albumin, and 5 mM HEPES (pH adjusted to 7.4 with Tris). The mixture was rapidly filtered under vacuum through a cellulose filter with 0.45-$\mu$m pores, and the filters were washed twice with 3 ml of wash solution. Radioactivity was determined by liquid scintillation spectrophotometry. The data were expressed as specific uptake determined by subtracting nonspecific uptake (samples containing 1 $\mu$M tetrodotoxin) from total uptake.

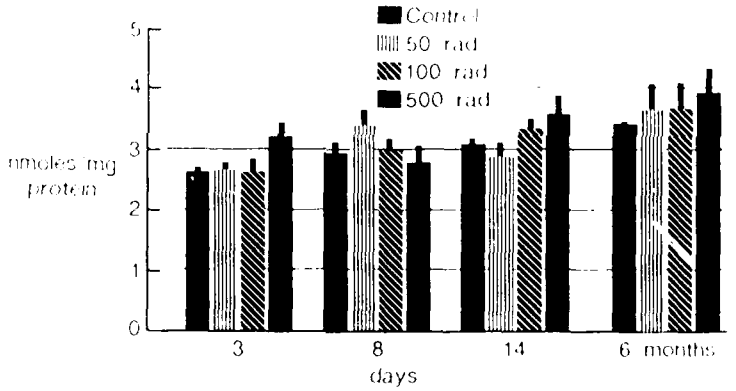


Fig. 3. $^{22}Na$ uptake after different doses of $^{56}Fe$ particles and different intervals after irradiation. No significant differences were observed under any of the experimental conditions studied.

Rats were irradiated with $^{56}Fe$ particles in the manner described above. Measurements of veratridine-stimulated sodium uptake in synaptosomes did not reveal any consistent and statistically significant changes after exposure of any of the four doses of radiation nor at any of the three intervals after irradiation (Fig. 3).

## GENERAL DISCUSSION OF RESULTS

The experiments completed to date demonstrate that $^{56}Fe$ particles can induce a CTA that may represent a state of illness, possibly nausea. These results along with those presented by Joseph et al. (1988) suggest that the behavioral effects of exposure to $^{56}Fe$ particles may be at least 10 times greater than those observed following exposure to gamma photons or high-energy electrons. They also may reflect a greater chance for the occurrence of nausea and emesis in astronauts exposed to a space radiation environment during longer term missions.

The successful completion of missions in space depends in part on behavioral and neural integrity of the astronauts. Given the potential significance of the data presented, it is important to seriously pursue an active program of research into the possible behavioral and neural deficits that might occur in space as a result of exposure to radiation. By combining sensitive behavioral assessments that can measure cognitive or motor performance with neurochemical analyses following HZE irradiation (e.g. Joseph et al., 1988), more information can be obtained concerning important behavioral and biological relationships that will aid in predicting and controlling possible performance deficits during manned space flight.

## ACKNOWLEDGEMENTS

The authors wish to acknowledge the assistance of Drs. E. John Ainsworth, Patricia Durbin, and Bernhard Ludewigt and the staff at the Lawrence Berkeley Laboratory without whose help these studies could not have been undertaken. This research was supported by the Armed Forces Radiobiology Research Institute, Defense Nuclear Agency, under work units B4098, B4123, and B4157. Views presented in this paper are those of the authors; no endorsement by the Defense Nuclear Agency has been given or should be inferred. Research was conducted according to the principles enunciated in the 'Guide for the Care and Use of Laboratory Animal Resources, National Research Council.'

## REFERENCES

Brizzee, K. R., 1970, Effect of localized brain stem lesions and supradiaphragmatic vagotomy on X-irradiation emesis in the monkey, Am. J. Physiol. 187:567.

Catterall, W. A., 1980, Neurotoxins that act on voltage-sensitive sodium channels in excitable membranes, Annu. Rev. Pharmacol. Toxicol. 20:15.

Catterall, W. A., 1982, The emerging molecular view of the sodium channel, Trends Neurosci. 5: 303.

Dey, M. S., Krueger, R. I., and Ritter, R. C., 1987, Paraquat-induced, dose-dependent conditioned taste aversions and weight loss mediated by the area postrema, Toxicol. Appl. Pharmacol., 87:212.

Garcia, J., Lasiter, P. S., Bermudez-Ratoni, F., and Deems, D. A., 1985, A general theory of taste aversion learning. Ann. NY Acad. Sci. 443:8.

Harding, R. K., Hugenholz, H., Keany, M., and Kucharczyk, J., 1985, Discrete lesions of the area postrema abolish radiation-induced emesis in the dog, Neurosci. Lett. 53:95.

Hodgkin, A. L. and Huxley, A. F., 1952, A quantitative description of membrane current and its application to conduction and excitation in nerve. J. Physiol. (London) 117:500.

Hunt, E. L., Carroll, H. W., and Kimeldorf, D. J., 1965, Humoral mediation of radiation-induced motivation in parabiont rats, Science, 150:1747.

Hunt, W. A., Rabin, B. M., and Lee, J., 1987, Ethanol-induced taste aversions: Lack of involvement of acetaldehyde and the area postrema. Alcohol 4:169.

Joseph, J. A., Hunt, W. A., Rabin, B. M., and Dalton T. K., 1988, Correlative motor behavioral and striatal dopaminergic alterations induced by $^{56}Fe$, in: 'Terrestrial Space Radiation and its Biological Effects', P. D. McCormack, C. E. Swenberg, and H. Bücker, eds., Plenum Press, New York.

Koester, J., 1981a, Resting membrane potential, in: 'Principles of Neural Science,' E. R. Kandel and J. H. Schwartz, eds., Elsevier/North Holland.

Koester, J., 1981b, Passive electrical properties of the neuron, in: 'Principles of Neural Science,' E. R. Kandel and J. H. Schwartz, eds., Elsevier/North Holland.

Koester, J., 1981c, Active conductances underlying the action potential, in: 'Principles of Neural Science,' E. R. Kandel and J. H. Schwartz, eds., Elsevier/North Holland.

Krueger, B. K., 1980, Sodium channels in presynaptic nerve terminals: Regulation by neurotoxins. J. Gen. Physiol. 76:287.

Mickley, G. A., Bogo, V., Landauer, M. R., and Mele, P. C., 1988, Current behavioral radiobiology research at the Armed Forces Radiobiology Research Institute. 'Terrestrial Space Radiation and its Biological Effects', P. D. McCormack, C. E. Swenberg, and H. Bücker, eds., Plenum Press, New York.

Mullin, M. J., Hunt, W. A., and Harris, R. A., 1986, Ionizing radiation alter the properties of sodium channels in rat brain synaptosomes. J. Neurochem. 47:489.

Ossenkopp, K. -P, 1983, Taste aversion conditioned with gamma radiation: Attenuation by area postrema lesions in rats. Behav. Brain Res. 7:295.

Rabin, B. M., and Hunt, W. A., 1986, Mechanisms of radiation-induced conditioned taste aversion learning. Neurosci. Biobehav. Rev. 10:55.

Rabin, B. M., Hunt, W. A., and Lee, J., 1983, Attenuation of radiation- and drug-induced conditioned taste aversions following area postrema lesions in the rat. Radiat. Res. 93:388.

Rabin, B. M., Hunt, W. A., and Lee, J., 1985, Intragastric copper sulfate produces a more reliable conditioned taste aversion in vagotomized rats than in intact rats. Behav. Neural Biol. 44:364.

Rabin, B. M., Hunt, W. A., Bakarich, A. C., Chedester, A. L., and Lee, J., 1986, Angiotensin II - Induced taste aversion learning in cats and rats and the role of the area postrema. Physiol. Behav. 36:1173.

Rabin, B. M., Hunt, W. A., and Lee, J., 1986, Effects of area postrema lesions on the behavioral toxicity of WR-2721 in the rat. Neurobehav. Toxicol. Teratol. 8:83.

Rabin, B. M., Hunt, W. A., Chedester, A. L., and Lee, J., 1986, Role of *the area postrema in* radiation-induced taste aversion learning and emesis in cats. Physiol. Behav. 37:815.

Rabin, B. M., Hunt, W. A., and Lee, J., 1987, Interactio ıs between radiation and amphetamine in taste aversion learning and the role of the area postrema in amphetamine-induced conditioned taste aversions. Pharmacol. Biochem. Behav. 27:677.

Ritter, S., McGlone, J. L. and Kelly, K. W., 1980, Absence of lithium-induced taste aversion after area postrema lesion. Brain Res. 201:501.

Tamkin, M. M. and Catterall, W. A., 1981, Ion flux studies of voltage-sensitive sodium channels in synaptic nerve endings. Mol. Pharmacol. 19:78.

Tamkin, M. M., Talvenheimo, J. A., and Catterall, W. A., The sodium channel from rat brain: Reconstitution of neurotoxin-activated ion flux and scorpion toxin binding from purified components. J. Biol. Chem. 259:1676.

Wang, S. C., Renzi, A. A., and Chinn, H. I., 1958, Mechanisms of emesis following X-irradiation, Am. J. Physiol. 193:335.

From: TERRESTRIAL SPACE RADIATION AND ITS BIOLOGICAL EFFECTS
Edited by Percival D. McCormack, Charles E. Swenberg,
and Horst Bücker
(Plenum Publishing Corporation, 1988)

# CORRELATIVE MOTOR BEHAVIORAL AND STRIATAL DOPAMINERGIC ALTERATIONS INDUCED BY $^{56}Fe$ RADIATION

J. A. Joseph, W. A. Hunt, B. M. Rabin, and T. K. Dalton

Department of Behavioral Sciences
Armed Forces Radiobiology Research Institute
Bethesda, MD 20814-5145

## INTRODUCTION

In recent years there has been increased interest in the study of mammalian organismic responses to heavy charged particles (HZE's). This interest has been generated from a variety of areas including space radiobiology (Grahn, 1973) and radiotherapy (Castro et al., 1985). While a great deal of information has been generated that is concerned with the mechanisms of HZE damage and repair (Curtis, 1986; Tobias, 1985) or the early and late effects of HZE damage (Ainsworth, in press), there have been few attempts to investigate the effects of these particles on any motor behavioral parameters. The potential for HZE's to alter behavioral performance becomes increasingly important when one considers that future space travelers, especially those who will be on long space voyages, or those who may be carrying out tasks outside the shelter of a space vehicle, may be exposed to HZE's that can create microscopic lesions in virtually all organs of the body (see Todd, 1983 for review). The questions as to whether or not such exposure results in performance deficits and the possible relationship of these deficits to the structural specificity of damage to the brain have not been addressed very extensively. There are indications, however, from at least one experiment (Philpott et al., 1985) that mice given brief exposure to low doses of $^{40}Ar$ particles showed time-dependent reductions in performance on a wire suspension task. Moreover, if one can extrapolate from studies in which organisms have been exposed to other

sources of radiation and behavioral performance examined, it might be postulated that decrements in such indices as motor behavior are a distinct possibility.

Several previous studies have indicated declines in motor performance of irradiated animals placed in tasks for which the organism is required to display physical strength, endurance, and coordination. For example, studies in irradiated lower animals assessing performance on psychomotor tasks have shown dose-dependent deficits (e.g., equilibrium platform, Barnes, 1966, 1968; accelerod, Bogo, 1984; activity wheel, Franz, 1985). These studies generally have utilized a variety of radiation sources ranging from mixed neutron-$\gamma$ (e.g., Franz, 1985) to high energy electrons (Bogo, 1984). The precise central locus of these deficits is still in question. There is, however, a great deal of evidence from non-irradiated organisms to suggest that the nigrostriatal system may be very important in mediating these types of motor behaviors.

It is becoming increasingly clear that the telencephalic end terminus of this system, i.e., the striatum, is one of the basic central processing areas involved in the mediation of motor behavior. This structure appears to control a wide variety of motor responses ranging from the simple (balance and coordination, see Steg and Johnels, 1979 for review) to the complex (e.g., the ordering and sequencing of intricate behavioral patterns directed by exteroceptive stimuli, Cools et al., 1984; Vrijmoed-de Vries & Cools, 1986). Since it can be postulated that control of such complicated patterns of behavior depends upon intrastriatal coordination of a host of neurotransmitters and neuromodulators, it would follow that if any of these interactions are altered as a result of heavy particle bombardment in a space environment, decrements in motor function may result.

Of the many intrastriatal neurotransmitter systems that may be involved in mediating these types of behaviors, two of the more important are the dopamine (DA) and acetylcholine (ACh) systems. It is believed that these neurochemicals exert part of their control through reciprocal inhibition. Any radiation-induced morphological or pharmacological alterations in their function may be translated into decreased reciprocal inhibitory control (RIC).

One area where this control becomes especially salient is concerned with the cholinergic regulation of striatal DA autoreceptors. Striatal DA autoreceptors are inhibitory, control DA release (Cebeddu and Hoffmann, 1982; 1983; Cohen and Berkowitz, 1976; Dubocovich and Weiner, 1981; Kelly, 1981; Plotsky et al., 1977; Westfall, et al., 1976) and may be of the $D_2$ subtype (Dreschin and Zahniser, 1986). If they are stimulated via DA agonists (e.g., apomorphine) or inhibited with DA antagonists (e.g., haloperidol), $K^+$-evoked release of DA will be respectively inhibited or enhanced. These receptors are in turn controlled by a group of inhibitory muscarinic heteroreceptors (Lehmann and Langer, 1982; Raiteri et al., 1982; 1984). Muscarinic agonists can activate the heteroreceptors, which inhibit the DA autoreceptors, and potentiate the $K^+$-evoked release of DA from the striatum (Lehmann and Langer, 1982; Plotsky et al., 1977; Raiteri et al., 1982).

In the present study, it became of interest to determine if there could be a radiation-induced reduction of autoreceptor function that could be related to the deficits in motor behavior that have been observed in irradiated animals. The present experiment was directed toward making these observations by examining motor behavioral performance in rats exposed to HZE's and relating the degree of alteration of such performance to any observed deficits in muscarinic enhancement of the $K^+$-evoked release of DA from superfused striatal slices.

## METHODS

### Animals

Male Sprague-Dawley Crl:CD(SD)BR rats (N = 180, Charles River Breeding Laboratories, Kingston, NY) weighing 200-300 g were used in these experiments. The rats were housed at the vivarium at the Lawrence Berkeley Laboratories, Berkeley, CA. The rats were maintained in polycarbonate cages which contained autoclaved hardwood contact bedding ("Beta Chip" Northeastern Products Corp., Warrensburg, NY). They were given food and water ad libitum. The animal holding rooms were kept at 21 $\pm$ 1° C with 50 $\pm$ 10% humidity.

## Procedure

### A. Radiation

The animals were divided into two groups (irradiated and control). The irradiated group was further subdivided into three groups and irradiated with one of three doses (0.5 Gy, 1.0 Gy, and 5.0 Gy) of 600 MeV $^{56}Fe$ delivered at maximum dose rate by the Bevalac at the Lawrence Berkeley Laboratory. Control animals were given sham exposure by being placed into a well-ventilated plastic restrainer for an equivalent length of time as that for the irradiated animals. Only one dose was administered on a particular day; so, the three doses were administered over three days. Behavioral and biochemical changes were then examined at 3, 8, and 14 days post-exposure or sham exposure in subsets of these animals (N = 10 control and 10 experimental animals at each time). Because of limitations imposed by other in vitro biochemical tests (not discussed here), one-half of each group was tested in the a.m. and the other half in the p.m.

### B. Behavior

The animals were tested on a battery of four motor tests:

1-2. Rod walking -- The ability of the rats to balance on stationary horizontal rods of two diameters: 12 mm (narrow rod) and wide 25 mm (wide rod) suspended 6.0 cm above a table was assessed. Each rat was given one trial and could achieve a maximum score of 60 sec (wide rod) or 120 sec (narrow rod). Animals were placed in the center of the rod and parallel to it. The time in seconds that the animal remained on the bar was recorded with a stopwatch. When the animal fell off the trial ended.

3. Wire suspension -- The prehensile reflex refers to an animal's ability to grasp a horizontal wire with its forepaws and to remain suspended. It is presumed to be a measure of muscle strength. In this test, individual rats were raised to an elevated hanging wire 8 cm above the table top and given one trial each, with total hanging time (in sec) recorded.

4. Inclined screen -- This test is purported to measure muscle tone and stamina. Each subject was placed in one of 5 separate compartments of a wire mesh screen inclined at a $60^{o}$ angle. The screen was suspended 60 cm above the table surface and the maximum time allowed on the screen was 1800 sec.

C. Muscarinic Control of Dopamine Release

Following the behavioral tests the animals were killed by decapitation, the brains quickly removed, and the striata dissected on ice. Slices (300 mμ) were prepared using a McIlwain tissue chopper. Striatal slices from each animal were placed into small glass vials containing a modified Krebs-Ringer basal release medium that had been bubbled for 30 minutes with 95% $O_2$/5% $CO_2$ and contained (in mM) $NaHCO_3$ 21, glucose 3.4, $NaH_2PO_4$ 1.3, EGTA 1, $MgCl_2$ 0.93, NaCl 127, and KCl 2.5 (pH 7.4). The slices were washed twice in this medium and aliquots placed into two chambers of a superfusion apparatus containing 16 parallel chambers. Since the apparatus only contained 16 chambers, only striata from 8 animals could be accommodated. Therefore, striata were examined from all of the experimental animals (5) and three of the five control animals (randomly selected) for each run. The tissue and buffer media were maintained at 37° C throughout the course of the experiment. Following placement into the superfusion chambers, the tissue was allowed to equilibrate for 30 minutes. It was continuously perfused with the oxygenated basal release medium at the rate of 124 μl/min. After the equilibration period, a 5 min baseline fraction was collected on ice and the medium was then switched to one containing (in mM) KCl 30, $CaCl_2$ 1.26 and NaCl 57 as well as the other components described above (pH 7.4) in the presence or absence of 500 μM oxotremorine. Following the switch, 5 min fractions continued to be collected on ice for 30 minutes.

The fractions were collected into tubes containing 0.3 ml of cold 0.4 N perchloric acid, 0.05% sodium metabisulfite, and 0.1% EDTA. These samples were then stored at -80° C until later analysis for DA via high performance liquid chromatography (HPLC) coupled to electrochemical detection.

The HPLC consisted of a Varian model 5000 ternary chromatograph, a Varian 401 data system, a Varian model 8055 autosampler, and a Valco air actuated injector with a 50 μl loop. The effluent was monitored with a bioanalytical systems LC-4B amperometric detector using a glassy carbon electrode. The detector potential was set at 0.72 V as a $Ag/AgCl_2$ reference electrode with a sensitivity of 10 nA/V. The mobile phase consisted of a filtered, degassed 100 mM $KH_2PO_4$ buffer containing 3 mM 1-heptanesulfonic acid, 100 μM EDTA, and 8% (V/V) acetonitrile (pH 3.6). The components were eluted off a Waters 10 μm particle, μBondapak $C_{18}$ reverse-phase

column (30 x 0.39 cm; flow rate = 1 ml/min) maintained at 30° C. Results were calculated relative to known previous standards that were analyzed on the HPLC under similar conditions. Data were expressed as pmoles/mg protein as analyzed by the Lowry procedure (1951).

Data Analysis

Data from the behavioral experiments were analyzed by using 4 (0, 0.5, 1.0, 5.0 Gy) by 3 (day) analyses of variance. Data from the perfusion experiments were analyzed by first computing difference scores by subtracting the pmoles of DA released to 0 $\mu$M oxotremorine from that released to 500 $\mu$M for each fraction and for each "striatal-channel" pair. These difference scores were then analyzed by 2 (control vs radiation) by 3 (day) by 7 (fractions) repeated measures (on the last factor) analyses of variance (one analysis for each radiation dose level). In addition, correlational analyses were carried out by correlating the peak DA release difference with the number of seconds that a particular animal remained suspended on the wire. The wire suspension task was used, since preliminary data analysis indicated that there were no significant radiation-induced deficits on the other behavioral tasks.

## RESULTS

### Behavior

The results of the wire suspension task are illustrated in Fig. 1. As can be seen from this figure, exposure to $^{56}Fe$ particles induced deficits in this task, and irradiated animals remained suspended on the wire for a shorter time than controls ($F\ (3/142) = 26.09\ p < 0.001$). There were, however, some differences in performance among the various radiation-treated groups especially at three days post-irradiation, where the animals that received 5 Gy did not show any deficits in performance on this task (Duncan's post test comparisons, 5 Gy vs control $p > 0.05$, 5 Gy vs 1 Gy $p < 0.01$, 5 Gy vs 0.5 Gy $p < 0.005$ df=11). At later time points (8 and 14 days), there were no differences among the radiation-treated groups (all comparisons $p > 0.05$), and all differed from controls (Fig. 1).

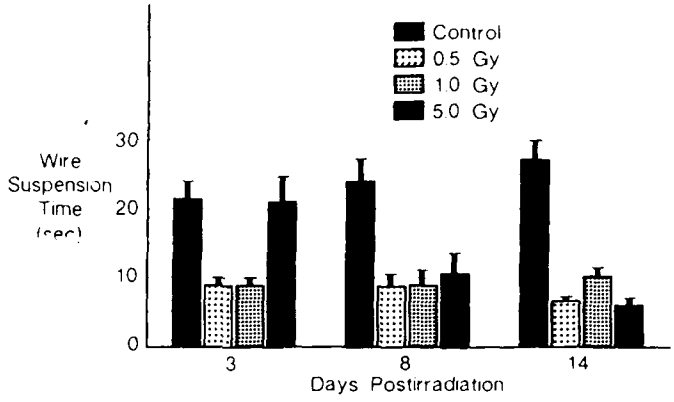


Fig. 1. Total time (in sec) that animals given one of three radiation doses or sham irradiated could remain on a taut, plastic coated wire with their forepaws as a function of days post-irradiation.

Results from the other behavioral tests indicated that performance of the irradiated groups did not differ from the control group on the wide rod or the inclined screen. However, there was a tendency for a greater number of the irradiated animals to fall off the narrow rod before the 120 sec maximum, especially at the later post-irradiation times (e.g., 5 Gy vs control at 14 days post-irradiation, 6/10 and 6/6, respectively).

DA Release

Analysis of the $K^+$-evoked release of DA at the 0 $\mu$M oxotremorine concentration indicated that striata from the irradiated groups showed greater release than controls (0.5 Gy, $F(12,468) = 2.58$ $p < 0.0025$; 1.0 Gy, $F(12,462) = 4.37$ $p < 0.0001$; 5.0 Gy, $F(12,468) = 2.71$ $p < 0.01$) and subsequent post hoc t-tests indicated that this difference was especially salient at 3 days post-irradiation. At later time points it was variable (Fig. 2). However, even though DA release to 30 mM KCl without oxotremorine was higher in irradiated animals (Fig. 3), analysis of oxotremorine enhancement of $K^+$-evoked release of DA indicated that such enhancement was reduced in the irradiated groups (overall radiation vs control by fraction, 0.5 Gy $F(6,468) = 31.36$ $p < 0.0001$; 1 Gy $F(6,462) = 17.54$ $p < 0.0001$; 5 Gy $F(6,468) = 9.72$ $p < 0.0001$).

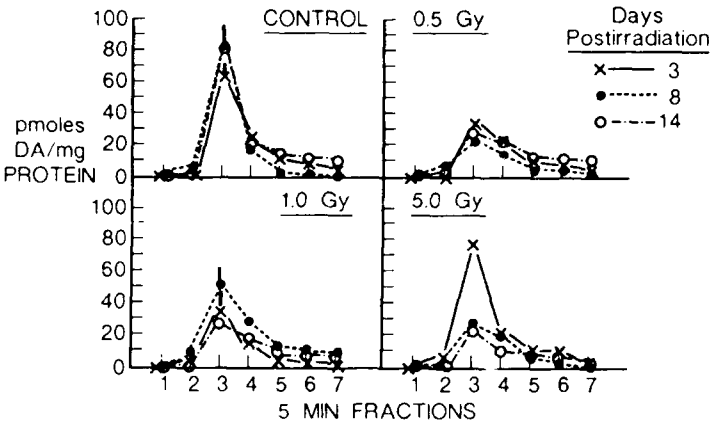


Fig. 2. Peak release of dopamine (DA) from superfused striatal tissue slices following stimulation by 30 mM KCl. Striata were obtained from Sprague-Dawley rats given one of three doses of $^{56}Fe$ or sham- irradiated and killed by decapitation at 3, 8, or 14 days post irradiation.

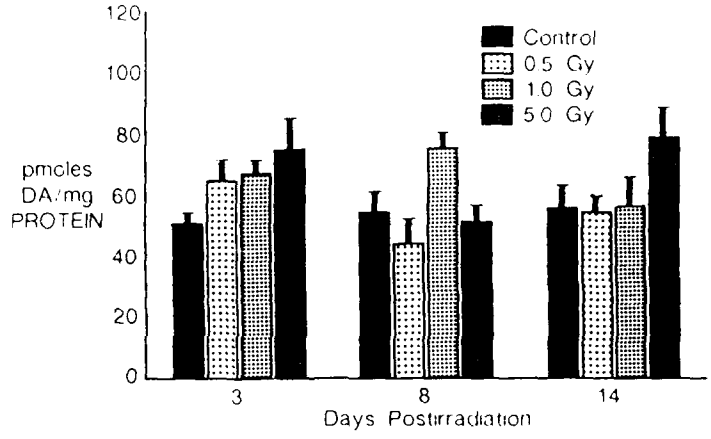


Fig. 3. DA release to 30 mM KCl superfused onto striatal slices as a function of days post-irradiation or sham-irradiation. (See Methods).

There was some indication, however, that the striata obtained from the group treated with 5 Gy initially (3 days) showed no reduction of enhancement of $K^+$-evoked release of DA. These deficits did not appear until the 8- and 14-day post-irradiation time points (radiation vs control by fraction by day $F(12,468) = 5.70$ $p< 0.0001$). In contrast to this group, attenuation appeared as early as 3 days in the other two radiation-treated groups, and response differences as a function of days were not observed ($F's < 1$, Fig. 2).

Interestingly, these response characterizations parallel the deficits observed with respect to wire suspension. This is more clearly seen by comparing Fig. 4 which shows the peak enhancement of $K^+$-evoked release of striatal DA with Fig. 1. It can be seen that the response profiles from both the biochemical and behavioral parameters are very similar. For example, the 5 Gy group showed neither behavioral deficits nor DA response reduction at 3 days post-irradiation, while at 8 and 14 days, deficits were observed in both response parameters. Subsequent correlational analysis indicated significant correlations between the time on the wire suspension task and degree of oxotremorine enhancement of $K^+$-evoked release of DA from the striatal slices (Fig. 5, 6, and 7) from the irradiated animals.

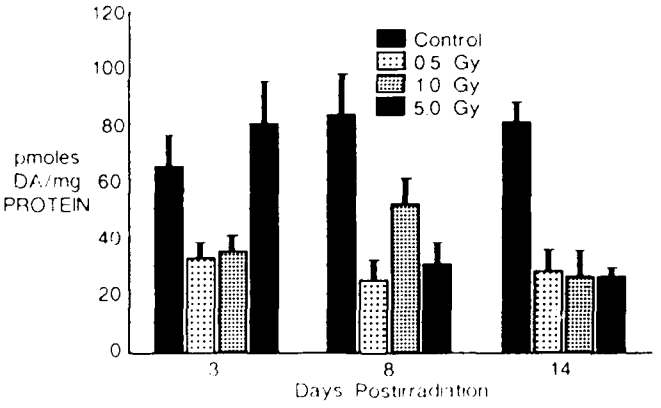


Fig. 4. Peak differences in DA release between 0 $\mu$M and 500 $\mu$M oxotremorine superfused onto striatal slices in the presence of 30 mM KCl as a function of days post-irradiation or sham-irradiation.

## DISCUSSION

The present results elucidate one possible mechanism by which motor deficits may occur following irradiation. It appears that there is an attenuation of muscarinic heteroreceptor responsivity in the striatum that is maximized in all groups within 8 days after exposure to $^{56}Fe$. This change is significantly correlated with at least one of the motor behaviors which assesses upper body muscle strength (i.e., wire suspension). There were also

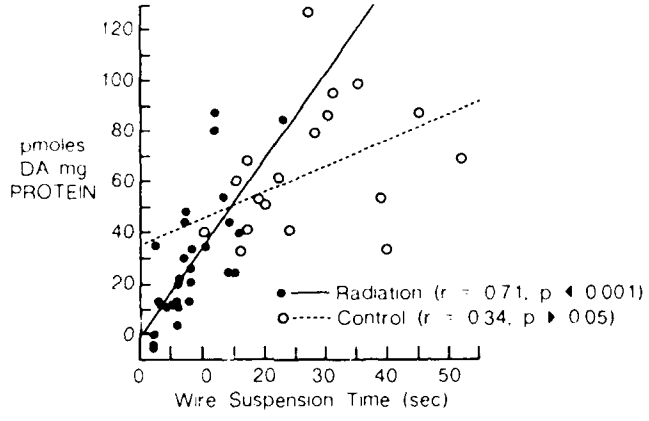


Fig. 5. Scatter plot of peak differences in DA release between 0 $\mu$m and 500 $\mu$M oxotremorine superfused onto striatal slices in the presence of 30 mM KCl for each animal as a function of its wire suspension time at the 0.5 Gy level.

deficits in the irradiated animal's ability to remain on the narrow rod which were greater as a function of the post-irradiation day on which they were tested. While the mechanism of these deficits is not clear, it has been hypothesized that these changes may be brought about by the destructive capabilities of free radicals generated by the irradiation (See below). If this is the case, then there should be other instances, perhaps in nonirradiated animals, in which damage from free radicals would produce similar kinds of effects.

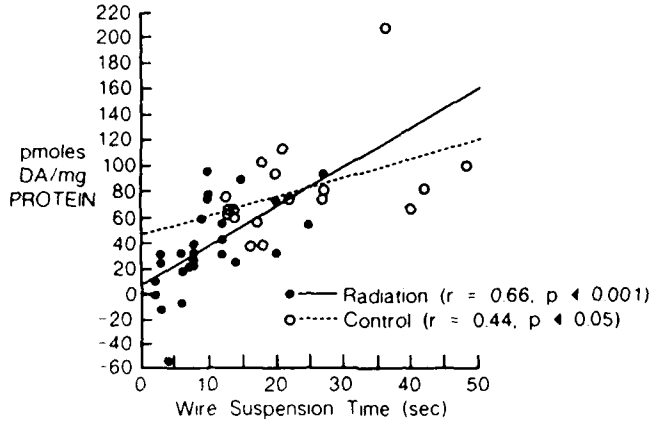


Fig. 6. Peak differences in DA release for each animal as a function of its wire suspension time at the 1.0 Gy level.

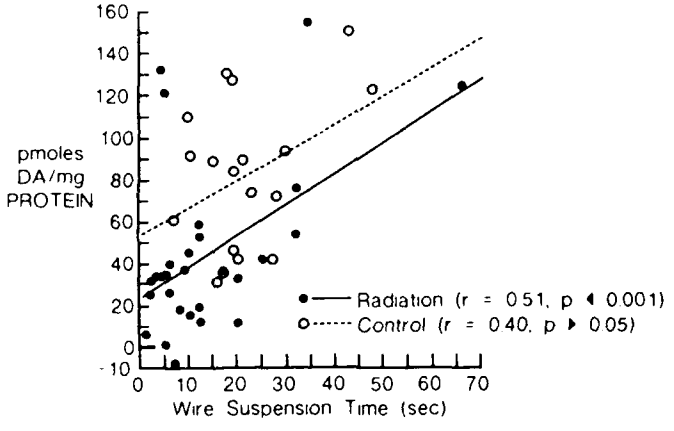


Fig 7. Peak differences in DA release for each animal as a function of its wire suspension time at the 5.0 Gy level.

One group of organisms where damage from free radicals seems to have taken its toll on central nervous function is made up by those that are senescent. It is believed that life-span effects of free radicals produced during the course of normal metabolism are believed to be responsible for the alterations in membrane structure and function seen in senescence (Schroeder, 1984). In the CNS, the transbilayer fluidity differences induced by peroxidation may be intimately involved in such factors as loss of neurotransmitter receptor function (Schroeder, 1981). In this regard, it is interesting to note that correlated striatal and motor behavioral deficits similar to these have been reported in the present study have been reported to occur as a function of aging. These experiments have indicated that there are age-related deficits in balance, strength, and coordination (for review, see Joseph et al., 1986) as assessed with some of the same tasks that were utilized in the present experiments. Moreover, these alterations occur in concert with specific striatal changes such as decreases in tyrosine hydroxylase activity (McGeer et al., 1977) and decreases in striatal $D_2$ (Joseph et al., 1978; Severson and Finch, 1980; Severson et al., 1982) and mACh (Morin and Wasterlain, 1980; Strong et al., 1984) receptor concentrations, as well as reduction of the muscarinic enhancement of the $K^+$-evoked release of DA (Joseph et al., in press).

While time-dependent assessments of the alterations in striatal $D_2$ and mACh receptor concentrations in animals irradiated with $^{56}Fe$ are presently being carried out, and we cannot say the parallel extends to these parameters, the present results provide, for the first time, strong evidence to suggest that there are radiation-induced alterations in the nigrostriatal system, an area that is one of the most sensitive to the ravages of time (Joseph et al., 1986), and that these changes can occur at relatively low radiation doses. A second area that appears to 'go gently into that good night and does not rage against the dying of the light' is the hippocampus. Numerous reports have indicated that this important 'working memory' control area is both structurally (e.g., Brizzee and Ordy, 1979) and functionally (Landfield, 1984) altered in senescence, and much like the striatum is affected by HZE's. In this case Philpott and his associates (1985) showed that morphological changes, which were assessed in mice at 6 and 12 months following exposure to 0.005 Gy or 0.5 Gy found that in the CA-1 area of the hippocampus, both the synaptic density and the synaptic spine length were lower in the irradiated animals relative to the controls.

These experiments provide further support for the 'age-radiation parallel' hypothesis which has been suggested in the literature for over 30 years (e.g., see Alexander, 1957; Upton, 1954). These early studies and later ones have suggested that radiation may have a life shortening effect (e.g., Ainsworth et al., 1976) and may bring about changes in biochemical (Upton, 1954; Adelman and Britton, 1975; Aiyar and De, 1978) and cellular (Ainsworth et al., 1976) parameters. Indeed, one study (De et al., 1983) has indicated that radiation exposure ($^{60}$Co source) resulted in enhanced accumulation of lipofuscin (the 'age pigment') in the brains, hearts, and intestines of the treated animals. Associated with these alterations were increases in lipoperoxidation in liver as well as increases in the activities of acid phosphatases and cathepsin in these same peripheral organs. All of these changes are associated with free radical damage, are similar to those which occur during aging, and are effectively prevented by dietary supplementation with the antioxidant BHT. In light of the 'free radical theory of aging' it is possible that changes induced by aging and those induced by radiation may share a common chemical/biochemical mechanism.

Thus, while there are numerous, parametric experiments concerned with dose, time, species, radiation source, etc., the results of earlier studies as well as the present one indicate that under the right conditions accumulating time in space can accelerate the aging process with some or all of its attendant motor and cognitive problems.

## ACKNOWLEDGMENTS

The authors wish to acknowledge the assistance of Drs. E. John Ainsworth, Patricia Durbin, and Bernhard Ludewigt and the staff at the Lawrence Berkeley Laboratory without whose help these studies could not have been undertaken. This work was supported by the Armed Forces Radiobiology Research Institute, Defense Nuclear Agency, under work unit B4166. Views presented in this paper are those of the authors; no endorsement by the Defense Nuclear Agency has been given or should be inferred. Research was conducted according to the principles enunciated in the 'Guide for the Care and Use of Laboratory Animals' prepared by the Institute of Laboratory Animal Resources National Research Council.

REFERENCES

Adelman, R. C. and Britton, G. W., 1975, The impaired capability for biochemical adaptation during aging, Bioscience 25:639.

Ainsworth, E. J., Fry, J. M., Brennan, P. C., Stearner, S. P., Rust, J. H., and Williamson, F. S., 1976, Life shortening, neoplasia and systematic injuries in mice after single or fractionated doses of neutron or gamma radiation. in: 'Biological and Environmental Effects of Low-Level Radiation Vol.' pp. 77-92 International Atomic Energy Agency, Vienna.

Ainsworth, E. J. Early and late mammalian responses to heavy charged particles, Adv. Space Res. In Press.

Alexander, P., 1957, Accelerated aging--a long term effect of exposure to ionizing radiations, Gerontologia 1:174.

Barnes, D. J., 1966, An initial investigation of the effects of pulsed ionizing radiation on the primate equilibrium function, Report No. TR-66-106. Brooks AFB, TX: United States Air Force School of Aerospace Medicine.

Barnes, D. J., 1968, Research with the primate equilibrium platform in a radiation environment. Report No. TR-68-81 Brooks AFB TX: United States Air Force School of Aerospace Medicine.

Bogo, V., 1984, Effect of bremsstrahlung and electron radiation on rat motor performance, Rad. Res. 100:313.

Brizzee, K. R. and Ordy, J. M., 1979, Age pigment, cell loss, and hippocampal function, Mech. Ageing and Dev. 9:143.

Castro, J. R. Chen, G. T. Y., and Blakely, E. A., 1985, Current considerations in heavy charged-particle radiotherapy: a clinical research trial of the University of California Lawrence Berkeley Laboratory, Northern California Oncology Group and Radiation Therapy Oncology Group, Rad. Res. 104:S-263.

Cohen, M. L. and Berkowitz, B. A., 1976, Vascular contraction: Effect of age and extracellular calcium, Blood Vessels 67:139.

Cools, A. R., Jaspers, R., Schwarz, M., Sontag, K. H., Vrijmoed-de Vries, M. and Van den Bercken, J., 1984, Basal ganglia and switching motor programs. in: 'Basal Ganglia, Structure and Function,'J. S. McKenzie, R. E. Kemm and L. N. Wilcock, eds., Plenum Press, pp. 513-544.

Cubeddu, L. X. and Hoffmann, I. S., 1982, Operational characteristics of the inhibitory feedback mechanism for regulation of dopamine release via presynaptic receptors, J. Pharmacol. Exp. Ther. 223:497.

Cubeddu, L. X. and Hoffmann, I. S., 1983, Frequency-dependent release of acetylcholine and dopamine from rabbit corpus striatum: Its modulation by dopaminergic receptors, J. Neurochem. 41:94.

Curtis, S. B., 1986, Lethal and potentially lethal lesions induced by radiation - a unified repair model, Rad. Res., 106:252.

De, A. K. and Aiyar, A. S., 1978, Alterations in tissue lipids of rats subjected to whole-body X-irradiation, Strahlentherapie 154:134.

De, A. K., Chipalkatti, S, and Aiyar, A. S., 1983, Effects of chronic irradiation on age-related biochemical changes in mice, Radiat. Res. 95:637.

Dubocovich, M. L. and Weiner, 1981, N. Modulation of the stimulation-evoked release of [$^3$H]-dopamine in the rabbit retina, J. Pharmacol. Exp. Ther. 219: 701.

Dwoskin, L. P. and Zahniser, N. R., 1986, Robust modulation of [$^3$H]-dopamine release from rat striatal slices by $D_2$ dopamine receptors, J. Pharmacol. Exp. Ther. 239:442.

Franz, C. G., 1985, Effects of mixed neutron-$\gamma$ total body irradiation on physical activity performance of Rhesus monkeys, Rad. Res. 101:434.

Grahn, D., 1973, HZE Particle effects in Manned Space Flight. National Academy of Science, Washington, DC.

Henry, J. M., Filburn, C. R., Joseph, J. A. and Roth, G. S., 1986, Effect of aging on striatal dopamine receptor subtypes in Wistar rats, Neurobiol. Aging, 7:357.

Joseph, J. A., Berger, R. E., Engel., B. T. and Roth, G. S., 1978, Age-related changes in the nigrostriatum: A behavioral and biochemical analysis, J. Gerontol. 33:643.

Joseph, J. A., Dalton, T. K. and Hunt, W. A. Age-related decrements in the muscarinic enhancement of $K^+$-evoked release of endogenous striatal dopamine: An indicator of altered cholinergic-dopaminergic reciprocal inhibitory control in senescence, Brain Res. in press.

Joseph, J. A., Roth, G. S., Lippa, A. and Antonian, L., 1986, Striatal dopamine receptor plasticity in senescence. in: 'Liver and Aging--Liver and Brain, 1986,' K. Kitani, ed., Elsevier/North Holland. pp. 141-159.

Kelly, M. J., 1981, An analysis of the effects of apomorphine and haloperidol on the release of [$^3$H]-dopamine and [$^3$H]-noradrenaline from rabbit brain slices, Arch. Int. Pharmacodyn. 250:18.

Landfield, P. W. and Pitler, T. A., 1984, Prolonged $Ca^{++}$-dependent afterhyperpolarizations in hippocampal neurons of aged rats, Science 276:1089.

Lehmann, J. and Langer, S. Z., 1982, Muscarinic receptors on dopamine terminals in the cat caudate nucleus: Neuromodulaton of [$^3$H]-dopamine release in vitro by endogenous acetylcholine, Brain Res. 248:61.

Lowry, O. H., Rosebrough, N. J., Farr, A. L. and Randall, R. J., 1951, Protein measurement with Folin phenol reagent, J. Biol. Chem. 193:265.

McGeer, P. L., McGeer, E. G., and Suzuki, J. S., 1977, Aging and extrapyramidal function, Arch. Neurol. 34:33.

Morin, A. M. and Wasterlain, C. G., 1980, Aging and rat brain muscarinic receptors as measured by quinuclidinyl benzilate binding, Neurochem. Res. 5:301.

Plotsky P. M., Wightman, R. M., Chey, W. and Adams, R. N., 1977, Liquid chromatographic analysis of endogenous catecholamine released from brain slices, Science, 197:904.

Philpott, D. E., Sapp, W., Miquel, J., Kato, K., Corbett, R., Stevenson, J., Black, S. Linseth, K. A., and Benton, E. V., 1985, The effect of high energy (HZE) particle radiation ($^{40}$Ar) on aging parameters of mouse hippocampus and retina, Scan. Elec. Micro., III 1177.

Raiteri, M., Marchi, M. and Maura, G., 1982, Presynaptic muscarinic receptors increase striatal dopamine release evoked by 'quasi-physiological' depolarization, Eur. J. Pharmacol. 83:127.

Raiteri, M., Riccardo, L., and Marchi, M., 1984, Heterogeneity of presynaptic muscarinic receptors regulating neurotransmitter release in the rat brain, J. Pharmacol. Exp. Ther. 228:209.

Schroeder, F., 1981, Use of a fluorescent sterol to probe the transbilayer distribution of sterols in biological membranes, FEBS Let. 135:127.

Schroeder, F., 1984, Role of membrane asymmetry in aging, Neurobiol. Aging 5:323.

Severson, J. A. and Finch, C. E., 1980, Reduced dopaminergic binding during aging in the rodent striatum, Brain Res. 192:147.

Severson, J. A. Marcusson, J., Winblad, B. and Finch, C. E., 1982, Age-related changes in dopaminergic biding sites in human basal ganglia, J. Neurochem. 39:1623.

Starke, K., Reimann, W., Zumstein, A. and Hertting, G., 1978, Effect of dopamine receptor agonists and antagonists on release of dopamine from rabbit caudate nucleus in vitro, Naunyn-Schmiedeberg's Arch. Pharmacol. 305:27.

Steg, G. and Johnels, B., 1979, Motor functions of the striatum in: 'The Neostriatum,' I. Divac and R. Oberg eds., Pergamon pp. 231-239.

Strong, R., Waymire, J. C., Samorajski, T. and Gottesfeld, Z., 1984, Regional analysis of neostriatal cholinergic and dopaminergic receptor binding and tyrosine hydroxylase activity as a function of aging, Neurochem. Res. 9:1641.

Todd, P., 1983, Unique biological aspects of radiation hazards -- an overview, Adv. Space Res. 3:187.

Upton, A. C., 1954, Ionizing radiation and aging, Gerontologia, 4:562.

Vrijmoed-de Vries, M. C. and Cools, A. R., 1986, Differential effects of striatal injections of dopaminergic, cholinergic and GABAergic drugs upon swimming behavior in rats, Brain Res. 364:77.

Westfall, T. C. Besson, M. J., Giorguieff, M. G. and Glowinski, J., 1976, The role of presynaptic receptors in the release and synthesis of [$^3$H]-dopamine by slices of rat striatum, Naunyn-Schmiedeberg's Arch. Pharmacol. 292:279.

RADIATION RESEARCH 117, 185–197 (1989)



# The Effect of γ Radiation on DNA Methylation

JOHN F. KALINICH,[1] GEORGE N. CATRAVAS, AND STEPHEN L. SNYDER

*Radiation Biochemistry Department, Armed Forces Radiobiology Research Institute, Bethesda, Maryland 20814-5145*

KALINICH, J. F., CATRAVAS, G. N., AND SNYDER, S. L. The Effect of γ Radiation on DNA Methylation. *Radiat. Res.* **117**, 185–197 (1989).

The effect of $^{60}$Co γ radiation on DNA methylation was studied in four cultured cell lines. In all cases a dose-dependent decrease in 5-methylcytosine was observed at 24, 48, and 72 h postexposure to 0.5–10 Gy. Nuclear DNA methyltransferase activity decreased while cytoplasmic activity increased in irradiated (10 Gy) V79A03 cells as compared to controls. No DNA demethylase activity was detected in the nuclei of control or irradiated V79A03 cells. Additionally, γ radiation resulted in the differentiation of C-1300 NIE-115 cells, a mouse neuroblastoma line, in a dose- and time-dependent manner. These results are consistent with the hypothesis that (1) genes may be turned on following radiation via a mechanism involving hypomethylation of cytosine and (2) radiation-induced hypomethylation results from decreased intranuclear levels of DNA methyltransferase. 

## INTRODUCTION

The methylation of DNA is a postreplicative process catalyzed by specific methyltransferases which transfer the chemically active methyl group from *S*-adenosylmethionine to carbon-5 of a cytosine residue (*1*). DNA methyltransferases can catalyze two methylation reactions on DNA:

1. *de novo* methylation, involving methylation of a cytosine residue on one strand even though the cytosine on the complementary strand is not methylated, and

2. maintenance methylation, in which the enzyme methylates a cytosine on one strand using a methylated cytosine on the other strand as a recognition signal.

Maintenance methylation constitutes the bulk of the methylation activity *in vivo* (*2*). In normal eukaryotic DNA, 5-methylcytosine appears as the only modified base (*3*) and then only in 5′-CpG-3′ sequences. The nonrandom distribution of 5-methylcytosine in eukaryotic DNA and the fact that not all potentially methylatable cytosines are methylated, along with the high metabolic cost of maintaining the methylation pattern, suggest an important regulatory function for this modified base. At present the methylation of DNA has been shown to play a major role in the packaging and repair of DNA (*4–6*), the control of gene expression (*7, 8*), carcinogenesis (*9–*

[1] Present address: Biochemistry Department, University of Texas Southwestern Medical Center at Dallas, 5323 Harry Hines Blvd., Dallas, TX 75235-9038.



0033-7587/89 $3.00

*11*), cellular development and differentiation (*12–14*), and the stabilization of DNA conformational states (*15*). The occurrence of 5-methylcytosine in DNA may also allow the cell to discriminate between strands in mismatch repair (*5, 6*). For example, damage to the 5-methylcytosine residue of DNA, resulting in deamination to form thymine, could be corrected by the appropriate repair enzymes using the undamaged methylated DNA strand as a template for repair. Methylated DNA also aids in the packaging of the DNA into nucleosomes. It has been shown that DNA containing 5-methylcytosine is packaged into nucleosomes (*4*) and is located primarily in the core particles (*16*).

Hypomethylation of DNA can result in activation of normally quiescent genes. Genes showing methylation-induced deactivation include hamster adenine phosphoribosyltransferase (*8*), HeLa cell and mouse hypoxanthine phosphoribosyltransferase (*17, 18*), and metallothionein (*19*). Most of the methylatable gene sequences important for determining expression are in the 5′-regions. Whether 5-methylcytosine prevents binding of the proteins needed for transcription or allows binding of repressor proteins is not yet known.

Ultraviolet radiation exposure results in a decrease in DNA methylation (*20–23*). A previous study investigating $\gamma$-radiation effects on DNA methylation in rat thymus and bone marrow *in vivo* (*24*) provided no clear-cut conclusion on the effect of $\gamma$ radiation on DNA methylation. In view of the important role DNA methylation appears to play in regulating gene expression and cell function, this study was undertaken to investigate the effect of $\gamma$ radiation on DNA methylation and its possible relationship to gene induction. It was also of interest to determine the effect of $\gamma$ radiation on intracellular distribution of DNA methyltransferase activity.

## MATERIALS AND METHODS

### *Cell Culture Conditions*

Nutrient Mixture F-12, $\alpha$ minimal essential medium, Eagle's minimal essential medium with Earle's salts, Dulbecco's modification of Earle's minimal essential medium, fetal calf serum, penicillin, streptomycin, gentamicin, and L-glutamine were purchased from GIBCO Labs (Grand Island, NY). *N*-2-Hydroxyethyl-piperizine-*N*′-2-ethane-sulfonic acid (Hepes) and dimethylsulfoxide (DMSO) were obtained from the Sigma Chemical Company (St. Louis, MO).

Chinese hamster ovary (CHO) clone K-1 was obtained from the American Type Culture Collection (Rockville, MD) and was maintained in Nutrient Mixture F-12 supplemented with 10% fetal calf serum, 100 units/ml penicillin, 100 $\mu$g/ml streptomycin, and 20 $\mu$g/ml gentamicin.

Chinese hamster lung fibroblast (V79) clone A03 was the kind gift of Dr. Tom Walden, AFRRI. It was maintained in $\alpha$ minimal essential medium supplemented with 10% fetal calf serum, 100 units/ml penicillin, 100 $\mu$g/ml streptomycin, 20 $\mu$g/ml gentamicin, and 2 m*M* L-glutamine. The medium was buffered with 25 m*M* Hepes.

HeLa clone S-3 was obtained from the American Type Culture Collection. It was maintained in M/3 medium (Dr. Pinhas Fuchs, personal communication). M/3 medium consisted of 1/3 vol Eagle's minimal essential medium with Earle's salts, 1/3 vol Nutrient Mixture F-12, and 1/3 vol Dulbecco's modification of Earle's minimal essential medium supplemented with 10% fetal calf serum, 100 units/ml penicillin, 100 $\mu$g/ml streptomycin, and 20 $\mu$g/ml gentamicin.

Mouse neuroblastoma C-1300 clone NIE-115 was the generous gift of Dr. David Krause of the Uniformed Services University of the Health Sciences (Bethesda, MD) and was maintained in M/3 medium.

All cell lines were maintained in monolayer at 37°C in a humidified 5% $CO_2$/95% air incubator. The medium on irradiated cells was changed daily to remove dead cells from the culture. Differentiation of mouse neuroblastoma cells was accomplished by adding dimethylsulfoxide to 2% and incubating for 2

days at 37°C. Phase contrast micrographs of Giemsa-stained neuroblastoma cells were taken with a Zeiss Axiophot photomicroscope.

*Radiation Conditions*

Irradiation was performed bilaterally at room temperature using the AFRRI $^{60}$Co γ-radiation source with a dose rate of 1 Gy/min. Total doses ranging from 0 to 10 Gy were given.

*Determination of 5-Methylcytosine Levels*

Cellular DNA was isolated using a modification of the method of Blin and Stafford (25, 26). The DNA was hydrolyzed to its deoxyribonucleotides (dNMP) following the enzymatic method of Christman (27). Separation of DNA dNMPs by high-pressure liquid chromatography was performed using a Beckman Model 344 gradient liquid chromatograph with an Altex Ultrasphere 5-μm particle octadecylsilane column (4.6 mm i.d. × 25 cm). Samples were eluted with 100 m*M* sodium phosphate buffer, pH 5.5, over 55 min at ambient temperature with a flow rate of 1 ml/min (27). Detection was at 254 nm with a detector sensitivity of 0.05 absorbance units full scale. Data were analyzed with an IBM System-9000 computer interfaced to the HPLC system. Deoxyribonucleotide standards were purchased from the Sigma Chemical Co.

*Acetylcholinesterase Assay of Mouse Neuroblastoma Cells*

Determination of acetylcholinesterase activity in cell homogenates of mouse neuroblastoma cells was performed using the method of Ellman *et al.* (28). The cells were harvested by forcefully pipetting a stream of medium over them. The cell suspension was centrifuged at 800*g* and 4°C for 10 min. The pellet was washed once with Hanks balanced salt solution (HBSS) and once with 100 m*M* sodium phosphate buffer, pH 8.0, resuspended in 2 ml of phosphate buffer, and homogenized by 10 strokes in a Dounce homogenizer. The reaction mixture consisted of 2.60 ml of 100 m*M* sodium phosphate buffer, pH 8.0, 0.40 ml of cell suspension, 0.10 ml of dithiobisnitrobenzoic acid (Calbiochem Biochemicals/Behring Diagnostics, La Jolla, CA), and 0.02 ml of acetylthiocholine iodide (Sigma) which was added to initiate the reaction. The absorbance at 412 nm was recorded for 5 min. Activity was determined using the change in absorbance per minute over a linear portion of the curve.

*Protein Determination*

The method of Lowry *et al.* (29) was used to measure protein content.

*Assay of DNA Methyltransferase Activity*

M13 single-stranded DNA, M13 17-base primer, *E. coli* DNA polymerase I, and T4 ligase were purchased from BRL (Bethesda, MD). ATP, dATP, dTTP, dCTP, and dGTP were obtained from Boehringer-Mannheim Biochemicals (Indianapolis, IN). 5-Methyl-dCTP was purchased from Pharmacia (Piscataway, NJ).

The method of Szyf *et al.* (30) was used to prepare unmethylated and hemimethylated DNA. Double-stranded DNA was synthesized *in vitro* using bacteriophage M13 single-stranded DNA as a template. Template DNA (100 μg) was incubated for 20 min at 15°C with 0.75 μg of M13 17-base primer. After incubation the following were added in a final reaction volume of 300 μl: dithiothreitol, (10 m*M*), Tris–HCl (pH 7.4, 66 m*M*), $MgCl_2$ (6.6 m*M*), ATP (0.1 m*M*), *E. coli* DNA polymerase I (large fragment, 7 units), T4 ligase (400 units), dATP (50 μ*M*), dTTP (50 μ*M*), and dGTP (50 μ*M*). For unmethylated DNA, dCTP was added to 50 μ*M*. For hemimethylated DNA, 5-methyl-dCTP was added to 50 μ*M*. The mixture was incubated at 12°C for 15 h and the reaction was terminated by the addition of EDTA to a final concentration of 20 m*M*.

*Extraction of DNA Methyltransferase*

The cell monolayer was washed once with HBSS and the nuclei were isolated using the Butler method (31). The nuclei were pelleted by centrifugation for 15 min at 800*g* and 4°C. The supernatant was saved and used to determine cytoplasmic DNA methyltransferase activity. The nuclei were washed twice with

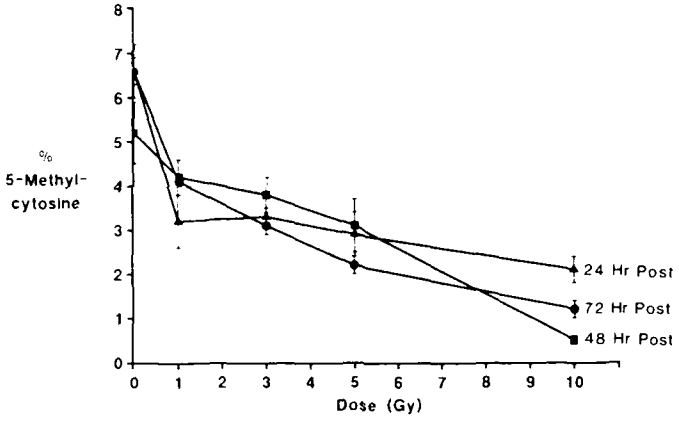


FIG. 1. 5-Methylcytosine changes in $\gamma$-$^{60}$Co irradiated CHO K-1 cells. Cells were exposed to 1, 3, 5, or 10 Gy of radiation. At 24, 48, or 72 h postirradiation, the cells were harvested, the DNA was isolated and hydrolyzed, and the resulting nucleotides were separated by HPLC. Data points are the average of nine determinations. Error bars are given in standard deviation.

HBSS, then resuspended in 0.5 ml of Tris–HCl, pH 7.6, containing 1 m*M* EDTA and 1 m*M* dithiothreitol. The nuclei were disrupted by 3 s of sonication after which the mixture was assayed for nuclear DNA methyltransferase activity.

*Assay of de Novo and Maintenance Activity*

The method of Szyf *et al.* (*30*) was used to assay for both *de novo* and maintenance methylation activity. The enzyme assay mixture contained, in a final volume of 25 $\mu$l, 0.3 $\mu$g of DNA (unmethylated for *de novo* methylation determination, hemimethylated for maintenance methylation determination), 16 $\mu M$ *S*-adenosyl-L-[*methyl*-$^3$H]methionine (15 mCi/mmol; Amersham, Arlington Heights, IL), and 3 $\mu$l of enzyme mixture in a buffer containing 20 m*M* Tris–HCl, pH 7.4, 25% glycerol (v/v), 10 m*M* EDTA, 0.2 m*M* PMSF, and 20 m*M* 2-mercaptoethanol. The mixture was incubated at 37°C for 60 min. The reaction was terminated by the addition of 100 $\mu$l of 10% sodium dodecyl sulfate and 100 $\mu$l of 1 *N* NaOH and incubated for an additional 2 h at 60°C. The mixture was extracted with 1 vol of a 1:1 mixture of chloroform:isoamyl alcohol. The layers were separated and 1 vol of 10% trichloroacetic acid (TCA) was added to the aqueous layer. The mixture was left on ice for 15 min after which the precipitate was collected on a Whatman GF/C glass microfiber filter. The filter was washed twice with 10% TCA containing 100 m*M* sodium pyrophosphate, washed twice with 70% ethanol, dried, and placed in a scintillation vial; 5 ml of a liquid scintillation counting fluid was added, and the incorporation of radioactivity was determined by liquid scintillation counting.

## RESULTS

### *5-Methylcytosine Changes*

The effect of various doses of $\gamma$ radiation on the percentage of 5-methylcytosine in cellular DNA is summarized in Figs. 1–4. CHO K-1, HeLa S-3, C-1300 N1E-115, and V79A03 cell lines irradiated with 1, 3, 5, or 10 Gy were harvested 24, 48, or 72 h postirradiation and the DNA was isolated and hydrolyzed. Following HPLC, the percentage of 5-methylcytosine was calculated and the distribution in irradiated cells was compared to that of unirradiated control cells.

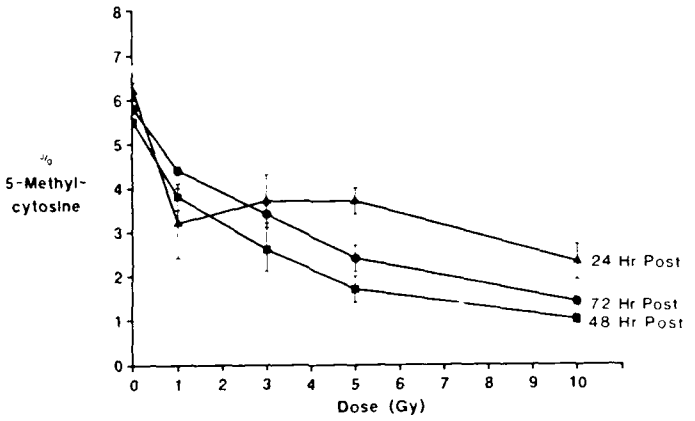


FIG. 2. 5-Methylcytosine changes in $\gamma$-$^{60}$Co irradiated HeLa S-3 cells. Cells were exposed to 1, 3, 5, or 10 Gy of radiation. At 24, 48, or 72 h postirradiation, the cells were harvested, the DNA was isolated and hydrolyzed, and the resulting nucleotides were separated by HPLC. Data points are the average of nine determinations. Error bars are given in standard deviation.

As shown in Fig. 1, 5-methylcytosine decreased in CHO K-1 cells following radiation exposure. The probability, based on Student's $t$ test, that the numbers are not significantly different was $P < 0.002$ in all cases.

Figure 2 shows the effect of radiation on 5-methylcytosine levels in HeLa S-3 cells. Again there is a decrease in 5-methylcytosine levels at all radiation doses and times ($P < 0.001$). As with CHO K-1 cells, HeLa S-3 cells exhibit dose-dependent decreases in 5-methylcytosine at 48 and 72 h postirradiation. However, from 1 to 5 Gy a plateau is seen at 24 h postirradiation.

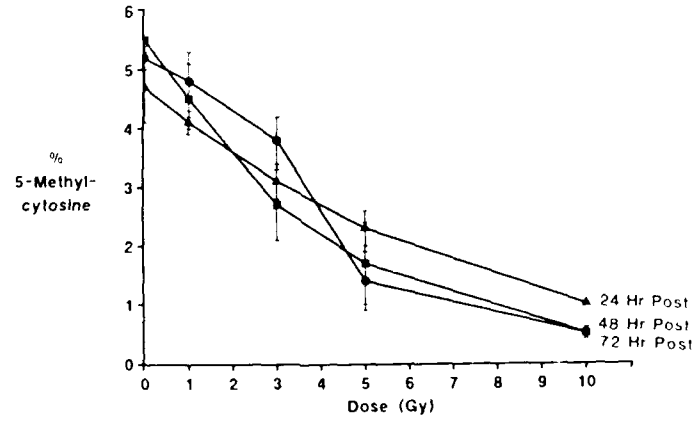


FIG. 3. 5-Methylcytosine changes in $\gamma$-$^{60}$Co irradiated V79A03 cells. Cells were exposed to 1, 3, 5, or 10 Gy of radiation. At 24, 48, or 72 h postirradiation, the cells were harvested, the DNA was isolated and hydrolyzed, and the resulting nucleotides were separated by HPLC. Data points are the average of nine determinations. Error bars are given in standard deviation.

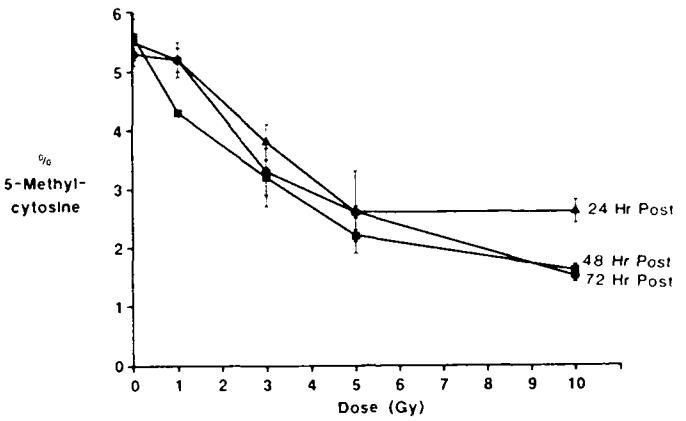


FIG. 4. 5-Methylcytosine changes in $\gamma$-$^{60}$Co irradiated C-1300 NIE-115 cells. Cells were exposed to 1, 3, 5, or 10 Gy of radiation. At 24, 48, or 72 h postirradiation, the cells were harvested, the DNA was isolated and hydrolyzed, and the resulting nucleotides were separated by HPLC. Data points are the average of nine determinations. Error bars are given in standard deviation.

The effect of $\gamma$ radiation on 5-methylcytosine levels in V79A03 cells is shown in Fig. 3. A dose-dependent decrease of 5-methylcytosine in irradiated cells is also observed; however, in this case the dose-dependent relationship is seen at all three times postirradiation. There is no 1- to 5-Gy plateau region at 24 h as seen in HeLa S-3 cells. Significance was at the $P < 0.001$ level in all but four cases. The most important of these are the 1-Gy values at 24, 48, and 72 h. At 24 and 48 h $P < 0.001$, but at 72 h $P < 0.1$, indicating that this value is not significantly different from the control.

The percentage of 5-methylcytosine in C-1300 N1E-115 cells is shown in Fig. 4. A dose-dependent decrease in 5-methylcytosine is seen at all three postirradiation times investigated. In all but two cases, 24 and 72 h at 1 Gy, the percentage 5-methylcytosine was significantly decreased ($P < 0.001$) relative to the controls.

### *DNA Methyltransferase Activity*

Experiments were performed to investigate the possibility that the decrease in 5-methylcytosine following radiation might be related to changes in the intranuclear methyltransferase (MT) activity. V79A03 cells were irradiated with 10 Gy of $\gamma$ radiation and harvested 24, 48, and 72 h postexposure. Maintenance and *de novo* MT activities were assayed in the nucleus and the cytoplasm of the cells. Tables I and II show the *de novo* and maintenance DNA methyltransferase activity of control and irradiated cells expressed as picomoles of $^3$H-methyl groups incorporated into DNA per 60 min incubation at 37°C/mg of protein.

Following radiation there was a redistribution of both maintenance and *de novo* methyltransferase activity from the nuclear to the cytoplasmic compartments. In the case of *de novo* MT activity, a decrease in the nucleus was apparent by 24 h, at which time there was a drop from 0.36 to 0.14 pmol tritium incorporated per hour (Table I). This decrease was paralleled by a concomitant increase in cytoplasmic *de novo*

TABLE I

*De Novo* DNA Methyltransferase Activity in V79A03 Cells

| | *Control* | | *10 Gy* | |
|---|---|---|---|---|
| | *pmol (M ± SD)* | *% Total activity* | *pmol (M ± SD)* | *% Total activity* |
| Nuclear activity | | | | |
| 24 h | 0.36 ± 0.06 | 5.6 ± 0.9 | 0.14 ± 0.02 | 2.3 ± 0.3 ($P < 0.001$) |
| 48 h | 0.38 ± 0.03 | 5.7 ± 0.4 | 0.14 ± 0.05 | 2.3 ± 0.8 ($P < 0.001$) |
| 72 h | 0.32 ± 0.03 | 4.9 ± 0.4 | 0.15 ± 0.01 | 3.2 ± 0.2 ($P < 0.001$) |
| Cytoplasmic activity | | | | |
| 24 h | 0.31 ± 0.02 | 4.8 ± 0.3 | 0.78 ± 0.02 | 12.4 ± 0.4 ($P < 0.001$) |
| 48 h | 0.28 ± 0.03 | 4.3 ± 0.5 | 0.54 ± 0.04 | 8.9 ± 0.6 ($P < 0.001$) |
| 72 h | 0.17 ± 0.06 | 2.6 ± 0.9 | 0.17 ± 0.03 | 3.7 ± 0.7 ($P < 0.010$) |

*Note.* Data are the mean of six determinations and are presented in activity units. One unit of activity is defined as the incorporation of 1 pmol of $^3H$ from *S*-adenosylmethionine into *DNA* when the reaction is incubated at 37°C for 60 min. Errors are given in standard deviation (SD). Significance was determined using Student's *t* test.

methylation activity from 0.31 to 0.78 pmol tritium incorporated per hour at 24 h postexposure. The *de novo* MT component found in the nucleus of irradiated cells remained depressed by approximately 50% relative to the controls during the 72-h period studied. Nuclear maintenance MT activity, which accounts for approximately 65% of the enzyme found within control cells, also decreased following radiation exposure, but in this case a significant decrease was not seen until 48 h postexposure (Table II). Once again the decrease in nuclear MT was accompanied by a comparable increase in cytoplasmic MT (Table II). During the course of these experiments there was also a decrease in the total cellular MT activity (*de novo* plus maintenance) following irradiation. For example, over the 72-h period investigated the total MT activity found in control cells remained constant at 6.4–6.6 pmol $^3H$ incorporated per hour while the MT in cells 72 h postirradiation had dropped to 4.7 pmol $^3H$ incorporated per hour.

### *Acetylcholinesterase Induction*

Figure 5 shows the effect of radiation on acetylcholinesterase activity in C-1300 N1E-115, a mouse neuroblastoma cell line. Acetylcholinesterase is a marker for cellular differentiation in C-1300 N1E-115 cells. Specific enzyme activity was determined in moles of substrate hydrolyzed per minute per milligram of protein. The results in Fig. 5 are given as percentage of control. Cells were irradiated with 0.5, 1, 3, 5, 7, or

TABLE II

Maintenance DNA Methyltransferase Activity in V79A03 Cells

| | *Control* | | *10 Gy* | |
|---|---|---|---|---|
| | *pmol M ± SD* | *% Total activity* | *pmol M ± SD* | *% Total activity* |
| Nuclear activity | | | | |
| 24 h | 4.28 ± 0.06 | 67.2 ± 0.9 | 3.95 ± 0.46 | 62.7 ± 7.0 ($P < 0.001$) |
| 48 h | 4.32 ± 0.18 | 65.8 ± 2.7 | 2.27 ± 0.30 | 37.6 ± 4.9 ($P < 0.001$) |
| 72 h | 4.22 ± 0.33 | 65.3 ± 5.1 | 2.28 ± 0.11 | 48.2 ± 2.4 ($P < 0.001$) |
| Cytoplasmic activity | | | | |
| 24 h | 1.43 ± 0.08 | 22.4 ± 1.2 | 1.42 ± 0.09 | 22.6 ± 1.4 ($P < 0.01$) |
| 48 h | 1.59 ± 0.07 | 24.2 ± 1.0 | 3.09 ± 0.27 | 51.2 ± 4.5 ($P < 0.001$) |
| 72 h | 1.76 ± 0.13 | 27.2 ± 2.1 | 2.13 ± 0.16 | 45.0 ± 3.5 ($P < 0.001$) |

*Note.* Data are the mean of six determinations and are presented in activity units. One unit of activity is defined as the incorporation of 1 pmol of $^3H$ from *S*-adenosylmethionine into DNA when the reaction is incubated at 37°C for 60 min. Errors are given in standard deviation (SD). Significance was determined using Student's *t* test.

10 Gy of γ radiation, harvested 1, 6, 24, 48, and 72 h postirradiation, and assayed for acetylcholinesterase activity. At 1 h postirradiation, enzyme activity levels were at or below the controls. Activities rose at 6 h postirradiation, but the increases were not significantly above controls, except for the 7- and 10-Gy points. At 24 h postirradiation all doses resulted in acetylcholinesterase levels greater than controls. Very little change was seen at 48 h postirradiation over 24 h except for 10 Gy which increased from 150 to 191% of control. The results obtained 72 h after radiation exposure showed increased enzyme activity over control at all doses in a dose-dependent manner. The greatest increase in activity was seen at 10 Gy 72 h postirradiation where acetylcholinesterase activity was 234% of control. This compares to an acetylcholinesterase activity 244% of control in neuroblastoma cells which had been differentiated with DMSO.

To determine if the increase in acetylcholinesterase activity was accompanied by morphological changes associated with differentiation, photomicrographs of control (undifferentiated), DMSO differentiated, and irradiated (10 Gy, 72 h postirradiation) neuroblastoma cells were taken. Figure 6 shows that both the DMSO-treated and irradiated cells exhibit axons indicative of differentiation in this cell line.

## DISCUSSION

Gene activation and inactivation, strand selection for repair, cellular differentiation, conformational transitions, and carcinogenesis are just a few of the processes in

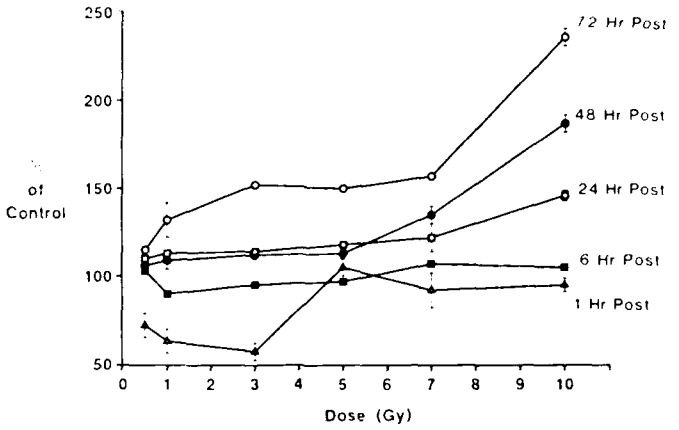


FIG. 5. Acetylcholinesterase activity in C-1300 N1E-115 cells following $^{60}$Co $\gamma$ exposure. Mouse neuroblastoma cells (C-1300 N1E-115) receiving various doses of $\gamma$ radiation were harvested at the indicated times, acetylcholinesterase activity was assayed, and the data were expressed as percentage of control (unirradiated) values. As a comparison, DMSO-differentiated neuroblastoma cells had acetylcholinesterase activity that was 244% of control. Data points are the average of nine determinations. Error bars are given in standard deviation.

which DNA methylation and 5-methylcytosine have been implicated. The deleterious effects of radiation are well known, but the mechanism by which damage is transmitted to the cell and the exact nature of the radiation target within the cell are still largely unknown. Since DNA methylation and 5-methylcytosine appear to play an important role in gene induction and DNA repair, we initiated this project to assess the effect of $\gamma$ radiation on DNA methylation.

In the present study 5-methylcytosine levels were found to decrease in a dose-dependent manner in cultured cells receiving up to 10 Gy $^{60}$Co $\gamma$ radiation. This decrease was seen at 24, 48, and 72 h postirradiation. The greatest decrease was seen at 10 Gy and 48 h postirradiation in all cells (Figs. 1–4). At 24 h there is a plateau region around 1 to 5 Gy in CHO K-1 and HeLa S-3 cells and 5 to 10 Gy in C-1300 N1E-115 cells. This appears to be a tissue-specific phenomenon since a plateau region is seen at 1 to 5 Gy in CHO K-1 and HeLa S-3 cells, both of which are epithelial lines. The plateau region is not seen until 5 to 10 Gy in C-1300 N1E-115 cells, a neuroblastoma line, and does not appear at all in V79A03 cells, a fibroblast line. At 72 h a slight increase in 5-methylcytosine levels over 48 h values was observed, possibly indicating the beginning of recovery.

Decreases in 5-methylcytosine content in DNA can result in the activation of normally quiescent genes (*7, 18, 19*). Hypomethylation of DNA has also been correlated with cellular differentiation (*13, 14*). C-1300 N1E-115 cells, a mouse neuroblastoma line used in this study, are maintained in culture in a nondifferentiated state but can be induced to differentiate by exposure to a chemical stimulus or X rays (*32–36*). Upon differentiation the cells exhibit axons (*36*) and produce acetylcholinesterase (*37*). Using acetylcholinesterase as an enzyme marker of cellular differentiation, the effect of $\gamma$ radiation on C-1300 N1E-115 cells was studied. Cells harvested 24, 48, and


FIG. 6. Phase contrast photomicrographs of Giemsa-stained C-1300 N1E-115 cells (500× magnification). (a) Control (unirradiated) cells. (b) DMSO-treated cells (2% DMSO/2 days). (c) Irradiated cells (10 Gy/72 h post). Both DMSO-treated and irradiated cells exhibit axon formation indicative of differentiation.

72 h postirradiation show dose- and time-dependent increases in acetylcholinesterase activity. It appears that, at 1 and 6 h postirradiation, the cells have not recovered from the radiation damage. Since radiation causes short-term inhibition of bulk protein synthesis (*38*), it may take up to 24 h postirradiation for the cells to express the products of the newly activated genes. Additionally, irradiated cells (10 Gy, 72 h postirradiation) are morphologically similar to DMSO-differentiated cells (Fig. 6). Thus our results show that radiation-induced hypomethylation may lead to differentiation of mouse neuroblastoma cells as indicated by increases in acetylcholinesterase activity and morphological changes (axon extension).

Finally, it was of interest to know whether the observed changes in the 5-methylcytosine content of DNA can be related to changes in nuclear DNA MT activity. Maintenance MT activity in the nuclei of irradiated cells decreased to approximately 50% of control at 48 and 72 h postirradiation (Table II). This decrease is paralleled by a concomitant increase in cytoplasmic maintenance MT activity 48 and 72 h postexposure. Our data also show a marked redistribution of *de novo* MT activity from the nuclear to the cytoplasmic compartment following radiation. These results indicate that DNA hypomethylation following radiation results, in large part, from radiation-induced leakage of MT from the nucleus to the cytoplasm. Alternatively, radiation damage to the nuclear envelope and/or pore complex may impair the transport of newly synthesized MT into the nucleus. Although a demethylase activity has been reported (*39*), we found no evidence suggesting that radiation-induced hypomethylation is due to the induction of a demethylase (data not shown).

Another factor that may result in hypomethylation after radiation is increased levels of an MT inhibitor. A preliminary report on a naturally occurring inhibitor of DNA MT has recently been published (*40, 41*). The inhibitor, a low molecular weight amine called methinin, was originally isolated from rabbit liver, but also has been found in human erythroleukemia cells. Although it is possible hypomethylation of DNA in irradiated cells could result from methinin inhibition of the methyltransferase, our results are more consistent with a redistribution of activity from the nucleus to the cytoplasm following radiation exposure.

We have demonstrated that $\gamma$ radiation interferes with the methylation of DNA and that the activation of certain genes can also occur following radiation exposure. Although our evidence is only suggestive, it seems reasonable to postulate that these phenomena may be related. Recently it has been shown that oncogenes can be induced by ionizing radiation (*42*). Whether there is a causal relationship between radiation-induced hypomethylation, oncogene induction, and tumorigenesis remains undetermined.

RECEIVED: November 25, 1987; REVISED: March 16, 1988

## REFERENCES


1. M. GOLD, J. HURWITZ, and M. ANDRES. The enzymatic methylation of RNA and DNA. II. On the species specificity of the methylation enzymes. *Proc. Natl. Acad. Sci. USA* **50,** 164–169 (1963).
2. E. L. KAUTIANEN and P. A. JONES. DNA methylation in mammalian nuclei. *Biochemistry* **24,** 5575–5581 (1985).
3. R. D. HOTCHKISS. The quantitative separation of purines, pyrimidines, and nucleosides by paper chromatography. *J. Biol. Chem.* **175,** 315–332 (1948).
4. R. L. P. ADAMS, E. L. MCKAY, T. L. DOUGLAS, and R. H. BURTON. Methylation of nucleosomal and nuclease sensitive DNA. *Nucleic Acids Res.* **4,** 3097–3108 (1977).
5. J. E. HARE and J. H. TAYLOR. One role for DNA methylation in vertebrate cells is strand discrimination in mismatch repair. *Proc. Natl. Acad. Sci. USA* **82,** 7350–7354 (1985).
6. M. JONES, R. WAGNER, and M. RODMAN. Mismatch repair of deaminated 5-methylcytosine. *J. Mol. Biol.* **194,** 155–159 (1987).
7. T. NAVEH-MANY and H. CEDAR. Active gene sequences are undermethylated. *Proc. Natl. Acad. Sci. USA* **78,** 4246–4250 (1981).
8. I. KESHET, J. YISRAELI, and H. CEDAR. Effect of regional DNA methylation on gene expression. *Proc. Natl. Acad. Sci. USA* **82,** 2560–2564 (1985).

9. I. I. J. BOEHM and D. DRAHOVSKY, Hypomethylation of DNA in Raji cells after treatment with *N*-methyl-*N*-nitrosourea. *Carcinogenesis* **2**, 39–42 (1981).
10. S. S. HECHT, N. TRUSHIN, A. CASTONGUAY, and A. RIVENSON, Comparative tumorigenicity and DNA methylation in F344 rats by 4-(methylnitrosamino)-1-(3-pyridyl)-1-butanone and *N*-nitrosodimethylamine. *Cancer Res.* **46**, 498–502 (1986).
11. I. J. LEVEL, G. R. BOSS, and R. W. ERBE, Decreased methylation rates of DNA in SV-40 transformed human fibroblasts. *Cancer* **57**, 764–768 (1986).
12. J. K. CHRISTMAN, N. WEICH, B. SCHOENBRUM, N. SCHNEIDERMAN, and G. ACS, Hypomethylation of DNA during differentiation of Friend erythroleukemia cells. *J. Cell Biol.* **86**, 366–370 (1980).
13. M. SHEFFERY, R. A. RIFKIND, and P. A. MARKS, Murine erythroleukemia cell differentiation: DNase I hypersensitivity and DNA methylation near the globin genes. *Proc. Natl. Acad. Sci. USA* **79**, 1180–1184 (1982).
14. A. RAZIN, C. WEBB, M. SZYF, J. YISRAELI, A. ROSENTHAL, E. NAVEH-MANY, N. SCIAKY-GALILI, and H. CEDAR, Variations in DNA methylation during mouse cell differentiation in vivo and in vitro. *Proc. Natl. Acad. Sci. USA* **81**, 2275–2279 (1984).
15. M. BEHE and G. FELSENFELD, Effects of methylation on a synthetic polynucleotide: the B–*Z* transition in poly(dG-m5C)·poly(dG-m5C). *Proc. Natl. Acad. Sci. USA* **78**, 1619–1623 (1981).
16. A. SOLAGE and H. CEDAR, Organization of 5-methylcytosine in chromosome DNA. *Biochemistry* **17**, 2934–2938 (1978).
17. R. IVARIE and J. A. MORRIS, Activation of a nonexpressed hypoxanthine phosphoribosyltransferase allele in mutant H23 HeLa cells by agents that inhibit DNA methylation. *Mol. Cell. Biol.* **6**, 97–104 (1986).
18. L. F. LOCK, D. W. MELTON, C. T. CASKEY, and G. R. MARTIN, Methylation of the mouse hprt gene differs on the active and inactive X chromosomes. *Mol. Cell. Biol.* **6**, 914–924 (1986).
19. S. J. COMPERE and R. D. PALMITER, DNA methylation controls the inducibility of the mouse metallothionein-I gene in lymphoid cells. *Cell* **25**, 233–240 (1981).
20. M. LOW, E. L. READ, and E. BOREK, Methylation of DNA in HeLa cells after ultraviolet irradiation. *Int. J. Radiat. Oncol. Biol. Phys.* **1**, 289–294 (1976).
21. O. NIWA and T. SUGAHARA, Inhibition of DNA methylation and radiation induction of murine endogenous viruses. *J. Radiat. Res.* **23**, 57 (1982).
22. M. W. LIEBERMAN, L. R. BEACH, and R. D. PALMITER, Ultraviolet radiation-induced metallothionein-I gene activation is associated with extensive DNA demethylation. *Cell* **35**, 207–214 (1983).
23. F. F. BECKER, P. HOLTON, M. RUCHIRAWAT, and J. N. LAPEYRE, Perturbation of maintenance and de novo DNA methylation in vitro by UV-B(280–340nm)-induced pyrimidine photodimers. *Proc. Natl. Acad. Sci. USA* **82**, 6055–6059 (1985).
24. I. A. RAKOVA, Post-radiation methylation of de novo synthesized DNA of rat bone marrow and thymus. *Radiobiologie* **19**, 413–416 (1979).
25. N. BLIN and D. W. STAFFORD, A general method for the isolation of high molecular weight DNA from eukaryotes. *Nucleic Acids Res.* **3**, 2303–2308 (1976).
26. T. MANIATIS, E. F. FRISCH, and J. SAMBROOK, *Molecular Cloning: A Laboratory Manual*, p. 468. Cold Spring Harbor Laboratory, 1982.
27. J. K. CHRISTMAN, Separation of major and minor deoxyribonucleoside monophosphates by reverse-phase high-performance liquid chromatography: A simple method applicable to quantitation of methylated nucleotides in DNA. *Anal. Biochem.* **119**, 38–48 (1982).
28. G. L. ELLMAN, K. D. COURTNEY, V. ANDRES, and R. M. FEATHERSTONE, A new and rapid colorimetric determination of acetylcholinesterase activity. *Biochem. Pharmacol.* **7**, 88–95 (1961).
29. O. H. LOWRY, N. J. ROSEBROUGH, A. L. FARR, and R. J. RANDALL, Protein measurement with the Folin phenol reagent. *J. Biol. Chem.* **193**, 265–275 (1951).
30. M. SZYF, E. KAPLAN, V. MANN, H. GILOH, I. KEDAR, and A. RAZIN, Cell cycle-dependent regulation of eukaryotic DNA methylase level. *J. Biol. Chem.* **260**, 8653–8656 (1985).
31. W. B. BUELL, Preparing nuclei from cells in monolayer cultures suitable for counting and for following synchronized cells through the cell cycle. *Anal. Biochem.* **141**, 70–73 (1984).
32. P. ZIMARSKI, D. J. SILVERMAN, and M. LUBIN, Expression of differentiated functions in mouse neuroblastoma mediated by dibutyryl-cyclic adenosine monophosphate. *Nature* **233**, 413–415 (1971).
33. K. N. PRASAD and A. W. HSIE, Morphologic differentiation of mouse neuroblastoma cells induced in vitro by dibutyryl adenosine 3′:5′-cyclic monophosphate. *Nature New Biol.* **233**, 141–142 (1971).

34. J. R. KATES, R. WINTERTON, and K. SCHLESSINGER, Induction of acetylcholinesterase activity in mouse neuroblastoma tissue culture cells, *Nature* **229,** 345–347 (1971).
35. Y. KIMHI, C. PALFREY, I. SPECTOR, Y. BARAK, and U. Z. LITTAUER, Maturation of neuroblastoma cells in the presence of dimethylsulfoxide, *Proc. Natl. Acad. Sci. USA* **73,** 462–466 (1976).
36. K. N. PRASAD, X-ray-induced morphological differentiation of mouse neuroblastoma cells in vitro, *Nature* **234,** 471–473 (1971).
37. T. AMANO, E. RICHELSON, and M. NIRENBERG, Neurotransmitter synthesis by neuroblastoma clones, *Proc. Natl. Acad. Sci. USA* **69,** 258–263 (1972).
38. N. L. OLENICK and R. C. RUSTAD, Interrelationships between ionizing radiation, protein synthesis, and the physiological expressions of radiation damage, In *Advances in Radiation Biology* (J. T. Lett and H. Adler, Eds.), pp. 107–160, Academic Press, New York, 1976.
39. R. A. GJERSET and D. W. MARTIN, Presence of a DNA demethylating activity in the nucleus of murine erythroleukemic cells, *J. Biol. Chem.* **257,** 8581–8583 (1982).
40. S. B. LYON and H. LINK, DNA methylation: The enzymes and a naturally occurring inhibitor, *Fed. Proc.* **45,** 1927 (1986).
41. S. B. LYON, L. BUONOCORE, and M. MILLER, Naturally occurring methylation inhibitor: DNA hypomethylation and hemoglobin synthesis in human K562 cells, *Mol. Cell. Biol.* **7,** 1759–1763 (1987).
42. M. J. SAWEY, A. T. HOOD, F. J. BURNS, and S. J. GARTE, Activation of c-myc and c-K-ras oncogenes in primary rat tumors induced by ionizing radiation, *Mol. Cell. Biol.* **7,** 932–935 (1987).

Exp Brain Res (1989) 75: 28–34

Experimental Brain Research





# Enhanced acoustic startle responding in rats with radiation-induced hippocampal granule cell hypoplasia

G. A. Mickley and J. L. Ferguson

Behavioral Sciences Department, Armed Forces Radiobiology Research Institute, Bethesda, MD 20814-5145, USA

**Summary.** Irradiation of the neonatal rat hippocampus reduces the proliferation of granule cells in the dentate gyrus and results in locomotor hyperactivity, behavioral perseveration and deficits on some learned tasks. In order to address the role of changes in stimulus salience and behavioral inhibition in animals with this type of brain damage, irradiated and normal rats were compared in their startle reactions to an acoustic stimulus. A portion of the brain of 10 rats was exposed to a fractionated total dose of 13 Gy during the first 16 days post partum. This procedure produced selective hypoplasia (91% reduction) of the granule cells in the hippocampal dentate gyrus. Other rats (N = 10) were sham irradiated. Sudden tones were presented to each adult rat at a rate of 1 every 30 s (spaced trials) during an initial 10-min session and 1 every 15 s (massed trials) during a subsequent session. Irradiated rats startled with a consistently higher amplitude than controls and were more likely to exhibit startle responses. These animals with hippocampal damage also failed to habituate to the startle stimulus and, under certain circumstances, showed potentiated startle responses after many tone presentations.

**Key words:** Startle – Hippocampus – Dentate gyrus – Granule cells – Radiation

## Introduction

The startle response consists of a characteristic sequence of rapid muscular contractions beginning at the mouth and sequentially involving the neck, forelegs and finally the whole body (Landis and Hunt 1939). Analyses of movements associated with startle are being used increasingly in the study of human behavior (Wilkins et al. 1986) and the behavior of other animals (Eaton 1984). Although the acoustic startle response is a relatively simple behavior, its sensitivity to a variety of experimental treatments has made it an important tool in pharmacology and toxicology (for review see Eaton 1984). In particular, brain mechanisms of sensation, learning (habituation, sensitization), memory and movement are being elucidated through measures of startle (Davis 1984).

The neurons that comprise the primary acoustic startle circuit reside entirely within the brain stem (Davis 1984). However, the nature of the extrinsic neural systems that modulate acoustic startle is not so well understood. Since the hippocampus has long been known to play a role in response inhibition (Douglas 1967; Kimble 1968; Altman et al. 1973) it is likely that this structure also influences startle responding. In support of hippocampally mediated behavioral inhibition other investigators have reported excitatory behaviors after hippocampal lesions. For example, rats with hippocampal lesions exhibit locomotor hyperactivity (Teitelbaum and Milner 1963; Means et al. 1971), response perseveration (Isaacson 1974), facilitated acquisition of active avoidance (Isaacson et al. 1961) and impaired performance on passive avoidance tasks (Blanchard and Fial 1968; Isaacson and Wickelgren 1962). More-selective hippocampal lesions of CA3 have also been reported to produce hyper-reactivity to sensory stimulation (Handelmann and Olton 1981). Still, the function of the hippocampus in startle responding is controversial. Some authors (Groves et al. 1974; Leaton 1981) have reported that lesions of the hippocampus do not consistently alter startle, while others (Coover and Levine 1972) have found increased acoustic startle after surgically induced hippocampal damage.

*Offprint requests to:* G. A. Mickley (address see above)

Bayer et al. (1973) have identified a number of similarities between the behavioral deficits observed in rats with selective hippocampal granule cell lesions and the behavioral dysfunctions found after hippocampectomy. This is not totally surprising since the perforant path (from the entorhinal cortex to the granule cells of the dentate gyrus) provides one of the major inputs to the hippocampus (O'Keefe and Nadel 1978). Lesions, specific to the granule cells, effectively reduce the targets of these entorhinal cortex neurons, significantly limit hippocampal afferents and disrupt a variety of hippocampal functions (Brunner and Altman 1974; Altman 1986; Wallace and Altman 1970a, b).

In the present experiment we produced granule cell hypoplasia in the fascia dentata by partial-head X-irradiation of neonatal rats (Bayer and Peters 1977). In order to address the role of stimulus salience and behavioral inhibition in animals with these selective hippocampal lesions, irradiated and normal adult rats were compared in their startle reactions to an acoustic stimulus.

## Material and methods

Time-pregnant female (Fl × CD/SD-BR) rats were purchased from Charles River Laboratories, Kingston, NY, for these experiments. Pregnant rats were quarantined on arrival and screened for evidence of disease. Upon release from quarantine, they were maintained in a facility accredited by the American Association for Accreditation of Laboratory Animal Care (AAALAC). Subjects were housed in Microisolator cages on hardwood chip contact bedding and provided with commercial rodent chow and acidified water ad libitum (Wadsworth 1979). Animal holding rooms were maintained at 24–25°C with 20–30% relative humidity using at least 20 air changes per hour of 100% conditioned fresh air. The rats were on a twelve hour light/dark full spectrum lighting cycle with no twilight. On the day of birth, litters were culled to include eight pups. Neonatal subjects were then randomly assigned to either 0 or X irradiated or the sham-irradiated control conditions. The sham-irradiated control rats were restrained under lead shielding in the same manner as the irradiated animals (see below) but were not exposed to X rays. Following weaning (at 24–30 days) rats were individually housed.

Portions of the brains of the experimental rats were exposed to 0 or X rays on postnatal days 1 and 2, and to 2.5 Gy on days 5, 7, 9, 12, 14, and 16. X irradiation was delivered at a rate of 0.39 Gy/min at a depth of 2 mm in tissue. The radiation source was a Phillips Industrial 300 kvp X-ray machine (Phillips Inc., Mahwah, NJ) operated with 2.5 mm of copper filtration. The half-value layer was 2.5 mm copper. Doses were determined by using Victoreen R-meter (ionization chambers with calibration traceable to the National Bureau of Standards). Following a technique described by Bayer and Peters (1977), X irradiation was delivered to a 2 mm-wide area on the coronal plane to expose the hippocampal primordium previously determined to contain the granule cell progenitors. The X-ray exposure was directed through a slot in a lead shield (1 cm thick). The slot width ranged from 7–12 mm depending on the size of the pup. A custom plastic mould was used to accommodate the curvature of the head over the course of the radiation treatments. The entire anterior–posterior extent of the hippocampus was irradiated as were brain areas dorsal to and ventral to this structure (Paxinos and Watson 1982). Brain areas anterior and posterior to the slot were shielded.

Despite the fact that much of the neonatal rat brain was exposed to X rays, only the precursors of the granule cells in the dentate gyrus were permanently altered by this procedure (Hicks 1958; Bayer and Peters 1977). Most of the rat brain develops prenatally. At the time of our radiation exposures the brain contains only 3 populations of dividing (and therefore radiosensitive) neuronal precursors: the granule cells of the hippocampus, cerebellum and olfactory bulbs (Bayer et al. 1973; Bayer and Altman 1975). Through our shielding we protected two of these neuronal precursor populations (in the cerebellum and olfactory bulbs). Our X rays hit only the mitotic (radiosensitive) granule cells of the dentate gyrus and the mature neurons (that are radioresistant; see Cassaret 1980; Hicks and D'Amato 1966) in other brain structures residing in the same coronal plane as the hippocampus. This procedure produces selective hypoplasia of granule cells in the dentate gyrus while sparing other brain structures. The technique has been validated through a variety of neuroanatomical methods (Hicks 1958; Bayer and Altman 1975; Zimmer et al. 1985) including the ones reported here (see below).

Acoustic startle was measured on a Columbus Instrument's (Columbus, OH) Responder IV within a sound-attenuating chamber (Model E10-20, Coulbourn Instruments, Lehigh Valley, PA). The startle apparatus consisted of a (15 × 30 cm) metal plate mounted on load cells allowing a measurement ("amplitude" of response) directly proportional to a sudden force applied to the plate. The rat to be tested was placed in a transparent plastic box (10 × 12 × 22 cm) with a perforated lid. The rat could sit in the box without touching the top or sides of the container. Subjects did not locomote within the startle chamber. The box was set on the sensing plate 2 cm beneath a speaker from which a 10 ms acoustic stimulus (90 dB, SPL, 10 kHz) was presented.

An equal number of experimental (X = 100) and control (X = 100) rats were selected from the same litters and allowed to mature (mean age = 210 days, SD = 30). Before behavioral testing, subjects were matched for weight (irradiated rat mean = 656 g, SD = 36; control rat mean = 684 g, SD = 28). Each rat was placed in the plastic chamber which was then set immediately on the sensing plate of the startle apparatus. During the first session (spaced trials) the sound pulse was presented every 30 s for 30 min. During the second session, 4 days later (massed trials), the stimulus was presented every 15 s for the 30 min. Relative amplitude measurements were recorded after each trial. The sensitivity on the startle apparatus was set at 0.5 (5% of full scale) with a sampling window of 50 ms following stimulus onset. Movements were not recorded as a "startle" if they failed to be detected within these measurement parameters. Output linearity and stability were confirmed by recording output amplitudes after dropping small weights (5 to 35 g) from 2 cm to the sensor plate, or by dropping a 40 g mass 0.6 cm to the plate when it was loaded with 550 to 1250 g of dead weight. The mean startle amplitude recorded for the 20 subjects was 545; this was equivalent to dropping a 17 g weight 2 cm to the non-loaded sensor plate.

Using irradiation procedures similar to ours, Bayer and Peters (1977) have previously determined that X irradiation destroys approximately 85% of the granular cells in the dentate gyrus of the hippocampus while sparing adjacent structures (Bayer et al. 1975). After behavioral testing our rats were anesthetized and perfused with heparinized saline followed by 10% buffered formalin. Brains were embedded in paraffin, serially sectioned (6 μm) on either the coronal or sagittal plane) and then stained with cresyl violet and luxol fast blue (LaBossiere 1976). All brains were viewed to confirm radiation-induced changes in the hippocampus. In addition, irradiated and sham-irradiated brains were selected at

**Table 1.** Histological data derived from analysis of sagittal sections of hippocampus

| | Irradiated (N = 9) | Sham Irradiated (N = 6) | % of control |
|---|---|---|---|
| Number of dentate granule cells | 177.2 (27.9) | 1966.2 (122)* | 9% |
| Dentate area [sq mm] | 0.4 (0.06) | 2.1 (0.02)* | 19% |
| Density of dentate granule cells [/sq mm] | 472.5 (43.8) | 971.3 (86.2)* | 48% |
| Thickness of dentate granule cell layer | 3.5 (0.2) | 8.1 (0.5)* | 43% |
| Thickness of CA1 pyramidal cell layer | 2.8 (0.2) | 2.8 (0.2) | 100% |

* Difference from sham-irradiated $P < 0.001$
Numbers are means with SEM in parentheses
Number of cells

random for a further cell counting analysis. One or two sections from each brain were selected for this review. Sagittal sections (used to count granule cells in the olfactory bulb, hippocampus and cerebellum) were 1.9 mm lateral from the midline. Coronal sections, used to count hippocampal and cerebellar granule cells, were 3.3 mm and 11.8 mm posterior to bregma, respectively (Paxinos and Watson 1982). We counted total granular cells in the dentate gyrus using an imaging system (Bioquant System IV, R&M Biometrics, Inc., Nashville, TN) we also derived the area of the dentate gyrus, computed the cellular density of the structure and the thickness of the granule cell layer. In order to confirm that the shielding of other brain areas was sufficient, we also counted granule cells in a 0.004 mm² area in the cerebellum and olfactory bulb and measured the area of the entire cerebellum. Further, we evaluated the sparing of other more-mature, and therefore less-radiosensitive, hippocampal structures by counting the thickness of the CA1 pyramidal cell layer that was dorsal to the dentate and directly in the path of the X radiation. Unless otherwise stated, statistical analyses of histological findings used data from the sagittal sections (see Table 1).

## Results

Our histological and behavioral data suggest that hippocampal granule cell hypoplasia enhances startle amplitude and frequency and limits startle habituation.

Exposure of the neonatal rat hippocampus to ionizing radiation produced a significant [$t(6) = 14.3$, $P < 0.001$] depletion of dentate granule cells (Table 1, Fig. 1). This damage was fully quantified only in the brains randomly selected for cell counting but was easily observed in all irradiated brains. Similarly, both the areas and the granule cell densities of the irradiated dentate gyri were significantly reduced compared to those of the control rats [$t(13) = 11.0$, $P < 0.001$ and $t(13) = 7.1$, $P < 0.001$, respectively]. The specificity of this damage is illustrated by the sparing of the post-mitotic pyramidal CA1 neurons that were directly in the path of the X rays. Irradiation produced no change in the thickness of the CA1 pyramidal cell layer, yet the thickness of the dentate granule cell layer was significantly reduced [$t(13) = 9.4$, $P < 0.001$]. The granule cell populations (i.e., number of cells/unit area) of the olfactory bulb and the cerebellum were not significantly altered by the irradiation although there was a slight trend toward more cells in these structures in irradiated rats. Further, exposure to ionizing radiation did not change the total area of the cerebellum when measured in coronal section. These data suggest that the shielding of the olfactory bulb and cerebellum during the irradiation treatment was effective.

Although there were different cell counts associated with the coronal and sagittal planes of section, the histological data derived from sections in either of these planes generally suggested identical conclusions. However, when we used sagittal sections to determine the total area of the cerebellum, this analysis revealed a radiation-induced reduction in overall cerebellar size [$t(13) = 2.7$, $P < 0.1$] whereas the review of the coronal sections did not indicate this difference. This fact, in itself, is not remarkable since others (Bayer and Altman 1975), have reported different results from measures of hippocampal anatomy depending on the plane of the brain section analyzed. The cerebellum was shielded during irradiation, the density of the granule cells present was normal and the organization of cells within this structure did not resemble that reported to occur when this brain area is exposed to ionizing radiation (Brunner and Altman 1974; Altman 1986). Further, a reduction in cerebellar height (in the coronal plane) has been observed in rats with radiation-induced cerebellar damage (Altman et al. 1968) but was not present in our subjects. It may be that reduced cerebellar size in the sagittal plane, but not the coronal plane, is due to overall cranial shortening since even partial head irradiation can reduce bone growth (both within and outside the head) (Mosier and Jansons 1970).

Although the origin of the singular cerebellar change reported here is currently unclear, cerebellar damage probably played a negligible role in the production of the behavioral results reported below. There is a dissimilarity between the behaviors charac-

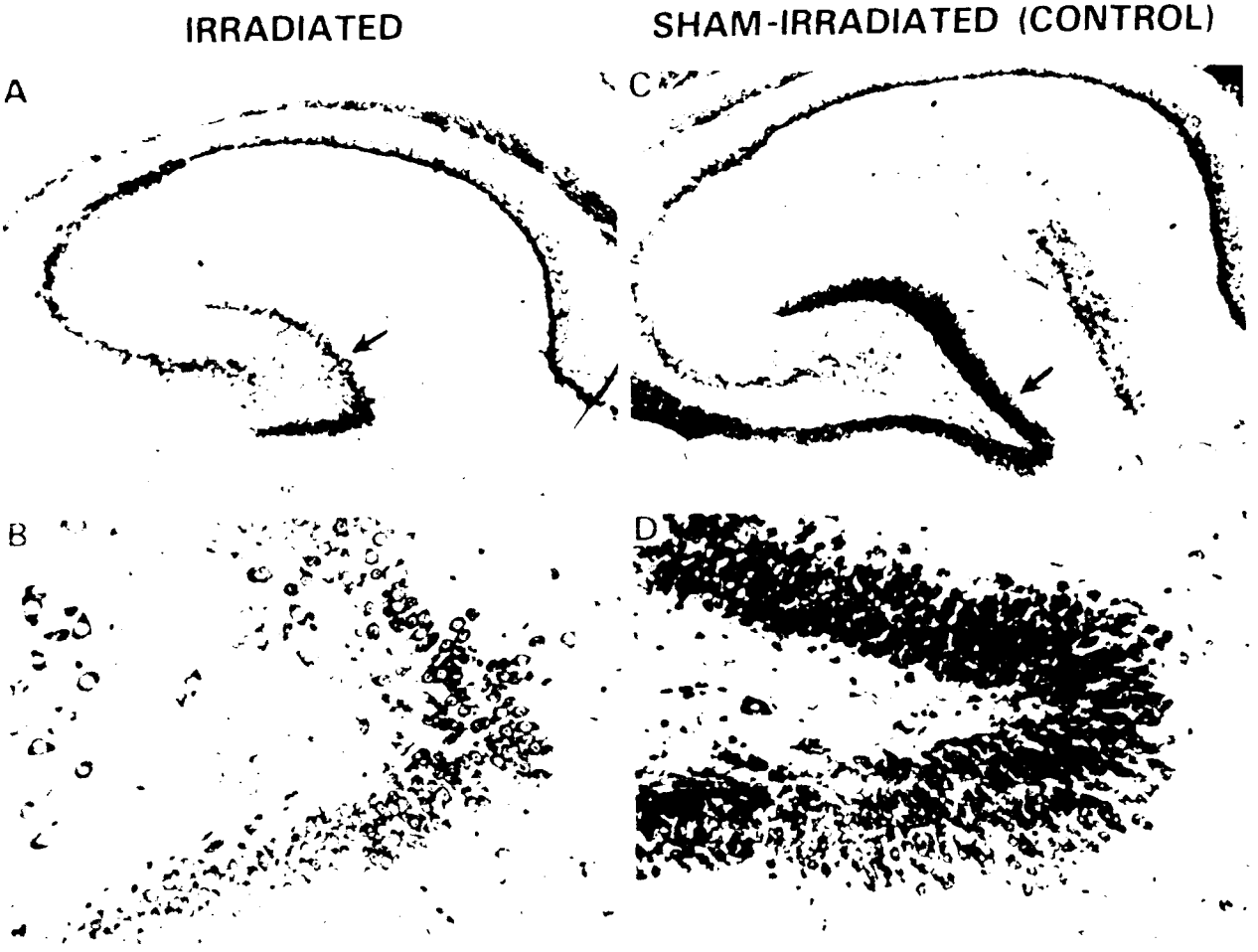


Fig. 1. Nissl stained sections of hippocampus from either an irradiated (**A**, **B**) or sham-irradiated control rat (**C**, **D**). Neonatal exposure to X-irradiation (see Experiment 1 for details) like that of Bayer and Peters [27] produced a significant reduction in size, cell number and thickness of the granule cell layer (GCL) of the dentate gyrus (DG) while sparing other adjacent brain structures. Enlargements (**B**, **D**) show the apex of the dentate gyrus in the region of the arrowheads in **A** and **C**.

teristic of cerebellar and hippocampal damage. For example, locomotor hypoactivity, observed in rats with radiation-induced cerebellar damage (Wallace and Altman 1970a, b; Brunner and Altman 1974) was not seen in rats with the same brain lesions as those reported here (Mickley et al. 1989).

Acoustic startle was markedly enhanced in subjects with radiation-induced hippocampal damage (see Fig. 2). This increase in amplitude occurred within spaced trials (tone presented each 30 s during the first session) [Mann-Whitney $U$ (150, 158) = 3498, $P < 0.001$] and within massed trials (tone presented each 15 s during the second session) [$U$ (123, 198) = 3603, $P < 0.001$].

Rats in the experimental and control groups were matched for body weight in order to attenuate any bias that this factor might have on the startle measure. However, in order to confirm our results of enhanced startle in subjects with hippocampal damage we performed an analysis of covariance which adjusted for the weight of the subjects. Within this analysis, it was clear that the mean startle responses exhibited by irradiated rats were significantly higher during both the first [$F(1,17) = 7.817$, $P = 0.012$] and second [$F(1,17) = 7.452$, $P = 0.014$] test sessions. Further, when we adjusted the data for the effect produced by the irradiation treatment it was apparent that heavier animals tended to have consistently higher startle responses: [session 1: $F(1,17) = 8.356$, $P = 0.01$; session 2: $F(1,17) = 8.699$, $P = 0.009$]. Although animal weight can influence acoustic startle measurements, our observation that startle is enhanced in rats with hippocampal damage was not confounded by this variable.

The apparent decline in acoustic startle (Fig. 2) between the first and second halves of session 1

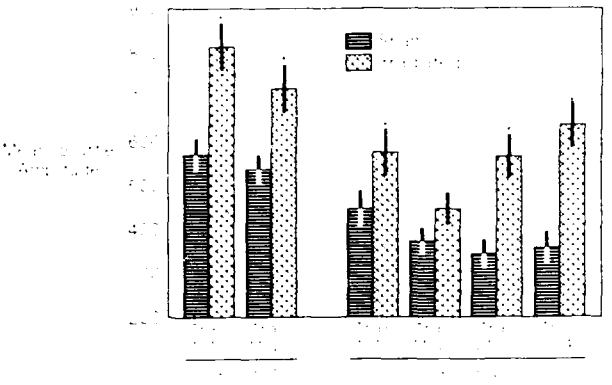

**Fig. 2.** Mean amplitude of acoustic startle responses exhibited by irradiated rats with hippocampal granule cell hypoplasia and control rats. Results from ten trial blocks are shown for each of two test sessions. In session 1, tone presentations were spaced (1 per 30 s) while in session 2 they were more frequent (massed at a rate of 1 per 15 s). Irradiated rats produced startle responses of greater amplitudes than those of controls. Through the course of the second session, habituation was observed in sham-irradiated rats but not in rats with hippocampal damage. Dispersion indicators are the standard errors of the means. * represents a statistically significant difference between the experimental and control groups at a particular time period. ($P < 0.05$, Mann-Whitney U.)

(spaced trials) was not statistically significant for either experimental or control animals (Mann-Whitney U). The responses in the first and second halves of session 2 (massed trials) revealed a statistically significant decline in the startles exhibited by the sham-irradiated rats [$U(67,56) = 2217$, $P = 0.04$]. However, for the irradiated rats with hippocampal damage, not only did startle amplitude fail to habituate during the second session but there was a trend toward potentiation of this response.

Because a rapid habituation of startle in rats with hippocampal damage has been reported (Leaton 1981) a comparison was made of the first and last 3 trials of the first 10 trial block during each session. In the first session there was a decline of 22% in startle amplitude of sham-irradiated rats [Mann-Whitney U (21,26) = 349.5, $P < 0.05$] and a decline of 8% for irradiated rats [not significant]. In the second session (massed trials) there was a 52% decline in startle amplitude for sham-irradiated rats [Mann-Whitney U (9,12) = 96, $P < 0.01$] and a 25% drop for irradiated rats [not a significant drop].

Not all tone presentations resulted in startles (i.e. movements that met the criteria established by our apparatus settings). During the first session (spaced trials) the irradiated rats tended to startle more frequently than the control rats but this difference was not statistically significant. During the second session (massed trials) the higher frequency of startle was reliable [$t(18) = 1.71$, $P = 0.05$] in the hippocampally damaged rats.

## Discussion

We report here a potentiation of the acoustic startle response in rats with radiation-induced hypoplasia of hippocampal dentate granule cells. This observation was made during 2 test sessions (separated by 4 days) in which tones were presented in either a spaced (1 per 30 s) or massed (1 per 15 s) format. Habituation of the acoustic startle response was not observed in animals with hippocampal damage.

The method of fractioned partial-brain x-irradiation used here has been shown to produce a selective reduction in the number of granule cells in the dentate gyrus (see present data and also: Hicks and D'Amato 1969; Bayer and Altman 1975; Bayer and Peters 1977). However, this damage in the neonatal hippocampus may also cause secondary anatomical changes. Zimmer and his colleagues (1985, 1986) have shown that the brain may compensate for this early radiation-induced damage to the hippocampal granule cells by stimulating dendritic growth. Their results demonstrate that a reduction of a specific neuronal population can induce: (1) a compensatory increase in the neuropil layers containing the dendrites of the remaining neurons, (2) a corresponding relative increase in their axonal projections, and (3) a shift and expansion of afferent projections to an adjacent neuronal population. Thus, although our hippocampal radiation produces damage specific to the granule cells, subsequent brain changes, in reaction to this initial damage, may produce more-pervasive changes in neuroanatomy. Although these data reflect changes in hippocampal afferents and intra-hippocampal neuroanatomy, the most dramatic and direct radiogenic damage observed in our experiment can be found within the granule cell layer of the dentate gyrus.

Some authors (Groves et al. 1974; Leaton 1981) have previously reported that lesions of the hippocampus do not consistently alter startle, while others (Coover and Levine 1972) have found increased acoustic startle after this surgery. The lesion/test interval may be a distinguishing feature between experiments that have found potentiated startle amplitudes and those studies not reporting these effects in rats with hippocampal damage. Enhanced startle has been found when there was a significant interval between the brain lesion and the startle test. In both the current experiment and that of Coover and Levine (1972) the lesion/test interval was long (approximately 194 and 70 days, respec-

tively). On the other hand, Leaton (1981) used a shorter interval (approximately 14 days) between lesioning and testing and reported little change in acoustic startle after hippocampectomy. These results paralled other data suggesting that acute startle changes following lesions of the inferior colliculus may be opposite those measured later (for review see Davies 1984). Still, a recent study reporting an early enhancement of acoustic startle 1 week after hippocampal damage has brought into question the universality of this lesion-test latency effect (Hilson et al. 1987).

Our startle data also suggest that the habituation recorded in control animals during the full course of 30 tone presentations was not evident in irradiated rats with hippocampal damage. In fact, experimental subjects exhibited a trend toward potentiation of their startle responding in the second half of our test session. On the surface our results appear to differ from those of Groves et al. (1974) and Leaton (1985) who have reported normal within-session startle habituation in rats with hippocampal damage. A closer analysis of the data helps reconcile these apparently divergent results. The habituation reported by other laboratories was evident within the first 20 stimulus presentations. Our startle sensitization required more than 20 trials to observe. Review of our data collected during the first 10 trials of each test session also revealed a tendency for sham-irradiated animals to habituate to the acoustic stimulus. While not statistically significant, a similar trend was observed during the first 10 startle trials in the irradiated subjects as well. However, on subsequent trials, startle amplitudes increased in the animals with hippocampal damage while startles of control rats continued to gradually decline in magnitude. Independent of these within-session comparisons, we also analyzed between-session changes in startle. Although a trend toward a decline was observed in both experimental and control subjects, there was no statistically significant change in startle amplitude between our test sessions. These data are consistent with others that have not detected recovery of habituated startle responding between test sessions (Leaton 1981). It should be noted that rats with radiation-induced hippocampal damage readily exhibit habituation of spontaneous locomotion within the same time parameters that we observed little startle habituation (Mickley et al. 1989). However, others have commented that habituation of exploratory behavior and habituation of elicited reflex-like responses depend on different underlying mechanisms and that hippocampal lesions do not produce general habituation deficits (for review see Leaton 1985).

The primary distinguishing features between the present startle study and others are the timing, method and anatomical result of the hippocampal lesion procedure. Our radiation-induced hippocampal lesion was produced in neonates and primary damage was confined to the granule cells of the dentate gyrus. Others (Leaton 1981; Groves et al. 1974; Coover and Levine 1972), relying on aspiration and electrolytic lesion techniques, have removed most of the hippocampus as well as portions of the cerebral cortex of the adult animal. Using a third procedure, additional investigators have used the neurotoxin colchicine to produce fairly selective damage to the granule cells of the adult hippocampal dentate gyrus. With neuroanatomical changes similar to the radiation-induced damage reported here, colchicine-injected rats have exhibited a significant enhancement of acoustic startle reactivity in one study (Hilson et al. 1987), but not in another that used auditory stimulus parameters different from our own (Walsh et al. 1986). Future experiments that systematically manipulate startle parameters as well as the timing and extent of hippocampal lesions may further develop our understanding of the role of hippocampus in startle responding. According to our data, however, the granule cells of the hippocampus exert an inhibitory influence on the primary acoustic startle circuit of the brainstem. With the loss of this tonic inhibitory influence, startle responding is greater in amplitude, more frequent and less likely to habituate.

*Acknowledgements.* The authors recognize the helpful technical assistance provided by Ms. Maureen A. Malvihill and Mr. Thomas J. Nemeth. The dosimetry and irradiations were performed by Mr. Douglas Eggleston and Mr. Ernest Golightly. Statistical advice was provided by Mr. William Jackson. We thank Ms. Lilly Heiman-Ackah for her excellent histological assistance. This research was supported by the Armed Forces Radiobiology Research Institute, Defense Nuclear Agency, under work unit B3363. Views presented in this paper are those of the authors and do not reflect official Defense Nuclear Agency position or policy unless so designated.

## References

Ahlsen G (1985) An electrophysiological [illegible] In: Lewis M, Sullivan J (eds) [illegible] Plenum Press, New York, pp 283–302

Ahlsen G, Andersson W, Wright K (1984) [illegible] Exp Neurol [illegible]

Ahlsen G, Rogers RC, Rose SA [illegible] Brain Res [illegible]

Bell SA, Altman J, Rogers RC [illegible] Exp Neurol [illegible]

Bayer SA, Peters PL (1977) A method for X-irradiating selected brain regions in infant rats. Brain Res Bull 2: 153–156

Bayer SA, Brunner RL, Hine R, Altman J (1973) Behavioural effects of interference with the postnatal acquisition of hippocampal granule cells. Nature New Biol 242: 222–224

Blanchard RJ, Hall RA (1988) Effects of limbic lesions on passive avoidance and reactivity to shock. J Comp Physiol Psychol (in press)

Brunner RL, Altman J (1974) The effects of interference with the maturation of the cerebellum and hippocampus on the development of adult behavior. In: Stein DG, Rosen JJ, Butters N (eds) Plasticity and recovery of function in the central nervous system. Academic Press, New York, pp 129–148

Casarett GW (1980) Radiation histopathology, Vol II. CRC Press, Boca Raton

Coover GD, Levine S (1972) Auditory startle response of hippocampectomized rats. Physiol Behav 9: 75–77

Davis M (1984) The mammalian startle response. In: Eaton RC (ed) Neural mechanisms of startle behavior. Plenum Press, New York London, pp 287–351

Douglas RJ (1967) The hippocampus and behavior. Psychol Bull 67: 416–442

Eaton RC (ed) (1984) Neural mechanisms of startle behavior. Plenum Press, New York London

Groves PM, Wilson CJ, Boyle RD (1974) Brain stem pathways, cortical modulation, and habituation of the acoustic startle response. Behav Biol 10: 391–418

Handelmann GE, Olton DS (1981) Spatial memory following damage to hippocampal CA3 pyramidal cells with kainic acid: impairment and recovery with preoperative training. Brain Res 217: 41–58

Hicks SP (1958) Radiation as an experimental tool in mammalian developmental neurology. Physiol Rev 38: 337–356

Hicks SP, D'Amato CJ (1966) Effects of ionizing radiations on mammalian development. In: Woollam DHM (ed) Advances in teratology. Logos Press, London, pp 195–250

Isaacson RL (1974) The limbic system. Plenum Press, New York

Isaacson RL, Wickelgren WO (1962) Hippocampal ablation and passive avoidance. Science 138: 1104–1106

Isaacson RL, Douglas RJ, Moore RY (1961) The effect of radical hippocampal ablation on acquisition of avoidance responses. J Comp Physiol Psychol 54: 625–628

Kimble DP (1968) Hippocampus and internal inhibition. Psychol Bull 70: 285–295

LaBossiere E (1976) Histological processing for the neural sciences. Thomas, Springfield, Ill

Landis C, Hunt WA (1939) The startle pattern. Farrar and Rinehart, New York

Leaton RN (1981) Habituation of startle response, lick suppression, and exploratory behavior in rats with hippocampal lesions. J Comp Physiol Psychol 95: 513–526

Means LW, Leander JD, Isaacson RL (1971) The effects of hippocampectomy on alternation behavior and response to novelty. Physiol Behav 6: 17–22

Mickley GA, Ferguson JL, Nemeth LJ, Mulvihill MA, Alderks CE (1989) Spontaneous perseverative turning and other behavioral changes in rats with radiation-induced hippocampal damage. Behav Neurosci (in press)

Mosier HD, Jansons RA (1970) Effect of x-irradiation of selected areas of the head of the newborn rat on growth. Radiat Res 43: 92–104

O'Keefe J, Nadel L (1978) The hippocampus as a cognitive map. Oxford University Press, Oxford

Paxinos G, Watson C (1982) The rat brain in stereotaxic coordinates. Academic Press, Sidney

Teitelbaum H, Milner P (1963) Activity changes following partial hippocampal lesions in rats. J Comp Physiol Psychol 56: 284–289

Tilson HA, Rogers BC, Grimes L, Harry GJ, Peterson NJ, Hong JS, Dyer RS (1987) Time-dependent neurobiological effects of colchicine administered directly into the hippocampus of rats. Brain Res 408: 163–172

Wallace RB, Altman J (1970a) Behavioral effects of neonatal irradiation of the cerebellum. I. Qualitative observations in infant and adolescent rats. Dev Psychobiol 2: 257–265

Wallace RB, Altman J (1970b) Behavioral effects of neonatal irradiation of the cerebellum. II. Quantitative studies in young-adult and adult rats. Dev Psychobiol 2: 266–272

Walsh TJ, Schulz DW, Tilson HA, Schmechel DE (1986) Colchicine-induced granule cell loss in rat hippocampus: selective behavioral and histological alterations. Brain Res 398: 23–36

Weisbroth SH (1979) Bacterial and mycotic diseases. In: Baker HJ, Lindsey JR, Weisbroth SH (eds) The laboratory rat: biology and diseases, Vol I. Academic Press, New York, pp 206–208

Wilkins DE, Hallett M, Wess MM (1986) Audiogenic startle reflex of man and its relationship to startle syndromes. Brain 109: 561–573

Zimmer J, Sunde N, Sorensen I (1985) Reorganization and restoration of central nervous connections after injury: a lesion and transplant study of the rat hippocampus. In: Will BE, Schmitt P, Dalrymple-Alford JC (eds) Brain plasticity, learning and memory. Plenum Publishing, London, pp 505–518

Zimmer J, Laurberg S, Sunde N (1986) Non-cholinergic afferents determine the distribution of the cholinergic septohippocampal projection: a study of the AChE staining pattern in the rat fascia dentata and hippocampus after lesions, X-irradiation, and intracerebral grafting. Exp Brain Res 64: 158–168

Received April 13, 1988. Accepted August 22, 1988

[illegible]
[illegible]

0891-5849/89 $3.00 + .00
1989 Pergamon Press plc



*Original Contribution*

# OXIDATIVE DAMAGE IN THE GUINEA PIG HIPPOCAMPAL SLICE

TERRY C. PELLMAR* and KATHRYN L. NEFF

*Physiology Department, Armed Forces Radiobiology Research Institute, Bethesda, MD 20814, U.S.A.*

*Received* 3 *May* 1988; *Revised* 29 *July* 1988; *Accepted* 8 *August* 1988)

**Abstract**—Free radicals and active oxygen compounds are implicated in brain ischemia and head trauma. Previous studies have shown that free radicals, generated by radiation and through the Fenton reaction, produce both synaptic and postsynaptic damage in the hippocampal brain slice. To evaluate the contribution of oxidation to the observed damage, the actions of the oxidants, chloramine T and N-chlorosuccinimide (NCS), were studied on electrophysiological responses in the hippocampal slice isolated from the brains of guinea pigs. Electrical stimulation of afferents to neurons of the CA1 region of hippocampus evoked a population postsynaptic potential (population PSP) in the dendritic layer and a population spike in the cell body layer. Chloramine-T (25–500 $\mu$M) and NCS (750–4000 $\mu$M) decreased the population spike in a dose dependent manner (ED$_{50}$ = 125 $\mu$M and 1100 $\mu$M, respectively). Input-output curves revealed that both the population spike and the population PSP were significantly reduced with both oxidants, but, the ability of the population PSP to produce a population spike was not impaired. These studies suggest that oxidation reactions can account for the synaptic component of the damage produced by free radicals but can not account for the postsynaptic effects.

**Keywords**—Chloramine-T, N-chlorosuccinimide, Oxidation, Free radical, Hippocampus.

## INTRODUCTION

Active oxygen compounds are generated normally in vivo[1–3] but the presence of superoxide dismutase, catalase, peroxidase and a variety of antioxidants limit the concentrations to non-toxic levels. In the event of an ischemic attack or head trauma, levels of these active oxygen species increase,[4] however the source of these compounds is unclear. Peroxide and superoxide could be generated from xanthine oxidase in local endothelial cells[5–7]. Beckman et al.[4] calculated concentrations of superoxide and peroxide as high as 70 $\mu$M/min and 170 $\mu$M/min, respectively, following an ischemic episode. Active oxygen compounds could also be secreted by the microglia invading a region of injury.[8] Another possible source is the generation of free radicals in neurons during reperfusion when a burst of oxidative metabolism results in the release of incompletely reduced oxygen (i.e., superoxide and peroxide).[9]

Previous studies have shown that active oxygen species produce functional damage in neurons.[10–12] Hydrogen peroxide and ionizing radiation decrease synaptic efficacy (synpatic damage) and impair mechanisms of spike generation (postsynaptic damage). The evidence suggests that the molecular mechanisms underlying synaptic and postsynaptic damage are different.[12] In the present study, the oxidants chloramine-T and N-chlorosuccinimide were tested to evaluate the contribution of an oxidation reaction to free radical damage. The results indicate that the oxidants can account for impairment of synaptic function but not for postsynaptic deficits.

## MATERIALS AND METHODS

Hippocampal slices were prepared from the brains of euthanized male Hartley guinea pigs as previously described.[13] The slices (400–450 $\mu$m thick) were incubated in artificial cerebrospinal fluid (ACSF) (composition in mM: 124 NaCl, 3 KCl, 2.4 $CaCl_2$, 1.3 $MgSO_4$, 1.24 $KH_2PO_4$, 10 glucose, 26 $NaHCO_3$, equilibrated with 95% $O_2$–5% $CO_2$) at room temperature for 1–2 hours to allow recovery from dissection. A slice was then transferred to a submerged slice recording chamber and continually perfused (1–2 ml/min) with oxygenated ACSF. All experiments were done at 30 ± 1°C. Solutions of chloramine-T (CT) and N-

*All correspondence and reprint requests should be addressed.

chlorosuccinimide (NCS) (Sigma Chemical Company) were prepared fresh daily.

Potentials were recorded with a high gain DC amplifier and were digitized, stored, and analyzed on an LSI 11/23 minicomputer. A bipolar stainless steel stimulating electrode (DKD) was positioned in stratum radiatum to activate the Schaffer collateral pathway as well as other afferents to the CA1 pyramidal cells. Constant current stimuli (0.1–1 mA, 200 $\mu$s) were provided at 0.20 Hz. Field potentials were recorded using glass microelectrodes filled with 2M NaCl and having a resistance of less than 10 MΩ. One recording electrode was placed in the cell body layer of CA1 region to record the somatic response (population spike). The population spike is the extracellularly recorded action potential occurring synchronously in a population of CA1 pyramidal cells. In some experiments, a second recording electrode was positioned in the stratum radiatum to record the dendritic response (population postsynaptic potential, population PSP) and the afferent volley. The population PSP is the extracellularly recorded synaptic potential activated synchronously in the dendrites of CA1 pyramidal cells. The afferent volley is the potential produced by the activation of fibers in the stimulated pathway.

Following placement of the electrodes, baseline recordings were obtained for a minimum of 30 min to ensure stability of the tissue. Stimulus intensity was set to a value that produced approximately a half-maximal response. If during this period the responses changed substantially, the experiment was discarded. A dose of either chloramine-T or NCS was then applied

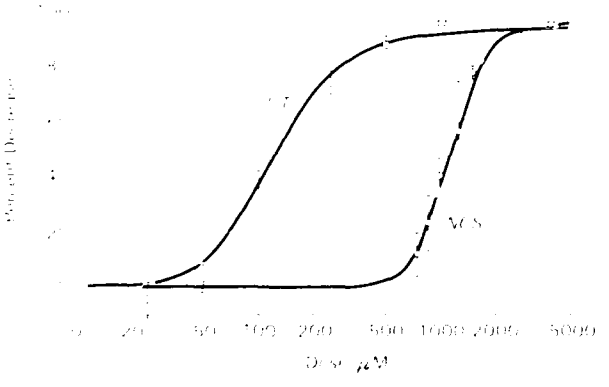


Fig. 1. Dose response curves for Chloramine-T (CT) and NCS. Varying doses of chloramine-T and NCS were applied to the hippocampal brain slice for 30 min. The percent decrease in the population spike at 30 min in comparison with control (i.e., before drug) is plotted vs. the dose of drug used. The number of experiments with Chloramine-T at 25 $\mu$M = 6; 50 $\mu$M = 7; 100 $\mu$M = 6; 250 $\mu$M = 7; 500 $\mu$M = 5; 1000 $\mu$M = 5. The number of experiments with NCS at 625 $\mu$M = 5; 750 $\mu$M = 4; 875 $\mu$M = 6; 1000 $\mu$M = 12; 1250 $\mu$M = 4; 1500 $\mu$M = 4; 4000 $\mu$M = 8. Squares = Chloramine-T. Circles = NCS.

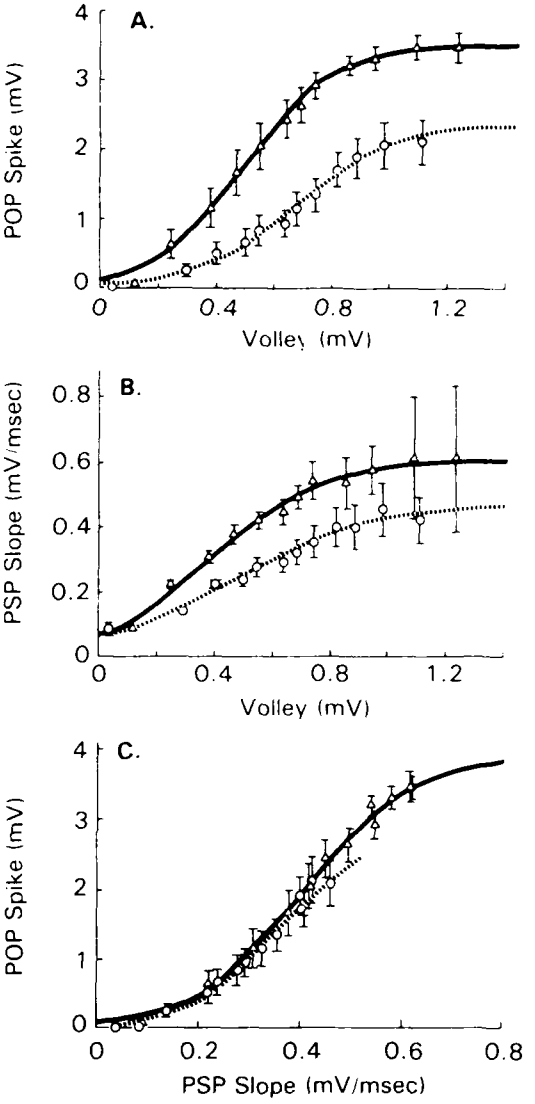


Fig. 2. Input-output curves averaged for 8 slices exposed to 100 $\mu$M chloramine-T. Control curves: solid line; chloramine-T curves: dotted line. A: Graph shows that chloramine-T reduces the population spike for [illegible] afferent volley amplitude. B: Chloramine-T decreases [illegible]y of the afferent volley to produce a synaptic respon[illegible]amine-T has no affect on the ability of a PSP to evoke an action potential. Chloramine-T causes synaptic but no postsynaptic defect.

continuously for thirty minutes. Electrophysiological responses were continuously monitored throughout this period; every 5 min 8 traces were averaged. Drug was then washed off and the tissue was perfused with ACSF for another 30 min. To determine the dose-response relationships, a minimum of four experiments at each dose of NCS and chloramine-T were performed. The effectiveness of the drug was expressed as the percentage decrease in amplitude at the 30 min time point as compared to control amplitude. The 30 min time point was chosen for 2 reasons: 1) The drug effects

frequently appeared to level off within this time period and 2) this protocol allowed comparison with previous experiments on hydrogen peroxide using a 30 min exposure. All experiments at a single dose were averaged and standard errors (SEM) were calculated.

Input-output (I-O) curves were constructed for each drug at a dose that produced approximately a 40% decrease in population spike amplitude. Somatic and dendritic traces ($n = 4$) were averaged at each stimulus intensity ranging from 0.1 to 1.0 mA. The data from 5 experiments for NCS and for 8 experiments for chloramine-T were averaged to obtain composite curves. The I-O curves consisted of three relationships: 1) volley vs. population spike 2) volley vs. population PSP, and 3) population PSP vs. population spike. The volley vs. population spike curve reflects the ability of the presynaptic activity to elicit an action potential in the postsynaptic cell. The population spike vs. population PSP reflects primarily postsynaptic mechanisms (i.e., the effectiveness of a postsynaptic depolarization to evoke an action potential). The volley vs. population PSP reflects the synaptic mechanisms (i.e., the ability of presynaptic activity to produce a synaptic potential). Thus, analysis of these curves provides information on the mechanisms of oxidative damage. The input-output data were computer-fitted with the equation for a sigmoid curve and analyzed as previously described. Differences between control and treated curves were tested for significance by comparing the residual sum of squares for the individual curves with the residual sum of squares for a curve fit to a composite of control and test data. Significance was accepted at $p = 0.05$.

## RESULTS

Chloramine-T decreased the amplitude of the population spike elicited by orthodromic stimulation of CA1 in a dose dependent manner (Fig. 1). Low doses of chloramine-T (25 $\mu$M) produced little or no effect during or after exposure to the drug. Intermediate doses (50–200 $\mu$M) noticeably decreased the amplitude of the population spike during the 30 minute exposure to chloramine-T. The response recovered approximately to its original size within a 30 min period of wash with normal ACSF. When exposed to higher doses of chloramine-T (250–1000 $\mu$M), the amplitude of the population spike decreased sharply during exposure and remained depressed throughout the wash. The dose response curve (Fig. 1) shows that the concentration for a half maximal effect is 125 $\mu$M. Chloramine-T is maximally effective at doses greater than about 500 $\mu$M.

The dose response curve for N-chlorosuccinimide (NCS) (Fig. 1) shows that NCS required higher concentrations than chloramine-T to produce comparable damage. The onset and reversal of NCS action was very similar to, although slightly more gradual than, that of chloramine-T. The dose of NCS to produce a half maximal effect was approximately 1.1 mM. Doses of 2 mM and greater caused a maximal decrease in the population spike amplitude.

Input-output (I-O) experiments were done to determine the site of damage of the oxidants. The dose of chloramine-T chosen for these experiments (100 $\mu$M) was expected from the dose response curve to produce, on the average, a 40% decrease in the population spike. The I-O curves ($n = 8$) show that for a given afferent volley input, both the population spike (Fig. 2A) and the popultion PSP (Fig. 2B) were significantly reduced by chloramine-T. The ability of the population PSP to produce a population spike, however, was not altered (Fig. 2C). The population PSP was equally effective in evoking a spike before and during exposure to the oxidant. Fig. 3 shows sample traces from a typical slice

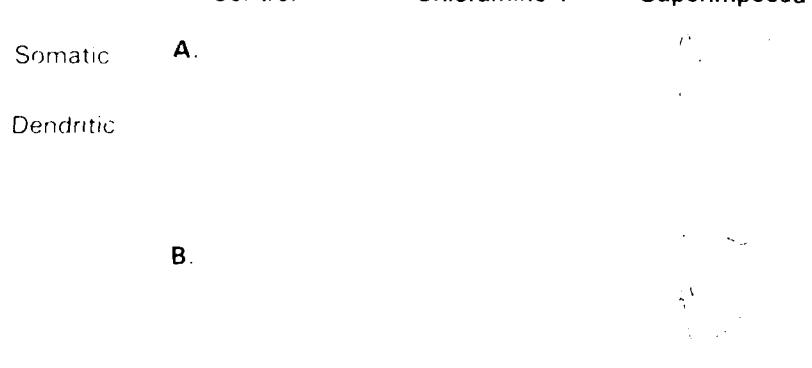


Fig. [illegible] Somatic and dendritic population spikes recorded from a single CA1 pyramidal cell before (control), during exposure to 100 μM chloramine-T, and after 30 min wash with normal ACSF. Control (left) and chloramine-T (middle) traces are superimposed on the right. A: Somatic spike recorded in stratum pyramidale. Chloramine-T causes a decrease in the amplitude of the population spike. B: Dendritic population PSP recorded in stratum radiatum. Chloramine-T causes a decrease in the amplitude of the population PSP. Calibration bars apply to all traces. Calibration bars apply to all traces. [illegible]

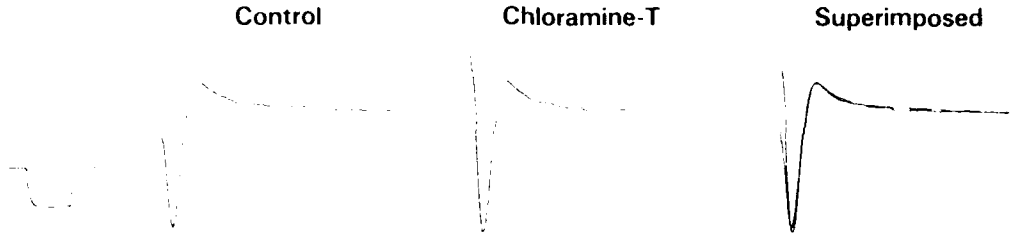


FIG. 4. The antidromic spike was evoked by stimulation of the alveus and recorded in the cell body layer of CA1. It was unaffected by 250 μM chloramine-T (center trace) and can be seen best when the traces are superimposed (right trace). Calibration (square wave on lower left): 1 mV, 2 ms.

treated with 100 μM chloramine-T. Both population spike and population PSP were reduced. If, while still in chloramine-T, stimulus strength was increased to produce a population PSP comparable to control, the evoked population spike is comparable in amplitude (Fig. 3B). These data suggest that the observed decrease in the population spike with exposure to chloramine-T is due completely to the reduction in the synaptic response.

Previous reports [ ] indicate that chloramine-T at similar doses removes sodium inactivation, broadening the sodium action potential in squid, crayfish, frog and toad axons. To evaluate the actions of chloramine-T directly on the sodium action potential in this preparation, *the effect on the antidromically elicited* population spike was evaluated. Axons of the CA1 pyramidal cells were stimulated with a bipolar stainless steel electrode in the alveus. The resulting antidromic spike was recorded from the cell body layer of CA1. At a dose that maximally reduced the synaptically-activated (orthodromic) population spike (250 μM), chloramine-T had no effect on the antidromic action potential (Fig. 4) ($n = 4$).

Input output experiments were repeated with NCS at a dose of 1.0 mM ($n = 5$). As with chloramine-T, the population spike (Fig. 5A) and the population PSP (Fig. 5B) evoked by equivalent afferent volleys were both reduced. Yet population PSPs of equivalent size, before and during exposure to NCS, produced equivalent population spikes (Fig. 5C). NCS reduced the population PSP *for the same size afferent volley, but* the effectiveness of that PSP was unaltered. As with chloramine-T, *these results demonstrate that only synaptic damage and no postsynaptic deficits were produced by NCS.*

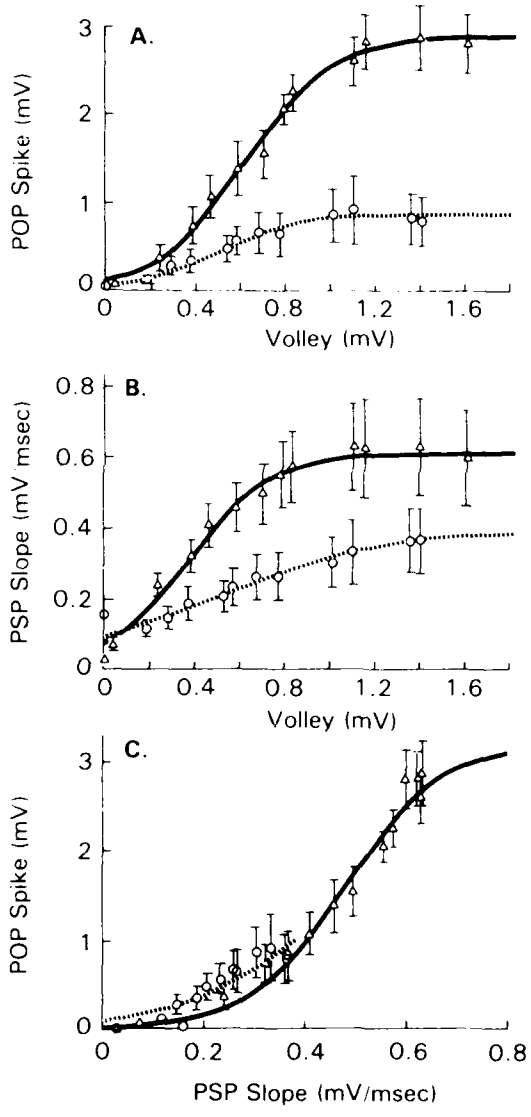


FIG. 5. Input output curves averaged for 8 slices exposed to 1 mM NCS. *The results are identical to those obtained for chloramine-T.* Control curves: solid line. NCS curves: dotted line. A: For a given afferent volley, the population spike is decreased. B: For a given afferent volley, the synaptic response is decreased. C: For a given synaptic response, the evoked population spike is the same both in control and in NCS. NCS causes only synaptic damage and no postsynaptic damage.

## DISCUSSION

The oxidants, chloramine-T and N-chlorosuccinimide, were observed to cause a decrease in the orthodromic potentials in the CA1 region of the hippocampus in vitro. While the synaptic potentials were reduced

in size, they were not impaired in their ability to evoke action potentials in the postsynaptic neurons. The reduced synaptic efficacy occurred at doses that did not alter the antidromically evoked spike in the same neuronal population.

Chloramine-T and NCS have been reported to remove inactivation of the sodium current in the giant axon of squid [17] and crayfish [7] and in the myelinated axons of the toad [18] and frog.[19] Although many of the studies used chloramine-T in higher doses (1 to 10 mM), Wang [18] reported that in toad fibers, a dose as low as 89 $\mu$M was effective in broadening the action potential 3-fold after only 7 min. Longer exposures further prolonged the action potential and began to reduce the amplitude. In contrast, in the present study in the hippocampal slice preparation 250 $\mu$M chloramine-T for 30 min did not alter the antidromic spike which is predominantly a sodium-dependent action potential. One major difference between the present experiments and those testing chloramine-T in axons is that in the present study, potassium currents were not pharmacologically blocked. The presence of the potassium component of the action potential could obscure an action of the oxidants to broaden the action potential through removal of sodium inactivation. In two studies [7,17] chloramine-T (1–14 mM) was also found to decrease the potassium current in toad and squid axons. Neither decreased sodium inactivation or decreased potassium current can account for the decrease in synaptic efficacy seen in the present study. If anything, one would predict that both mechanisms would increase the duration of the action potential, increase the presynaptic calcium influx and enhance transmitter release.

Previous studies [1,2] showed that ionizing radiation and hydrogen peroxide could produce damage in an isolated neuronal system. In an aqueous environment ionizing radiation produces free radicals including $^{\cdot}OH$ and $O_2^{\cdot-}$. Hydrogen peroxide can react with iron and through the Fenton reaction produce hydroxyl free radicals. Both procedures decreased synaptic responses produced by orthodromic stimulation of stratum radiatum suggesting either a decrement in presynaptic release or impaired function of the postsynaptic receptor ionophore complex (synaptic damage). In addition, the synaptic potentials that were elicited were less capable of evoking an action potential in the hippocampal neurons suggesting that membrane properties of the soma or axon hillock were altered in some way (postsynaptic damage). Two separate mechanisms were postulated for these two actions since they showed very different dependencies on the dose rate of radiation. Since free radicals produced by ionizing radiation (such as the hydroxyl free radical) and hydrogen peroxide are oxidants, the contribution of an oxidative reaction to the observed damage was considered.

Chloramine-T and NCS are oxidizing agents that appear to be fairly specific for methionine and cysteine residues of membrane proteins.[17] These actions are similar to the oxidizing effects of hydrogen peroxide.[7] The oxidants in the present study were able to produce damage in the hippocampal brain slice, but they could not completely mimic the effects of radiation and peroxide. This provides further support for the hypothesis that two separate mechanisms underlie the synaptic and the postsynaptic damage produced by radiation and by peroxide. The present study showed that the oxidants specifically impaired synaptic efficacy, suggesting that an oxidation reaction could account for the peroxidative and radiation damage at this site. Yet, the oxidants had no effect on postsynaptic generation of action potentials. The limited dose rate dependence of radiation damage [2] and the iron potentiation of peroxide damage [1] are also more consistent with a lipid peroxidation mechanism than with an oxidation reaction.

In conclusion, the observations reported here suggest that oxidative damage may account for the synaptic component of free radical damage in the nervous system but can not account for the postsynaptic deficits.

*Acknowledgement*—We thank Dr. P. Gunter Smith for helpful comments on the manuscript. Supported by the Armed Forces Radiobiology Research Institute, Defense Nuclear Agency, under work unit 00105. Views presented in this paper are those of the authors, no endorsement by the Defense Nuclear Agency has been given or should be inferred. Research was conducted according to the principles enunciated in the "Guide for the Care and Use of Laboratory Animals" prepared by the Institute of Laboratory Animal Resources, National Research Council.

## REFERENCES

1. Pellmar T., Electrophysiological correlates of peroxide damage in guinea pig hippocampus in vitro, *Brain Res.* **346**, 377–381 (1986).
2. Pellmar T., Peroxide alters neuronal excitability in CA1 region of guinea pig hippocampus in vitro, *Neurosci. Lett.* **23**, 447–456 (1981).
3. Tolliver T. M., Pellmar T. C., Effects of ionizing radiation on hippocampal excitability, *Radiation Res.* **112**, 558–563 (1987).
4. Smet, P. M., Heikkila, R. E., Cohen, G., Hydrogen peroxide production by rat brain in vivo, *J. Neurochem.* **34**, 1421–1428 (1980).
5. Fridovich I., Superoxide radical: an endogenous toxicant, *Ann. Rev. Pharmacol. Toxicol.* **23**, 239–257 (1983).
6. Halliwell, B., Gutteridge, J. M. C., Oxygen radicals and the nervous system, *Trends in Neurosci.* **8**, 22–26 (1985).
7. Demopoulos, H. B., Flamm, E., Seligman, M., Pietronigro, D. D., Oxygen free radicals in central nervous system ischemia and trauma. In: Xotor, A. P. (ed.), *Pathophysiology*, New York: Academic Press, 1982, pp. 177–188.
8. Kogure, K., Arai, H., Abe, K., Nakano, M., Free radical damage of the brain following ischemia, *Prog. Brain Res.* **63**, 237–250 (1985).
9. Beckman, J. S., Ischiropoulos, H., Beckman, J. K., Freeman, B. A. and Rosen, G. M., Oxygen radicals and xanthine oxidase, *Ann. N.Y.*

[illegible] *Neurosci. Abstr.* **13** 1498 abstr. 598.

Rosen, G. M., Rauckman, B. S. Detection of superoxide generated by endothelial cells. *Proc. Natl. Acad. Sci. USA* **81** 2265–2267, 1984.

Saran, M., Gilbert, D. L. Protection by superoxide dismutase of CNS neurotoxicity. *Neurochem. Int.* **7** 283–288, 1985.

Wang, G. K. Blockade by chloramine-T of sodium channel activation and fast inactivation in voltage-clamped frog myelinated fibers. The oxidant chloramine-T. *J. Physiol.* **346** 277–290, 1984.

Wang, G. K. Modification of sodium channel inactivation in [illegible] by the oxidant chloramine-T. *Biochim. Biophys. Acta* **946** 125–138, 1988.

Wang, G. K., Brodwick, M. S., and Eaton, D. C. Removal of sodium channel inactivation in squid axon by the oxidant chloramine T. *J. Gen. Physiol.* **86** 289–302, 1985.

Drews, G. Effects of chloramine T on charge movement and reaction of open channels in frog nodes of Ranvier. *Pflügers Arch.* **409** 251–257, 1987.

Huang, L. M. C., Tanguy, J., Yeh, J. Z. Removal of sodium inactivation and block of sodium channels by chloramine-T in crayfish and squid axons. *Biophys. J.* **52** 155–163, 1987.

Means, G. E., Feeny, R. E. Chemical modification of proteins. San Francisco: Holden-Day, 1971.

Schechter, Y., Burstein, Y., and Patchornik, A. Selective oxidation of methionine residues in proteins. *Biochemistry* **14** 4497–4502, 1975.

Life Sciences, Vol. 44, pp. 1185-1191 Pergamon Press
Printed in the U.S.A.



# RADIATION-INDUCED VOLATILE HYDROCARBON PRODUCTION IN PLATELETS

E. Radha*, Y. N. Vaishnav, K. S. Kumar, and J. F. Weiss

Radiation Biochemistry Department, Armed Forces Radiobiology Research Institute, Bethesda, MD 20814-5145

(Received in final form February 20, 1989)

## Summary

Generation of volatile hydrocarbons (ethane, pentane) as a measure of lipid peroxidation was followed in preparations from platelet-rich plasma irradiated in vitro. The hydrocarbons in the headspace of sealed vials containing irradiated and nonirradiated washed platelets, platelet-rich plasma, or platelet-poor plasma increased with time. The major hydrocarbon, pentane, increased linearly and significantly with increasing log radiation dose, suggesting that reactive oxygen species induced by ionizing radiation result in lipid peroxidation. Measurements of lipid peroxidation products may give an indication of suboptimal quality of stored and/or irradiated platelets.

Thrombocytopenia plays an important role in the development of the postirradiation hemorrhagic syndrome (1). Although destruction of platelet precursors in bone marrow is a major effect of high-dose radiation exposure, the effects of radiation on preformed platelets are unclear. The latter is also of concern with respect to blood-banking practices since platelets are often irradiated at doses in the range of 20-50 Gy before transfusions to prevent graft-versus-host disease. With increasing emphasis on allogenic and autologous bone marrow transplantation, transfusions of irradiated platelets are likely to rise. Transfusions of platelets were critical in the treatment of Chernobyl radiation-accident victims (2).

The effect of in vitro irradiation of platelets has been the subject of a number of studies, but there is no consensus on the subject. The survival of platelets exposed to radiation doses up to 750 Gy before transfusion remained unchanged (3,4). Another study, however, indicated that irradiation with 50 Gy before transfusion to normal subjects resulted in decreased platelet recovery, although platelet function did not appear to be affected (5). In most in vitro studies of irradiated platelets, no changes in the structural, functional, and metabolic properties of platelets were observed even at high radiation doses (6-8). However, irradiation of experimental animals appears to alter the function of surviving platelets (1,9).

Radiation injury is most often attributed to cellular DNA damage, and since platelets do not have nuclei they are good models for studying the effects of radiation on the functional characteristics of membranes. Free radicals, especially the hydroxyl radical generated during radiation exposure, can promote membrane lipid peroxidation (10) and alter the properties of cell membranes. Irradiation of platelets (100 Gy and greater) under conditions promoting hydroxyl radical or hydrogen

*Present address: DCLD, Food and Drug Administration, 8757 Georgia Ave., Silver Spring, MD 20910

0024-3205/89 $3.00 + .00

peroxide formation resulted in inhibition of ADP-induced platelet aggregation (11). Whole-body irradiation has been shown to alter the lipid composition and arachidonic acid metabolism in rat platelets (9). Lipid peroxidation is more pronounced in old than in young circulating platelets, and it has been suggested that this may be a cause of platelet aging (12).

In the present study, we quantified radiation-induced lipid peroxidation in vitro by the evolution of volatile hydrocarbons, a method we used previously to demonstrate radiation-induced lipid peroxidation in microsomes (13).

## Methods

Platelet-rich plasma (PRP) was prepared from whole-blood donations by centrifuging at 100 g for 20 min. PRP thus separated was irradiated at 50, 100, 200, and 400 Gy (10 Gy/min) using a cobalt-60 source. Platelet counts were done in control and irradiated samples using a Coulter counter. Hydrocarbon generation was measured in PRP, platelet-poor plasma (PPP), and washed platelets. The irradiated PRP was split into subsamples to prepare PPP and washed platelets. Washed platelets were resuspended in Hank's buffer, pH 7.4. Cell counts were adjusted to $10^9$/4 ml in PRP and washed platelets. Four-ml aliquots of PRP, PPP, and washed platelets were taken in 10 ml siliconized glass vials, which were sealed with Teflon-coated butyl rubber septa with aluminum caps and star springs (Perkin-Elmer, Rockville, MD). Gas in the headspace of the vials was sampled with a gas-tight syringe for analysis of volatile hydrocarbons by gas chromatography using a Perkin-Elmer Sigma 3B FID chromatograph with Sigma 15 data system. Analyses were done isothermally (60°C) with a stainless steel column (3.2 mm x 2 m) containing Porasil B (80/100 mesh, Applied Science Labs, State College, PA). Hydrocarbon standards (approx. 100 ppm in helium) were obtained from Scott Specialty Gases, Plumsteadville, PA, and scientific grade air, helium, and hydrogen were purchased from MG Industries, Valley Forge, PA. The first samples (zero time) were analyzed within 30 min after radiation exposures were terminated, and the same preparations were analyzed at different time points.

## Results and Discussion

Pentane evolution as a function of radiation dose and time after irradiation in PRP, PPP, and washed platelets is shown in Figs. 1, 2, and 3, respectively. A significant increase in lipid peroxidation as measured by pentane evolution was observed in all fractions after 50-Gy exposure. The increase in pentane evolution appears linear at lower radiation doses and earlier time periods. The relation to pentane evolution and radiation dose is best described by a logarithmic plot; Fig. 4 shows pentane evolution in the three fractions at the 6-hr time period. Extension of the lines to a point where there would be no detectable effect suggests that there would be no significant increase in pentane production at radiation doses less than 25 Gy. The slope of pentane evolution with respect to log dose was different for washed platelets than for PPP and PRP.

In general, ethane evolution followed the same pattern as pentane evolution, but the ethane concentrations were much lower. Evolution of the two hydrocarbons was not strictly correlated, e.g., the slope of pentane concentration with log radiation dose was steeper compared to the slope of ethane evolution (Fig. 5). Similarly the slope of pentane production versus time was steeper (data not shown).

The spontaneous release of pentane over time in platelets (controls, Figs. 1-3) indicates that lipid peroxidation occurs in stored platelets. In vitro irradiation of platelets induces lipid peroxidation in a dose- and time-dependent manner. If it can

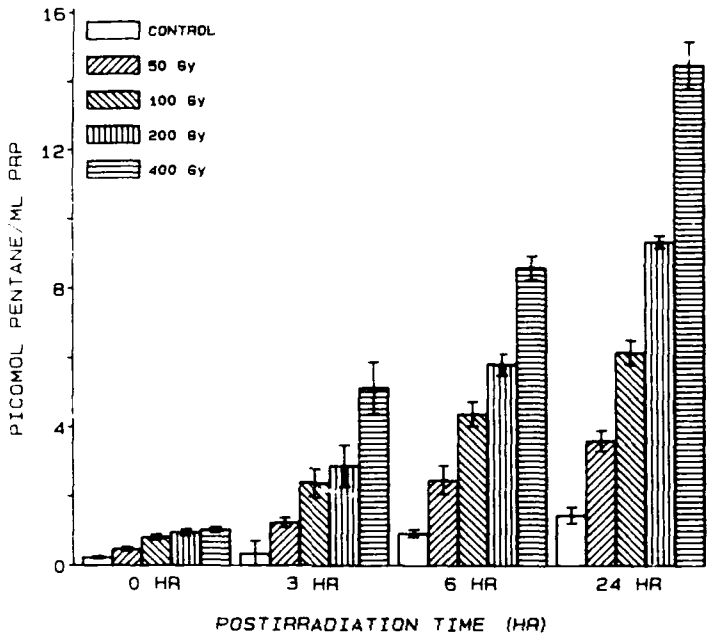


Fig. 1. Radiation-induced pentane generation in platelet-rich plasma (PRP). Values are means of 6 determinations ± SEM.

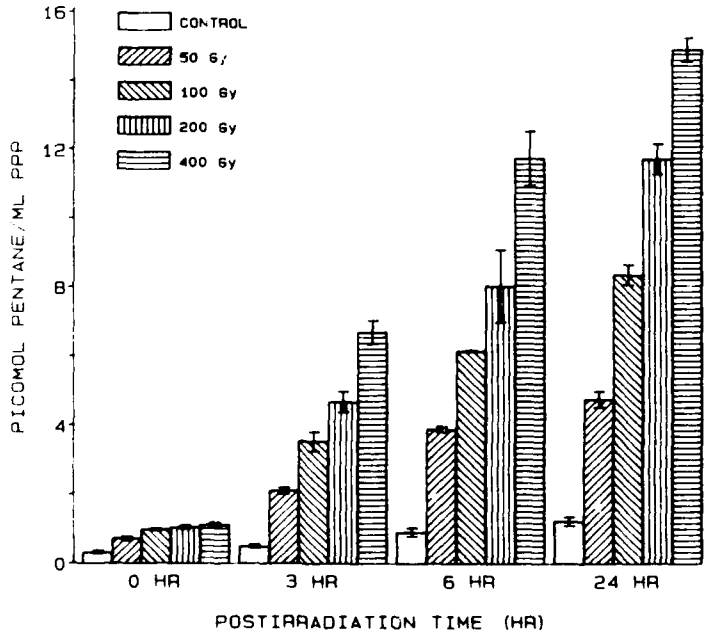


Fig. 2. Radiation-induced pentane generation in platelet-poor plasma (PPP). Values are means of 6 determinations ± SEM.

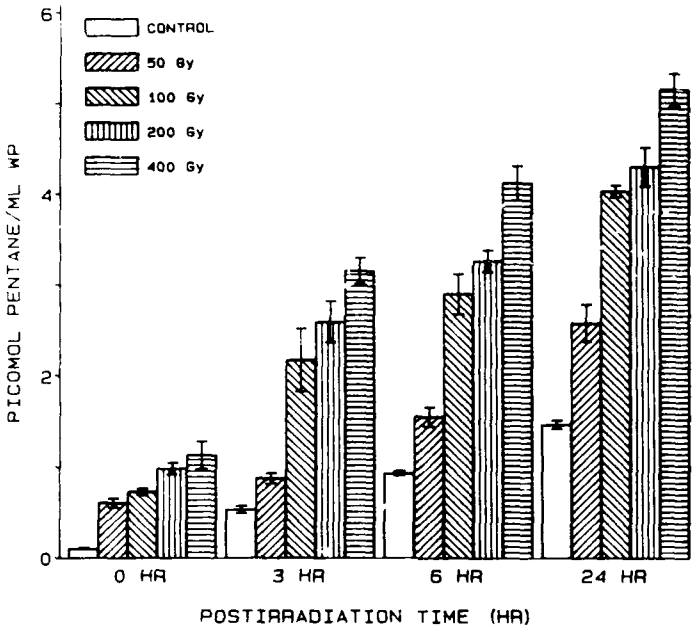


Fig. 3. Radiation-induced pentane generation in washed platelets (WP). Values are means of 6 determinations ± SEM.

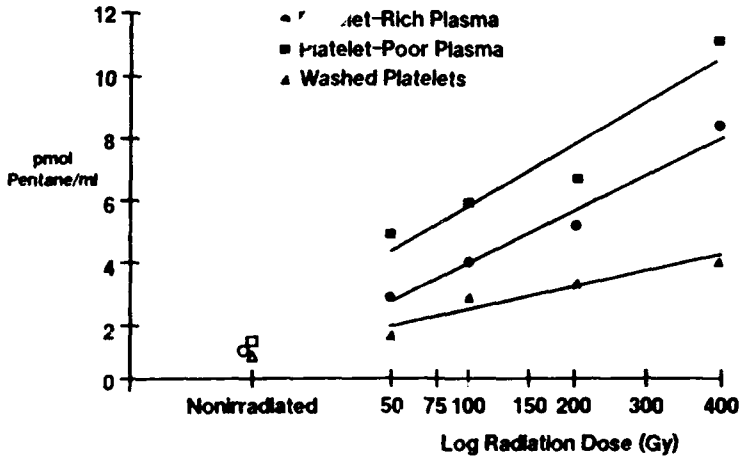


Fig. 4. Comparison of pentane generation from PRP, PPP, and WP at 6 hr after irradiation. Values are means of 6 determinations.

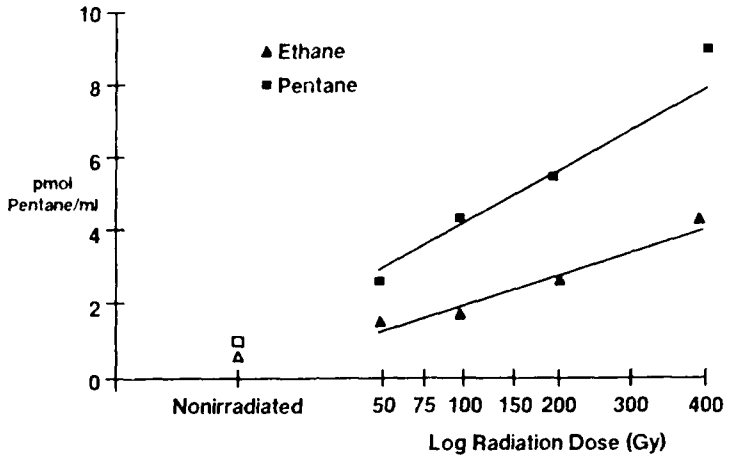


Fig. 5. Comparison of ethane and pentane generation in PRP at 6 hr after irradiation. Values are means of 6 determinations.

be shown definitively that lipid peroxidation is related to detrimental effects in platelets, then precautionary measures can be taken with respect to storage and irradiation procedures in blood banks. The dose of radiation used in this study, at which there was an increase in lipid peroxidation, was comparable to that used in removing lymphocytes in the preparation of PRP. It is interesting to note that there was less lipid peroxidation in washed platelets than in PRP. One possible explanation is that platelets contain efficient defense mechanisms against oxidative damage. It appears, for example, that platelets have the inherent capacity to regenerate glutathione in vitro, at least for 48 hr, but total glutathione decreases upon storage (14). PPP showed the largest amount of radiation-induced lipid peroxidation.

The major hydrocarbon formed, pentane, is derived from the oxidation of omega-6 fatty acids, predominantly arachidonic acid. The minor hydrocarbon formed, ethane, is derived from omega-3 fatty acids, mainly linoleic acid. Pentane production may be related not only to nonspecific membrane lipid peroxidation but also to the high degree of oxidative arachidonic acid metabolism involved in the formation of prostaglandins and leukotrienes in platelets. The relatively nonspecific indicator of lipid peroxidation, malondialdehyde, has been used as an indicator of prostaglandin endoperoxide formation by the platelets, occurring during release reactions (15). Malondialdehyde formation has also been considered a sensitive indicator of platelet hyperaggregatability seen in certain disease states such as diabetes (16). The exact relationship between pentane formation and "normal" oxidative metabolism of arachidonic acid in relation to platelet function, as opposed to "uncontrolled" peroxidation of arachidonic acid, requires further investigation.

The relationship between the observed radiation-induced lipid peroxidation and changes in platelet function postirradiation is also not clear. We have shown hyperaggregatability of platelets irradiated in vitro. There is also some indication from in vivo studies that their function (platelet aggregation) is increased shortly

after irradiation, before platelet numbers decrease (1). Platelet activation is often associated with an increase in cytosolic free calcium concentration, partly due to calcium release from the dense tubular system (17). We have also found an increase in intracellular calcium concentration in irradiated platelets (18). Peroxidation of membrane lipids is often acccompanied by structural and functional changes resulting in impairment of ion homeostasis leading to $Ca^{2+}$ overload and cell death. In the case of resistant cells, such as platelets, cell death does not occur readily, and gross changes are difficult to observe after oxidative damage, such as radiation exposure. Our results do suggest that radiation-induced lipid peroxidation may result in alteration of calcium homeostasis that is reflected in observable functional alterations. Further studies are needed to understand the exact nature of lipid peroxidation involvement in platelet aggregation. From a practical point of view, the effect of the oxidative changes due to aging, radiation, and other storage conditions is relevant to platelet therapy.

## Acknowledgements

This research was supported by the Armed Forces Radiobiology Research Institute, Defense Nuclear Agency (DNA), under work unit 00162. Views presented in this paper are those of the authors; no endorsement by DNA has been given or should be inferred. Dr. Radha was a National Research Council research associate at the Armed Forces Radiobiology Research Institute The assistance of William E. Jackson III for statistical analysis is gratefully acknowledged.

## References

1. T. P. U. WUSTROW, H. M. FRITSCHE and O. MESSERSCHMIDT, The Pathophysiology of Combined Injury and Trauma (R. I. WALKER, D. F. GRUBER, T. J. MacVITTIE and J. J. CONKLIN, eds.), pp. 125-135, University Park Press, Baltimore (1985).
2. R. W. YOUNG, Pharmac. Ther. 39 27-32 (1988).
3. M. L. GREENBERG, A. D. CHANANA, E. P. CRONKITE, L. M. SCHIFFER and P. A. STRYCKMANS, Radiat. Res. 35 147-154 (1968).
4. L. N. BUTTON, W. C. DeWOLF, P. E. NEWBURGER, M. S. JACOBSON and S. V. KEVY, Transfusion 21 419-426 (1981).
5. A. E. KALOVIDOURIS and A. G. PAPAYANNIS, Acta Radiol. [Oncol.] 20 333-336 (1981).
6. M. J. STUART, Transfusion 23 106-108 (1983).
7. M. V. PILLAI, G. D. QURESHI, R. HOWELLS, N. NARASIMHACHARI, E. G. BEHM and T. A. HAZRA, Milit. Med. 150 496-498 (1985).
8. G. MOROFF, V. M. GEORGE, A. M. SIEGL and N. L. C. LUBAN, Transfusion 26 453-456 (1986).
9. J. L. LOGNONNE, R. DuCOUSSO, G. ROCQUET and J. F. KERGONOU, Biochimie 67 1015-1021 (1985).
10. J. C. EDWARDS, D. CHAPMAN, W. A. CRAMP and M. B. YATVIN, Prog. Biophys. Mol. Biol. 43 71-93 (1985).
11. N. I. KRINSKY, D. G. SLADDIN and P. H. LEVINE, Oxygen and Oxy-Radicals in Chemistry and Biology (M. A. J. Rodgers and E. L. Powers, eds.), pp. 153-160, Academic Press, New York (1981).
12. M. OKUMA, M. STEINER and M. BALDINI, Blood 34 712-716 (1969).
13. C. R. DOBBS, K. S. KUMAR, J. F. WEISS and G. N. CATRAVAS, Int. J. Radiat. Biol. 39 445-449 (1981).
14. E. RADHA, T. D. HILL, G. H. R. RAO and J. G. WHITE, Thromb. Res. 40 823-831 (1985).
15. J. B. SMITH, C. M. INGERMAN and M. J. SILVER, J. Lab. Clin. Med. 88 167-172 (1976).
16. M. J. STUART, Thromb. Haemost. 42 649-65 (1979).

AD-A212 928 AFRRI (ARMED FORCES RADIOBIOOGY RESEARCH INSTITUTE) 2/2
REPORTS APRIL-JUNE 1989(U) ARMED FORCES RADIOBIOLOGY
RESEARCH INST BETHESDA MD JUL 89

UNCLASSIFIED F/G 6/7 NL

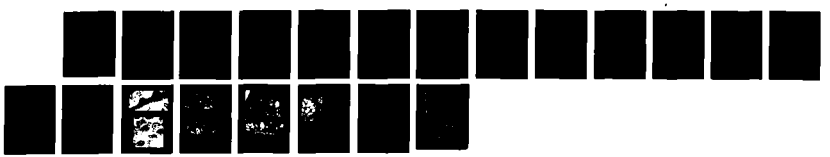

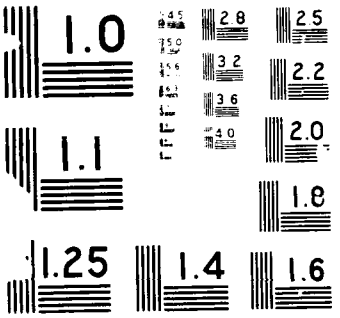
1.0
1.1
1.25
1.4
1.6
1.8
2.0
2.2
2.5
2.8
3.2
3.6
4.0

Exp Hematol 17:411–417 (1989)


*Experimental* Hematology



# Long-term Culture of Canine Bone Marrow Cells

Friedrich G. Schuening, Rainer Storb, Joey Meyer, and Sondra Goehle

Clinical Research Division, Fred Hutchinson Cancer Research Center, Seattle, Washington, USA

*Received* 12 June 1988; *revised and accepted* 10 October 1988; *accepted* 7 November 1988

**Abstract.** Conditions that allow the growth of canine marrow cells in long-term marrow culture are described. The quality of the culture conditions was evaluated based on the weekly number of granulocyte–macrophage colony-forming units (CFU-GM) in the nonadherent cell fraction. Using this parameter, the highest number of CFU-GM was obtained when marrow cells were incubated at 37°C in RPMI-1640 or McCoy's 5A medium supplemented with 20% prescreened horse serum without addition of hydrocortisone. CFU-GM colonies could be regularly grown out of the nonadherent cell fraction for 20–31 weeks, after recharging the cultures with $2.5 \times 10^6$ mononuclear autologous marrow cells 1 week after establishing the stromal cell layer.

**Key words:** Canine long-term marrow culture — Culture conditions — CFU-GM production

Long-term bone marrow cultures offer an in vitro approach for studying regulatory mechanisms controlling hemopoietic cell development. This method was first described for long-term culture of mouse bone marrow cells [1], which produced both spleen colony-forming units (CFU-S) and granulocyte–macrophage colony-forming units (CFU-GM) for periods of 5 months or more, depending on mouse strain [2]. Hemopoiesis in this system was dependent upon the presence of an adherent layer of marrow-derived stromal cells consisting of a heterogeneous population of cell types, including phagocytic mononuclear cells, endothelial cells, and giant lipid-laden adipocytes [1].

In addition to reports on murine long-term marrow cultures, similar long-term cultures for Syrian hamster [3], prosimian *Tupaia glis* (tree shrew) [4], and human marrow [5] have been described. So far, there has been no report on long-term cultures of canine bone marrow cells. We were interested in establishing a method for the long-term culture of canine marrow cells for two reasons: first, maintaining marrow cells in long-term culture might be used as a means of depleting malignant cells from the marrow, as has been suggested by studies with murine lymphoblastic leukemia [6] and in patients with acute nonlymphoblastic or chronic myeloblastic leukemia [7, 8]. This approach could be similarly effective in removing lymphoma cells from canine marrow and thus improve our results of autologous marrow transplantation for spontaneous canine non-Hodgkin's lymphoma [9]. Second, we are currently searching for methods to improve the efficiency of retroviral gene transfer into canine hemopoietic progenitor cells cultured for 24 h with virus-producing packaging cells [10]. One possible method could be to increase the time that marrow cells are exposed to retroviral vectors by combining 24-h cocultivation on packaging cells with long-term marrow culture fed repeatedly with virus-containing supernatant.

In this study we describe a method for the long-term culture of canine marrow cells, based on modifications of the murine system.

## Materials and methods

*Experimental animals.* A total of 12 canines of both sexes and various breeds (beagles, fox hounds, and mongrels), 6–14 months of age, were used as marrow donors in these experiments. Animals were either raised at the Fred Hutchinson Cancer Research Center or purchased from commercial United States Department of Agriculture-licensed dealers. Dogs were quarantined on arrival, screened for evidence of disease, and conditioned for a minimum of 2 months before being released for use. All dogs were dewormed and vaccinated for rabies, distemper, leptospirosis, hepatitis, and parvovirus. They were group housed in an American Association for Accreditation of Laboratory Animal Care (AAALAC)-accredited facility in standard indoor runs, and provided commercial dog chow and chlorinated tap water ad libitum. Animal holding areas were maintained at 70° ± 2°F with 50% ± 10% relative humidity using at least 15 air changes per hour of 100% conditioned fresh air. The dogs were on a 12-h light dark full spectrum lighting cycle with no twilight.

*Bone marrow aspiration.* All dogs were anesthetized by i.v. injection of Fentanyl (Innovar-Vet) at 0.03 mg/kg body weight and the collection site aseptically cleansed with a povoiodine scrub and alcohol rinse. Bone marrow was obtained from the humoral condyle via needle aspiration using a sterile 20-ml syringe and 14-gauge disposable needle. Ten ml of bone marrow were collected from each dog at 3-week intervals.

*Establishment of long-term marrow cultures.* Mononuclear marrow cells (MNC; $6 \times 10^7$) were cultured in 75-cm² canted-neck flasks (Corning, Corning, New York) at $2 \times 10^6$ MNC/ml in 30 ml RPMI-1640 medium (M.A. Bioproducts, Walkersville, Maryland) supplemented with 20% prescreened heat-inactivated horse serum (lot no. 272 111 37; Flow Laboratories, Rockville, Maryland), $10^{-4}$ M hydrocortisone-21-phosphate (Sigma, St. Louis, Missouri), 1% nonessential amino acids, 1% pyruvate, 2% L-glutamine, and 1% penicillin–streptomycin. In some experiments RPMI-1640 medium was replaced with either alpha minimum essential medium (M.A. Bioproducts), McCoy's 5A medium (GIBCO, Grand Island, New York), or Fischer's medium (GIBCO). Cultures were maintained at 37°C in a humidified atmosphere of 5% $CO_2$ in air. After 1 week of culture, nonadherent cells and medium were removed from the flasks and

Views presented in this paper are those of the authors; no endorsement by the Defense Nuclear Agency has been given or should be inferred. Research was conducted according to the principles enunciated in the Guide for the Care and Use of Laboratory Animals prepared by the Institute of Laboratory Animal Resources of the National Academy of Sciences National Research Council.

*Address reprint requests to* Dr. F.G. Schuening, Fred Hutchinson Cancer Research Center, 1124 Columbia Street, Seattle, WA 98104, USA

**Table 1.** Comparison of canine long-term marrow cultures established at identical culture conditions

| | Flask 1 | | Flask 2 | | Flask 3 | | Flask 4 | | Flask 5 | |
|---|---|---|---|---|---|---|---|---|---|---|
| Week | Nonadherent cells (× 10⁶) | CFU-GM | Nonadherent cells (× 10⁶) | CFU-GM | Nonadherent cells (× 10⁶) | CFU-GM | Nonadherent cells (× 10⁶) | CFU-GM | Nonadherent cells (× 10⁶) | CFU-GM |
| 1 | 200 | 0 | 152 | 0 | 163 | 0 | 152 | 0 | 220 | 850 |
| 2 | ND | | ND | | ND | | ND | | ND | |
| 3 | 160 | 0 | 80 | 298 | 80 | 416 | 40 | 1612 | 80 | 2600 |
| 4 | 48 | 1112 | 48 | 3920 | 78 | 3218 | 40 | 2704 | 60 | 3354 |
| 5 | 32 | 1989 | 30 | 2184 | 60 | 1860 | 10 | 247 | 45 | ND |
| 6 | 40 | 5304 | 40 | 1248 | 110 | 3003 | 52 | 1960 | 50 | 2080 |
| 7 | 80 | 2338 | 80 | 1788 | 100 | 1300 | 120 | 2808 | 65 | 592 |
| 8 | 32 | 1839 | 110 | 1001 | 130 | 1352 | 55 | 429 | 62 | 884 |
| Σ | 832 | 12,282 | 867 | 10,316 | 778 | 10,849 | 469 | 9760 | 882 | 10,363 |

All cultures were recharged 1 week after establishing an adherent cell layer with $4.8 \times 10^6$ MNC containing 585 CFU-GM. ND, not done. Σ, sum of weekly counts.

centrifuged at 400 *g* for 20 min. Half of the used medium (5 ml) together with 5 ml of fresh medium and $6 \times 10^6$ freshly aspirated autologous mononuclear marrow buffy coat cells obtained from the same dog used for establishing the stromal cell layer and centrifuged at 800 *g* for 10 min) were returned into each flask (marrow boost). CFU-GM in the nonadherent population harvested at the time of feeding were assayed as described below.

*CFU-GM assay.* Primary or cultured bone marrow cells were assayed for CFU-GM content as described [11, 12]. MNC ($0.075 \times 10^5$/plate) were cultured for 10 days at 37°C in a humidified atmosphere of 5% $CO_2$ in air in 35-mm plastic petri dishes containing 2 ml of agar medium. The agar medium consisted of an equal volume mixture of 0.6% (wt/vol) Bacto-agar (Difco, Detroit, Michigan) and double-strength Dulbecco's modified Eagle's medium (GIBCO) containing 40% (vol/vol) heat-inactivated human AB plasma. Phytohemagglutinin (PHA)-stimulated dog lymphocyte-conditioned medium was added to the petri dishes (0.1 ml/plate) prior to the agar medium mixture containing the bone marrow cells.

*Electron microscopy.* Specimens for electron microscopy were fixed in a 1:1 mixture of half-strength Karnovsky's fixative and RPMI-1640 medium for 2 h, rinsed in cacodylate buffer, and postfixed in 1% collidine-buffered osmium tetroxide for 1 h. After dehydration in a graded ethanol series the cells were infiltrated and embedded in Poly Bed 812 embedding media, thin sectioned at 80–100 nm, and stained with uranyl acetate and Millonig's lead stain. Sections were photographed using a JEOL 100-S electron microscope operating at 80 kV.

## Results

### *Comparison of long-term marrow cultures established with identical culture conditions*

Five long-term marrow cultures were established at the same time from the same marrow aspiration at the same culture conditions to determine at weekly intervals whether the numbers of nonadherent cells in the flasks were similar and whether the nonadherent cell fractions contained similar amounts of CFU-GM. One week after establishing an adherent cell layer, the five culture flasks were recharged with the same number of marrow cells from the same marrow aspiration. At weekly intervals, cells nonadherent to the culture flasks were counted and plated in CFU-GM assays. Table 1 shows the weekly counts of the nonadherent cells in each flask and the number of CFU-GM in this nonadherent cell fraction.

**Table 2.** Comparison of two different culture temperatures in canine long-term marrow culture

| | Flask at 37°C | | Flask at 33°C | |
|---|---|---|---|---|
| Week | Nonadherent cells (× 10⁶) | CFU-GM | Nonadherent cells (× 10⁶) | CFU-GM |
| 1 | 290 | 2639 | 490 | 0 |
| 2 | 98 | 764 | 91 | 0 |
| 3 | 26 | 3515 | 9 | 0 |
| 4 | 34 | 1635 | 2 | 57 |
| 5 | 20 | 11,518 | 3 | 4 |
| 6 | 12 | 15,194 | 0 | |
| Σ | 480 | 35,265 | 595 | 61 |

Cultures were recharged 1 week after establishing an adherent cell layer with $5.3 \times 10^6$ MNC containing 18,603 CFU-GM.

The sums of the nonadherent cells as well as the sums of the CFU-GM produced over a period of 8 weeks in each of the five long-term marrow cultures were quite similar. This shows that long-term marrow cultures set up at the same time from the same marrow aspiration at the same culture conditions contain similar quantities of CFU-GM in the nonadherent cell fraction during the same culture time, a finding that has been confirmed in three independent experiments (data not shown). This result is important for the following experiments comparing the growth-promoting qualities of different culture conditions. Because the weekly numbers of CFU-GM in long-term cultures were similar when using the same culture conditions, differences in CFU-GM number seen when changing one of the culture conditions could then most probably be contributed to this change. It was therefore possible to compare different culture conditions based on CFU-GM number in the nonadherent cell fraction during the culture time.

### *Comparison of different culture temperatures*

We studied the influence of culture temperature on CFU-GM number in long-term marrow culture by incubating a

**Table 3.** Comparison of different culture media in canine long-term marrow culture

| | RPMI-1640 medium | | McCoy's 5A medium | | Alpha medium | | Fischer's medium | |
|---|---|---|---|---|---|---|---|---|
| Week | Nonadherent cells (× 10⁴) | CFU-GM | Nonadherent cells (× 10⁴) | CFU-GM | Nonadherent cells (× 10⁴) | CFU-GM | Nonadherent cells (× 10⁴) | CFU-GM |
| 1 | 388 | 1862 | 340 | 9724 | 406 | 6334 | 291 | 1892 |
| 2 | 380 | 19,568 | 20 | 1014 | 32 | 998 | 17 | 309 |
| 3 | 10 | 221 | 12 | 412 | 18 | 374 | 5 | 143 |
| 4 | 32 | 841 | 14 | 109 | 5 | 5230 | 11 | 143 |
| 5 | ND | | ND | | ND | | ND | |
| 6 | 22 | 114 | 16 | 125 | 16 | 0 | 13 | 0 |
| Σ | 772 | 22,303 | 402 | 11,384 | 477 | 12,936 | 337 | 2487 |

All cultures were recharged 1 week after establishing an adherent cell layer with $6.4 \times 10^7$ MNC containing 41,600 CFU-GM.

**Table 4.** Comparison of different amounts of hydrocortisone in canine long-term marrow culture

| | No hydrocortisone | | 0.05 μM hydrocortisone | | 0.1 μM hydrocortisone | | 0.2 μM hydrocortisone | | 0.4 μM hydrocortisone | |
|---|---|---|---|---|---|---|---|---|---|---|
| Week | Nonadherent cells (× 10⁴) | CFU-GM | Nonadherent cells (× 10⁴) | CFU-GM | Nonadherent cells (× 10⁴) | CFU-GM | Nonadherent cells (× 10⁴) | CFU-GM | Nonadherent cells (× 10⁴) | CFU-GM |
| 1 | 1090 | 670,241 | 890 | 259,168 | 1000 | 44,200 | 1160 | 1508 | 1130 | 30,849 |
| 2 | 130 | 14,027 | 60 | 53,508 | 96 | 12,979 | 62 | 37,398 | 50 | 2990 |
| 3 | 36 | 24,617 | 15 | 49,937 | 10 | 30,914 | 9 | 25,459 | 3 | 0 |
| 4 | 15 | 15,113 | 24 | 38,314 | 18 | 30,046 | 8 | 15,215 | 6 | 3726 |
| 5 | 22 | 22,108 | 24 | 19,375 | 35 | 30,940 | 6 | 5561 | 2 | 1250 |
| Σ | 1293 | 746,106 | 1013 | 417,302 | 1159 | 149,079 | 1245 | 85,141 | 1191 | 38,815 |

All cultures were recharged 1 week after establishing an adherent cell layer with $4.5 \times 10^7$ MNC containing 257,400 CFU-GM.

culture flask at either 33° or 37°C. Both flasks were recharged after 1 week with the same number of marrow cells ($53 \times 10^7$ MNC containing 18,603 CFU-GM) from the same marrow aspiration. At weekly intervals, cells nonadherent to the flasks were counted and plated in CFU-GM assays. Table 2 shows the weekly counts of nonadherent cells in each flask and the number of CFU-GM in the nonadherent cell fraction. The sum of the weekly CFU-GM counts was highest for the flask incubated at 37°C. The superiority of 37°C has been confirmed in two independent experiments (data not shown).

*Comparison of different culture media and sera*

One week after inoculating marrow cells into culture flasks to form an adherent cell layer, marrow cultures were recharged with an equal number of marrow cells obtained from the same marrow aspiration. Each flask contained a different culture medium, either RPMI-1640, McCoy's 5A, Fischer's, or alpha medium. All four media were supplemented with 20% horse serum from the same lot. At weekly intervals, nonadherent cells were counted and plated in CFU-GM assays. Five independent experiments were performed. RPMI-1640 and McCoy's 5A medium gave equally good results. Both showed in two of the five experiments the highest sum of weekly CFU-GM counts. Flasks containing alpha medium were intermediate, having the highest CFU-GM counts in only one of the five experiments, whereas Fischer's medium showed the lowest or second lowest CFU-GM counts in all five experiments. Table 3 shows the results of one of the five experiments.

Next, we set up a long-term culture with RPMI-1640 medium supplemented with 20% prescreened fetal calf serum instead of horse serum. The flask was recharged after 1 week with $57 \times 10^7$ MNC containing 311,961 CFU-GM. The culture was maintained for 8 weeks. The number of MNC in the nonadherent cell fraction rapidly declined. There was no CFU-GM growth during the culture period of 8 weeks when plating the nonadherent cells in a CFU-GM assay. This finding has been confirmed in a second separate experiment. In parallel with the culture containing RPMI-1640 medium and 20% fetal calf serum, we set up a culture with RPMI-1640 medium supplemented with a mixture of 10% horse serum and 10% fetal calf serum. The flask was recharged after 1 week with $57 \times 10^7$ MNC from the same marrow aspiration containing 311,961 CFU-GM. During the 8-week culture period, a total of only 5000 CFU-GM were grown out of the nonadherent cell fraction. This result has been confirmed in a second separate experiment. Based on these experimental results, we decided to use RPMI-1640 medium supplemented with 20% prescreened horse serum in the following experiments.

*Comparison of different amounts of hydrocortisone*

The effect of hydrocortisone on CFU-GM number in long-term marrow culture was studied. One week after establishing

**Table 5.** Comparison of different amounts of marrow cells used for recharging canine long-term marrow cultures

| Week | 15 × 10⁶ MNC boost | | 30 × 10⁶ MNC boost | | 60 × 10⁶ MNC boost | | 120 × 10⁶ MNC boost | | 240 × 10⁶ MNC boost | |
|---|---|---|---|---|---|---|---|---|---|---|
| | Non-adherent cells (× 10⁶) | CFU-GM | Non-adherent cells (× 10⁶) | CFU-GM | Non-adherent cells (× 10⁶) | CFU-GM | Non-adherent cells (× 10⁶) | CFU-GM | Non-adherent cells (× 10⁶) | CFU-GM |
| 1 | 167 | 30,611 | 650 | 5070 | 998 | 16,866 | 1840 | 4784 | 570 | 30,381 |
| 2 | 26 | 0 | 34 | 4111 | 134 | 18,465 | 201 | 24,301 | 146 | 68,138 |
| 3 | 33 | 44,788 | 3 | 4701 | 8 | 5362 | 16 | 13,478 | 18 | 17,644 |
| 4 | 7 | 4908 | 5 | 5394 | 8 | 5283 | 26 | 8754 | 87 | 39,811 |
| 5 | 13 | 10,686 | 78 | 608 | 39 | 0 | 17 | 950 | 32 | 416 |
| 6 | 40 | 1716 | 15 | 449 | 20 | 5226 | 27 | 1474 | 17 | 862 |
| | 283 | 92,709 | 785 | 20,333 | 1207 | 51,202 | 2127 | 53,741 | 870 | 157,252 |
| Percent recovery of starting numbers of CFU-GM in marrow boost | | 40 | | 4 | | 6 | | 3 | | 4 |

All cultures were recharged 1 week after establishing an adherent cell layer with 15, 30, 60, 120, or 240 × 10⁶ MNC containing 229,710, 459,420, 918,840, 1,837,680, or 3,675,360 CFU-GM.

an adherent cell layer, flasks were recharged with the same number of marrow cells (45 × 10⁶ MNC, containing 257,400 CFU-GM) from the same marrow aspiration. Culture medium (RPMI-1640 plus 20% horse serum) was used either without hydrocortisone or supplemented with 0.05, 0.1, 0.2, or 0.4 μM hydrocortisone. As shown in Table 4, the sum of weekly CFU-GM counts in the nonadherent cell fraction was highest for the flask without hydrocortisone. This has been confirmed in a second independent experiment (data not shown).

### *Comparison of different amounts of marrow cells used for recharging long-term marrow cultures*

Long-term marrow cultures were started and then recharged after 1 week with either 15 × 10⁶, 30 × 10⁶, 60 × 10⁶, 120 × 10⁶, or 240 × 10⁶ mononuclear marrow buffy coat cells obtained from the same marrow aspiration. The sum of the weekly CFU-GM counts in the nonadherent cell fraction was highest in the flask recharged with 240 × 10⁶ marrow cells (Table 5). However, when compared to the number of CFU-GM inoculated into the culture flasks at the time of the marrow boost, most CFU-GM were obtained from the flask recharged with 15 × 10⁶ marrow cells. After 6 weeks, 40% of the number of CFU-GM contained in the marrow boost were obtained from the flask recharged with 15 × 10⁶ marrow cells compared to 3%–6% in the flasks boosted with 30–240 × 10⁶ marrow cells. This finding has been confirmed in a second independent experiment.

### *Comparison of recharging long-term marrow cultures with autologous or allogeneic dog leukocyte antigen DLA-nonidentical marrow cells*

The following experiments were done in order to find out whether the marrow cells used to recharge long-term marrow cultures need to be autologous compared to the cells of the adherent layer or whether they can be allogeneic, DLA-nonidentical. Cultures were started by incubating 6 × 10⁶ MNC from the same marrow aspiration in culture flasks. Flasks were either not recharged or boosted after 1, 2, or 3 weeks with 2 × 10⁶ MNC derived either from the same donor used for establishing the stromal cell layer or from a DLA-nonidentical unrelated donor. Results are shown in Figure 1. When cultures were recharged 1 week after establishing the stromal layer, the flask recharged with autologous marrow showed a higher sum of weekly CFU-GM counts in the nonadherent cell fraction compared to the flask boosted with DLA-nonidentical marrow (at week 20, the week before the first flask became contaminated, 796,337 compared to 175,014). Especially during the first 5 weeks, the weekly CFU-GM count was lower in the flask recharged with DLA-nonidentical marrow compared to the flask boosted with autologous marrow cells. Overall, the sum of the weekly CFU-GM counts in the flask boosted with DLA-nonidentical marrow was as low as the control flask that was not recharged. In contrast, culture flasks recharged 2 or 3 weeks after establishing the stromal layer showed a similar sum of weekly CFU-GM counts independent of whether boosted with autologous or DLA-nonidentical marrow cells. As shown in Figure 1, the sum of weekly CFU-GM at week 20 was 400,314 when the flask was recharged 2 weeks after establishing the adherent cell layer with autologous marrow cells, compared to 483,377 CFU-GM colonies when recharged with DLA-nonidentical marrow. When boosting the culture flasks after 3 weeks with autologous marrow cells, the sum of weekly CFU-GM at week 20 was 213,529 compared to 171,939 CFU-GM colonies when boosting with DLA-nonidentical marrow.

Results presented in Figure 1 also show that CFU-GM can be harvested from canine long-term marrow cultures for a prolonged period of time. We kept seven cultures until contamination occurred and we could obtain CFU-GM out of the nonadherent cell fraction for 20 to 31 weeks.

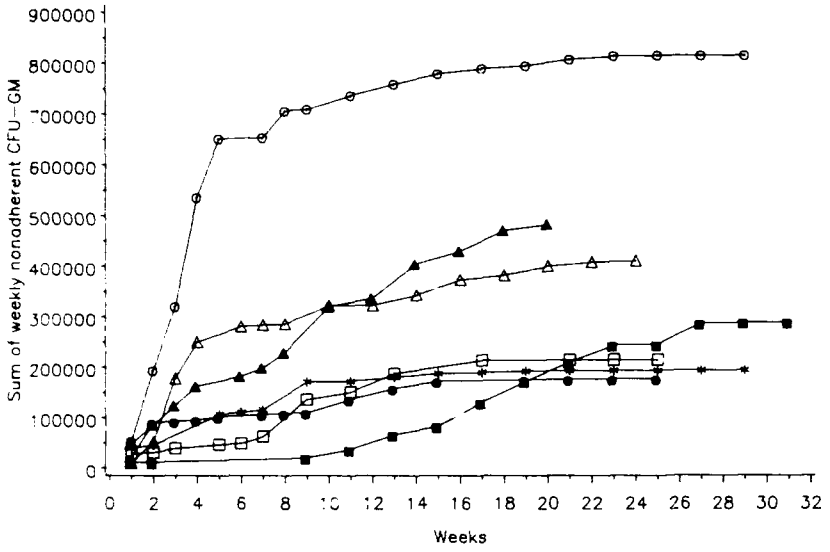


**Fig. 1.** Cumulative weekly CFU-GM in the nonadherent cell fraction of canine long-term marrow cultures recharged with autologous or allogeneic DLA-nonidentical marrow cells after 1, 2, or 3 weeks. Cultures were started by incubating $6 \times 10^7$ MNC from the same marrow aspiration in 75-cm² canted-neck flasks at $2 \times 10^7$ MNC/ml in RPMI-1640 medium supplemented with 20% prescreened heat-inactivated horse serum. Flasks were either not recharged (*) or boosted after 1, 2, or 3 weeks with $2 \times 10^7$ MNC derived either from the same donor as used for establishing the stromal cell layer (○, 1-week boost; △, 2-week boost; and □, 3-week boost) or from a DLA-nonidentical unrelated donor (●, 1-week boost; ▲, 2-week boost; and ■, 3-week boost). At weekly intervals nonadherent cells were plated in triplicate in CFU-GM assay. Each *point* represents the cumulative number of weekly CFU-GM.

*Ultrastructural analysis of canine long-term marrow cultures*

Canine long-term marrow cultures form a dense adherent cell layer relatively quickly, only 1 week after inoculating marrow cells into the culture flask. Ultrastructural analysis of the adherent cell layer 1–3 weeks after starting the culture showed that the dominant cells were macrophages. The second most frequent cell type seen was adipocytes containing numerous fat droplets in the cytoplasm. Close to or in direct contact with macrophages were hemopoietic cells at different stages of maturation.

## Discussion

In addition to their use as a system in which to study the regulation of hemopoiesis, long-term canine marrow cultures were of interest to us for two reasons. First, this culture method has been suggested as a means of depleting malignant cells from the marrow [6–8]. Dogs with spontaneous non-Hodgkin's lymphoma represent a potentially important model system in which the clinical utility of this approach could be tested [9]. Second, keeping marrow cells in long-term cultures fed repeatedly with virus-containing supernatant could allow a sufficient increase in the exposure of marrow to retroviral vectors and thus increase the efficiency of retroviral gene transfer into canine marrow cells. Indeed, in recent experiments we showed that we could increase the efficiency of gene transfer by culturing marrow cells for 24 h with virus-producing packaging cells and then for another 6 days in long-term culture (fed with virus supernatant) compared to results obtained with the 24-h cocultivation only [13].

The culture conditions described in this study allow canine hemopoietic precursor cells to be grown in long-term marrow culture regularly for 20 to 31 weeks. These culture conditions are based on findings first made in murine long-term cultures [1]. Similar to the growth requirements originally described for murine long-term cultures, we also found it to be important for canine cultures to first establish an adherent layer and then to recharge the cultures with fresh marrow. Another factor crucial for murine as well as canine cultures is to find the right lot of horse serum that supports culture growth. Yet culture conditions for canine marrow cells differ in several aspects from the one found to give best results in murine long-term cultures. Canine cultures give best results, i.e., highest number of CFU-GM, when incubated at 37°C, and show no or very little CFU-GM production when kept at 33°C. In contrast, cultures of murine marrow produce more CFU-GM as well as CFU-S when incubated at 33°C compared to 37°C [1]. In human long-term cultures, an incubation temperature of 33°C also seems to be superior to 37°C in terms of CFU-GM production [5]. Coulombel et al. reported equally good results in establishing human long-term cultures as judged by recoveries of erythroid burst-forming units (BFU-E) and CFU-GM, when incubating marrow cells for the first 3–4 days at 37°C, and then at 33°C for the remaining culture period [14]. Long-term cultures of Syrian hamster [3] and *Tupaia glis* [4] marrow cells grow best at 37°C, as judged by progenitor recoveries, similar to canine marrow. It is unclear why these species differences with regard to optimal culture temperature exist. Incubating mouse marrow cells at 33°C improves the development of the stromal adherent layer [1]. Because the adherent layer is known to be important for supporting long-term hemopoiesis, this may explain the better results seen when incubating murine cultures at 33°C. In canine long-term cultures, growth of adherent cells was better at 37°C, which again may explain the superiority of the culture results seen at 37°C. But in human culture, whereas 37°C favors development of the stromal adherent layer [8], 33°C seems to be superior in terms of supporting long-term hemopoiesis. Culture temperature, therefore, appears to be influencing additional factors relevant for the quality of long-term marrow cultures.

The growth medium conventionally used in murine long-term marrow cultures is Fischer's medium [1] but McCoy's 5A or alpha medium can be substituted [15]. Syrian hamster marrow grows best in RPMI-1640 medium [3] and *Tupaia* marrow has been cultured in Fischer's medium [4]. The growth medium for human long-term cultures can be alpha medium

[14], but Fischer's [5] and McCoy's 5A [16] medium have also been used. In contrast to murine and *Tupaia* marrow, canine marrow cells did not grow well in Fischer's medium. Best results were obtained in either RPMI-1640 or McCoy's 5A medium.

As mentioned above, the success of murine as well as canine long-term cultures is dependent on the growth-supporting qualities of selected lots of horse serum. Greenberger [17] reported that in murine cultures the quality of "deficient" lots of horse serum could be improved by supplementing them with glucocorticoid. Addition of $10^{-6}$ M hydrocortisone increased the number of adipocytes as well as the total adherent and nonadherent populations. Dexter et al. found that horse serum batches differ widely in their level of free corticosteroids [18]. Serum with a relatively low corticosteroid level was invariably poor in maintaining hemopoiesis, whereas serum with a relatively high level showed good growth-supporting qualities. When "poor" batches were supplemented with hydrocortisone, their quality improved considerably in terms of long-term culture hemopoiesis. The growth of human long-term marrow cultures is also improved when $10^{-6}$ M hydrocortisone is added, mainly because of improved development of the adherent layer [5]. In contrast to the positive influence of hydrocortisone on murine and human long-term cultures, we found best results in those canine long-term cultures that were not supplemented with hydrocortisone. With the addition of corticosteroid to canine cultures, a dose-dependent decrease in weekly CFU-GM number was observed. Long-term cultures of Syrian hamster [3, 19] or *Tupaia glis* [4, 20] marrow as well do not require supplementation with hydrocortisone.

The reasons for this species difference are unknown. In murine and human long-term cultures, hydrocortisone stimulates the development of stromal cells and adipocytes. Both cell types are thought to be important for establishing and maintaining hemopoietically active murine and human long-term cultures. Bone marrow cultures from the Syrian hamster produce stem cells that proliferate and differentiate for ~12 weeks in the absence of an adherent layer [3]. The fact that hamster long-term cultures can grow without a stromal layer may explain why they also do not require supplementation with hydrocortisone, which stimulates the development of an adherent cell layer. In contrast, both *Tupaia* and canine long-term marrow cultures depend on the presence of an adherent cell layer but seem to grow without supplementation of hydrocortisone. The adherent hemopoietic microenvironment of *Tupaia* long-term cultures shows as a specific characteristic a periodic detachment of adherent cells at intervals of 1–2 months followed by subsequent regeneration of the adherent cell layer [4]. This regenerative capacity of the adherent microenvironment seems to be sufficient for maintaining the *Tupaia* long-term cultures, thereby rendering addition of hydrocortisone unnecessary. The growth of canine long-term cultures has been strongly dependent on certain lots of horse serum. It could therefore be that when screening different lots of horse serum, we were selecting for those with a relatively high corticosteroid level. Adding hydrocortisone to the cultures could thus have increased the corticosteroid level in the cultures into a toxic range causing inhibition of culture growth. We did not test the utility of hydrocortisone additions to suboptimal lots of horse serum.

One of the problems faced when setting up several long-term cultures from the same dog is to obtain enough marrow cells 1 week later for recharging the cultures with autologous marrow cells. We therefore compared long-term cultures boosted with marrow cells that were either autologous or allogeneic DLA-nonidentical compared to the cells of the stromal layer. Cultures boosted after 1 week with DLA-nonidentical marrow cells contained less CFU-GM than those charged with autologous marrow, but the difference between autologous and allogeneic cultures disappeared when recharged 2 or 3 weeks after establishing the stromal layer. This may be due to the inability of the culture system to support survival and proliferation of T-lymphocytes or other cell types that can exert an inhibitory effect on the DLA-nonidentical cells of the marrow boost. The results of allogeneic cultures recharged after 2 or 3 weeks are similar to observations made by Dexter et al. [21] and Moore and Dexter [22] in murine long-term cultures demonstrating that major H-2 differences do not impair the capacity of the adherent microenvironment to sustain allogeneic stem cell proliferation.

In summary, we have described culture conditions that allow for the growth of canine marrow cells in long-term culture. CFU-GM colonies could be regularly grown out of the nonadherent cell fraction for 20–31 weeks. We are currently studying how long pluripotent stem cells survive in canine long-term cultures by transplanting autologous marrow cells kept in long-term cultures for different periods of time into lethally irradiated marrow donors. Also the effects of added hemopoietic growth factors on the longevity of pluripotent stem cells in canine long-term cultures are being studied. The results of these experiments may be relevant for a number of studies, including purging autologous marrow grafts of dogs with spontaneous lymphoma and for increasing the efficiency of retroviral-mediated gene transfer into canine hemopoietic stem cells.

## Acknowledgments

We thank Dr. Paul Simmons for helpful advice and discussion, and Ted Graham, Robert Raff, Liz Caldwell, Judy Groombridge, Lori Ausburn, Wally Meyer, and the Shared Word Processing Department for expert technical assistance. This work was supported in part by Grants CA 15704, CA 18105, CA 18221, and CA 31787 awarded by the National Cancer Institute, HL 36444 awarded by the National Health, Lung and Blood Institute, National Institutes of Health, Department of Health and Human Services, and by the Armed Forces Radiobiology Research Institute, Defense Nuclear Agency, under contract DNA-001-86C-0192.

## References

1. Dexter TM, Allen TD, Lajtha LG (1977) Conditions controlling the proliferation of haemopoietic stem cells in vitro. J Cell Physiol 91:335
2. Sakakeeny MA, Greenberger JS (1982) Granulopoiesis longevity in continuous bone marrow cultures and factor-dependent cell line generation: significant variation among 28 inbred mouse strains and outbred stocks. J Natl Cancer Inst 68:305
3. Eastment CE, Denholm E, Katsnelson L, Arnold E, Ts'o POP (1982) In vitro proliferation of hematopoietic stem cells in the absence of an adherent monolayer. Blood 60:130
4. Moore MAS, Sheridan APC, Allen TD, Dexter TM (1979) Prolonged hemopoiesis in a primate bone marrow culture system: characteristics of stem cell production and the hematopoietic microenvironment. Blood 54:775

5. Gartner S, Kaplan HS (1980) Long-term culture of human bone marrow cells. Proc Natl Acad Sci USA 77:4756
6. Hass EE, Hale F (1982) Growth of normal hemopoietic cells in cultures of bone marrow from leukemic mice. Eur J Cancer Clin Oncol 18:413
7. Chang J, Morgenstern G, Deakin D, Testa NG, Coutinho L, Scarffe JH, Harrison C, Dexter TM (1986) Reconstitution of haemopoietic system with autologous marrow taken during relapse of acute myeloblastic leukaemia and grown in long-term culture. Lancet i:294
8. Coulombel L, Kalousek DK, Eaves CJ, Gupta CM, Eaves AC (1983) Long-term marrow culture reveals chromosomally normal hematopoietic progenitor cells in patients with Philadelphia chromosome positive chronic myelogenous leukemia. N Engl J Med 308:1493
9. Appelbaum FR, Deeg HJ, Storb R, Self S, Graham TC, Sale GE, Weiden PL (1985) Marrow transplant studies in dogs with malignant lymphoma. Transplantation 39:499
10. Kwok WW, Schuening F, Stead RB, Miller AD (1986) Retroviral transfer of genes into canine hemopoietic progenitor cells in culture: a model for human gene therapy. Proc Natl Acad Sci USA 83:4522
11. Schuening F, Emde C, Schaefler UW (1983) Improved culture conditions for granulocyte-macrophage progenitor cells [abstr]. Exp Hematol [Suppl 14] 11:205
12. Schuening F, Storb R, Goehle S, Meyer J, Graham T, Deeg HJ, Pesando J (1987) Canine pluripotent hematopoietic stem cells and CFU-GM express Ia-like antigens as recognized by two different class II-specific monoclonal antibodies. Blood 69:165
13. Schuening F, Storb R, Nash R, Stead RB, Kwok WW, Miller AD (1988) Retroviral transfer of genes into canine hematopoietic progenitor cells. In: Tavassoli M, Zanjani ED, Ascensao JL, Abraham NG, Levine AS (eds) Molecular biology of hemopoiesis. New York: Plenum, p 9
14. Coulombel L, Eaves AC, Eaves CJ (1983) Enzymatic treatment of long-term human marrow cultures reveals the preferential location of primitive hemopoietic progenitors in the adherent layer. Blood 62:291
15. Spooncer E, Dexter TM (1984) Long-term bone marrow cultures. Bibl Haematol 48:366
16. Greenberg HM, Newburger PE, Parker LM, Novak T, Greenberger JS (1981) Human granulocytes generated in continuous bone marrow culture are physiologically normal. Blood 58:724
17. Greenberger JS (1978) Sensitivity of corticosteroid-dependent insulin-resistant hypogenesis in marrow preadipocytes of obese-diabetic (db/db) mice. Nature 275:752
18. Dexter TM, Spooncer E, Simmons P, Allen TD (1984) Long-term marrow culture: an overview of techniques and experience. In: Wright DG, Greenberger JS (eds) Long-term bone marrow culture. New York: Alan R Liss, p 57
19. Eastment CE, Ruscetti FW, Denholm E, Katznelson L, Arnold E, Ts'o POP (1982) Presence of mixed colony-forming cells in long-term hamster bone marrow suspension cultures: response to pokeweed spleen conditioned medium. Blood 60:495
20. Moore MAS, Sheridan APC (1979) Pluripotential stem cell replication in continuous human, prosimian and murine bone marrow culture. Blood Cells 5:297
21. Dexter TM, Moore MAS, Sheridan APC (1977) Maintenance of hemopoietic stem cells and production of differentiated progeny in allogeneic and semiallogeneic bone marrow chimeras in vitro. J Exp Med 145:1612
22. Moore MAS, Dexter TM (1978) Stem cell regulation in continuous hematopoietic cell culture. Transplant Proc 10:83

J. RADIAT. RES., 29, 255 – 260 (1988)



*Short Communication*

# Radioprotection of Mouse Hematopoietic Stem Cells by Leukotriene $A_4$ and Lipoxin $B_4$

THOMAS L. WALDEN, JR.

Radiation Biochemistry Dept., Armed Forces Radiobiology Research Institute,
Bethesda, Maryland 20814-5145 U.S.A.

*(Received August 3, 1988)*
*(Accepted September 8, 1988)*

**Radioprotection Leukotriene $A_4$ Lipoxin $B_4$ Endogenous spleen colony formation Mouse hematopoietic stem cell**

The potent cyto-radioprotective biological activity induced by leukotrienes prompted a search for other lipoxygenase products exhibiting similar properties. Pretreatment of mice with 1 to 20 μg of leukotriene $A_4$ before sublethal irradiation induced an increase in the number of endogenous hematopoietic stem cells. Radioprotection was also provided by pretreatment with lipoxin $B_4$, but not with lipoxin $A_4$ or with potential lipoxin precursors 5-HETE, 15-HPETE, 15-HETE, and arachidonic acid. The degree of protection induced by leukotriene $A_4$ or lipoxin $B_4$ is less than that previously reported for an equivalent dose of leukotriene $C_4$. Administration of the lipoxins did not result in any visibly detectable side effects such as diarrhea or ataxia.

## INTRODUCTION

The cytoprotective properties of eicosanoids were used for both cyclooxygenase products[1-3] and, more recently, lipoxygenase products to induce radioprotection[4,5]. This protection was shown with cells in culture[2,4], mouse hematopoietic stem cells *in vivo*[1,5], and with whole animal survival[1-3]. DRF's of 1.7 or greater can be obtained with DiPGE$_2$, a synthetic derivative of the naturally occurring prostaglandin E$_2$[1], and with LTC$_4$[5]. These cytoprotective radioprotective properties have significance in normal physiological processes and also in cancer biology where some tumors produce elevated levels of eicosanoids[6] and may influence therapeutic efficacy.

Pretreatment with LTC$_4$ provides a DRF of 2.01 for protection of mouse granulocyte-macrophage progenitor stem cells[5]. Because of the significant DRF by this one lipoxygenase product, the potential for other protective lipoxygenase products including the hydroxy fatty acids and lipoxins, was examined. Lipoxins are derived through the interaction of more than one type of lipoxygenase[7,8]. Although they may be formed by several biosynthetic routes, the best

characterized pathway involves the action of a 5-lipoxygenase on a 15-lipoxygenase product, either 15-HPETE, or 15-HETE. The two primary naturally occuring lipoxins are $LXA_4$ and $LXB_4$. Lipoxin production has been demonstrated in human neutrophils[9], rat basophilic leukemia cells[10], alveolar macrophages[209], and mastocytoma cells[11]. Their biological activities include smooth muscle contraction[12], inhibition of natural killer cell activity[13], vasoactivation[12], and as chemotactic factors for granulocytes[14]. The potential radioprotective properties of $LXB_4$ as well as that of $LTA_4$, a precursor of the lipoxins and leukotrienes, on hematopoietic stem cells (E-CFU) are presented in this paper.

## MATERIALS AND METHODS

*Compounds.* Synthetic $LXA_4$ and $B_4$, 15-HPETE, 15-HETE, and 5-HETE were obtained from BioMol Research Laboratory (Philadelphia, PA). Arachidonic acid was obtained from Nu Chek Prep, Inc. (Elysian, MN). $LTA_4$ methyl ester was the generous gift of Dr. Joshua Rokach (Merck Frosst Laboratories, Pointe Claire-Dorval, Canada). The free acid of $LTA_4$ was prepared from the methyl ester by saponification in methanol 50% sodium hydroxide (9:1, v:v) on ice for 4 hr. The pH was then adjusted to 7.0 with dilute HCl. Each eicosanoid was evaporated to dryness under nitrogen and resuspended in ethanol. Ethanol solutions containing the appropriate eicosanoid concentration were adjusted to 0.4% ethanol in Hanks' buffered salt solution (Gibco Biological Laboratories, Grand Island, NY). Compounds were administered by subcutaneous injection in the nape of the neck in a volume of 100 μl, 15 min before irradiation. Previous studies have shown that the optimal administration time for other eicosanoids using the E-CFU assay described below is 15 min prior to irradiation[1,5].

*Mice.* Male CD2F1 mal. mice, 10 to 12 weeks old, were obtained from Charles River (Kingston, NY). Animals were quarantined for a period of 2 weeks and examined for pathological or serological indications of illness or *Pseudomonas* infection (representative sampling). Mice were housed 8-10 to a cage in Microisolator cages on hardwood-chip contact bedding, maintained in conventional animal holding rooms in an AAALAC-accredited facility. Rooms were maintained at 21 ± 1°C with 50% relative humidity with 12 room changes of 100% conditioned fresh air per hour. Mice were maintained on a 12-hr light-dark cycle and provided with Wayne Rodent Blox diet (Continental Grain Co., Inc., Chicago, IL) and acidified water (pH, 2.5) *ad libitum*. At the time of the experiments, animals weighed 20-25 g.

*Irradiation.* Mice were irradiated in a bilateral cobalt-60 gamma radiation field at a dose rate of 1 Gy/min to a total dose of 7.25 Gy, as previously described[5].

*Hematopoietic Stem Cell Assay.* E-CFU formation was assayed by the method of Till and McCullough[15], as previously described[5]. Briefly, mice received 7.25 Gy of irradiation. They were killed at 10 days postirradiation by asphyxiation in a charged $CO_2$ chamber, and their spleens were removed and fixed in Bouin solution. The number of colonies per spleen were determined, and the mean and standard error were reported. Statistical significance was determined by analysis of variance or Student's t-test. The reported increases in E-CFU numbers are reproducible.

## RESULTS

Pretreatment with $LTA_4$ induced a dose-dependent radioprotection of E-CFU's (Figure 1). A 20 μg dose (not in figure) provided twice the protection of a 10 μg dose by increasing the number of surviving E-CFU's to 31.4 ($n = 5$). $LTA_4$ doses of 10 μg or greater produced ulceration at the site of injection in 80% of the mice. No ulceration was produced by the other eicosanoids.

Administration of 0.1 to 10 μg of $LXA_4$ 15 min before receiving 7.25 Gy of $^{60}$Co gamma radiation did not increase E-CFU numbers in the spleens at 10 days postirradiation (Figure 1). Unlike $LXA_4$, pretreatment with $LXB_4$ ($n = 5$) induced a small statistically significant increase in E-CFU numbers (Table 1). E-CFU's per spleen increased from 0.6 ± 0.2 (standard error) in control mice to 2.8 ± 0.6 in mice that received 10 μg of $LXB_4$. 15-HPETE, 15-HETE, 5-HETE, and arachidonic acid did not increase E-CFU numbers at the concentrations examined (Figure 1 and Table 1).

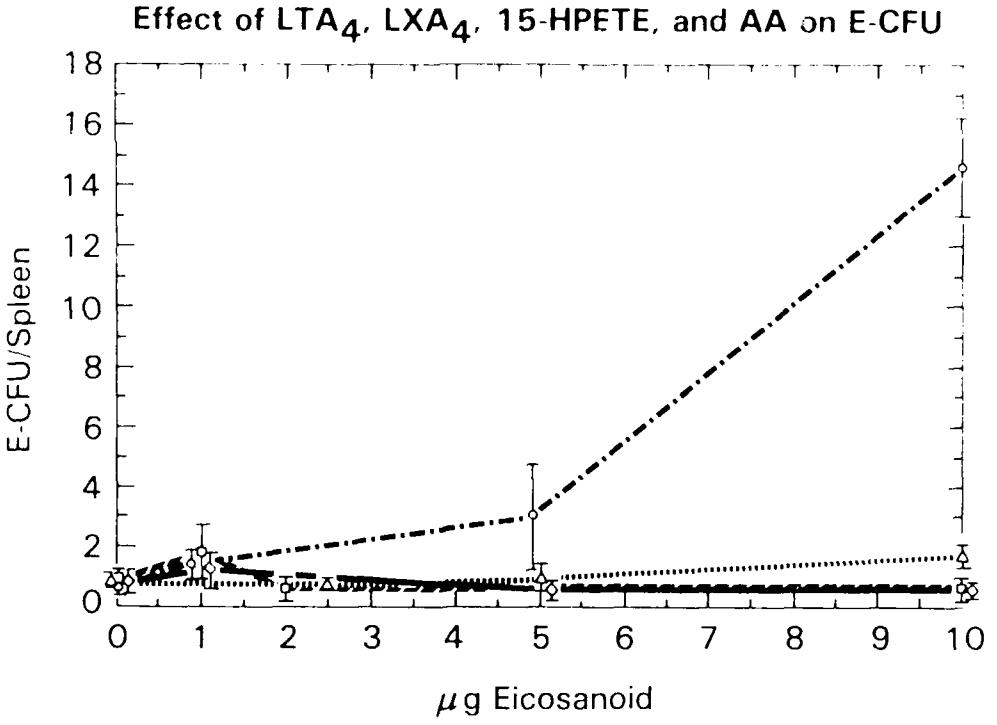


**Fig. 1.** Effect of lipoxygenase product pretreatment on E-CFU radiation survival. Mice ($n = 5$) were pretreated with the indicated concentration of eicosanoid 15 min before receiving 7.25 Gy of $^{60}$Co γ-radiation at a dose rate of 1 Gy/min. The number of E-CFU were determined on day 10 postirradiation. $LXA_4$ (◇); 15-HPETE (□); arachidonic acid (△); and $LTA_4$ (○). Each data point represents the mean ± the standard error of the mean. Only the $LTA_4$ data were significant, using analysis of variance.

Table 1. [illegible]

| [illegible] | [illegible] | E-CFU (± SEM) |
|---|---|---|
| [illegible] | | [illegible] |
| [illegible] | [illegible] | [illegible] |
| [illegible] | [illegible] | [illegible] |
| [illegible] | [illegible] | [illegible]** |

[illegible]

## DISCUSSION

A previous report demonstrated that $LTC_4$ and $LTB_4$ induced radioprotection of mouse hematopoietic stem cells[1] and prompted further investigation for other lipoxygenase products that induced cytoprotection/radioprotection. Of the additional products examined in the present study, $LTA_4$ provided the greatest degree of protection, but was not as effective as that reported for $LTC_4$. It is not clear whether $LTA_4$-induced radioprotection is a direct effect or mediated through conversion to other leukotrienes such as $LTC_4$.

Pretreatment with $LXB_4$, but not $LXA_4$, resulted in a small enhancement of E-CFU's in the spleens of sublethally irradiated mice. $LXB_4$ was approximately one-third as effective as an equivalent dose of $LTB_4$[1]. Enhancement was not observed for possible lipoxin precursors 15 HPETE, 15 HETE, or 5 HETE. Although in theory the survival of one pluripotent hematopoietic stem cell can prevent radiation-induced hematopoietic death, the $LXB_4$ E-CFU numbers are probably too low to increase animal survival. On a comparative basis for E-CFU radioprotection, $LTC_4 > LTA_4$, $DiPGE_2 > LTB_4 > LTE_4 > LTD_4 > LTE_4 > LXB_4$[1,2]. The lack of protection by arachidonic acid itself might be attributable to dilution through metabolism to a number of eicosanoids.

Administration of radioprotective concentrations of $DiPGE_2$ has been reported to cause diarrhea and ataxia[3]; however, none of the LXs or other lipoxygenase products examined produced diarrhea. In addition, no deaths resulted from toxicity, and no visible decrements in locomotor activity during the first 30 min posttreatment were apparent.

The mechanism for eicosanoid radioprotection in general remains unknown[5,46], but they are not thought to act by direct free radical scavenging[51] or by modification of DNA repair[47]. Prostacyclin-induced cytoprotection of the gastric mucosa in swine has been attributed to increased blood flow mediated by cAMP[52]. Lipoxins, like most eicosanoids, are vasoactive[12]. They do not stimulate cAMP production[13], but are potent activators of protein kinase C[49]. $LTA_4$- and $LXB_4$-induced radioprotection may be a hormonal response through direct influences on hematopoiesis. Prostaglandins, for example, stimulate hematopoiesis[20] while $LTC_4$ influences myeloid stem cell response to colony-stimulating factor[21]. Similar roles for LX's must await further research. Some tumor cells produce LX's[9,11] and therefore, LX-induced protection could

have implications for altered fibrinolysis.

## ACKNOWLEDGEMENTS

This research was supported by the Armed Forces Radiobiology Research Institute, Defense Nuclear Agency, under Research Work Unit 00152. The views presented in this paper are those of the author. No endorsement by the Defense Nuclear Agency has been given or should be inferred. Research was conducted according to the principles enunciated in the *Guide for the Care and Use of Laboratory Animals*, prepared by the Institute of Laboratory Animal Resources, National Research Council.

## REFERENCES

1. Walden, T. L., Jr., Parsons, M. L. and Snyder, S. L. (1987) 16,16-dimethyl prostaglandin E$_2$ increases survival of mice following irradiation. Radiat. Res. **109:** 440–448.
2. Prasad, K. N. (1972) Radioprotective effect of prostaglandin and an inhibitor of cyclic nucleotide phosphodiesterase on mammalian cells in culture. Int. J. Radiat. Biol. **22:** 187–189.
3. Landauer, M. R., Walden, T. L., Jr., Davis, H. D. and Dominitz, J. A. (1987) Alterations in locomotor activity induced by radioprotective doses of 16,16-dimethyl prostaglandin E$_2$. In "Prostaglandins and Lipid Metabolism in Radiation Injury", Ed. T. L. Walden and H. N. Hughes, pp. 244–251. Plenum Press, New York.
4. Walden, T. L., Jr., Hofelstein, J. V. and Catravas, G. N. (1986) Development of a model system to study leukotriene-induced modification of radiosensitivity in mammalian cells. Lipids Res. **25:** 587–590.
5. Walden, T. L., Jr., Patchen, M. L. and MacVittie, T. J. (1988) Leukotriene induced radioprotection of hematopoietic stem cells in mice. Radiat. Res. **113:** 388–395.
6. Bertazzo, A. (1987) In "Biological Protection with Prostaglandins" Ed. M. M. Cohen, Vol. 2, pp. 73–80. CRC Press, New York.
7. Parker, C. W., and Walden, T. L., Jr. (1988) Structures and actions of lipoxins: A review. Pros. Prostaglandins Leukotrienes Essential Fatty Acids, in press.
8. Serhan, C. N., Hamberg, M. and Samuelsson, B. (1984) Lipoxins: Novel series of biologically active compounds formed from arachidonic acid in human leukocytes. Proc. Natl. Acad. Sci. USA **81:** 5335–5339.
9. Ng, C. F., Lam, B. K., Pritchard, K., Stemerman, M. and Wong, P. Y.-K. (1988) Generation of lipoxin A$_4$ from rat basophilic leukemia cell (RBL-1). FASEB Journal **2:** A1265 (abstract).
10. Kot, S. L. (1988) Formation of lipoxins by alveolar macrophages. Biochem. Biophys. Res. Comm. **150:** 870–876.
11. Lazarus, S. C. and Zocca, E. (1988) Production of lipoxins by canine mastocytoma cells. FASEB Journal **2:** A409 (abstract).
12. Dahlén, S. E., Raud, J., Serhan, C. N., Björk, J. and Samuelsson, B. (1987) Biological activities of lipoxin A: Rabbit aortic strips contraction and dilation of arterioles *in vivo*. Acta. Physiol. Scand. **130:** 643–647.
13. Ramstedt, U., Ng, J., Wigzell, H., Serhan, C. N. and Samuelsson, B. (1985) Novel action of eicosanoids lipoxins A and B on human natural killer cell cytotoxicity: Effects on intracellular cAMP and target cell binding. J. Immunol. **135:** 3434–3438.
14. Palmblad, J., Gyllenhammer, H., Ringertz, B., Serhan, C. N., Samuelsson, B. and Nicotera, K. C. (1987) Effects of lipoxin A and B on functional responses of human granulocytes. Biochem. Biophys. Res. Comm. **145:** 168–175.

5. [illegible] and McCulloch, E. A. (1963) Early repair processes in marrow cells irradiated and proliferating in vitro. Radiat. Res. **18**: 96–101.
6. Walden, T. L., Jr. (1987) A paradoxical role for eicosanoids: Radioprotectants and radiosensitizers. In *Prostaglandins and Lipid Metabolism in Radiation Injury*, Ed. T. L. Walden, Jr. and H. N. Hughes, pp. 263–275. Plenum Press, New York.
7. Hanson, W. R., Frankenfield, D. L. (1987) Radiation-induced single-strand breaks in the intestinal mucosal DNA of mice and their modification by the radioprotectors WR-2721 or 16,16-dimethyl prostaglandin E$_2$. Int. J. Radiat. Biol. **52**: 67–76.
8. Robert, A., Nezamis, J. E., Lancaster, C. and Davison, A. V. (1982) Prostacyclin-mediated gastric cytoprotection: Is it dependent on mucosal blood flow? J. Supramol. Res. **33**: 140–145.
9. Hansson, A., Serhan, C. N., Haeggstrom, J., Iradman-Sandberg, M., Samuelsson, B. and Morris, J. (1986) A novel pathway of prostaglandin E$_2$ conversion by lipoxin A and other eicosanoids. Intracellular action of oxygenation products of arachidonic acid. Biochem. Biophys. Res. Comm. **134**: 1215–1222.
10. Dicke, P. P., Steele, N. V., Hammond, D., Ortega, J. A. and Datta, M. C. (1973) Enhancement of colony growth by prostaglandins. J. Lab. Clin. Med. **82**: 704–712.
11. Zhang, A. Y., Wong, J., Wu, M. C. and Yamms, A. Y. (1986) Modulation of colony stimulating factor-induced granulocyte-macrophage colony formation by N-peptido-lipoxygenase products. Cancer Res. **46**: 600–603.


**Abbreviations:** DRF, dose reduction factor; E-CFU, endogenous spleen colony forming unit; E-CSC, endogenous hematopoietic stem cell; LTA$_4$, leukotriene A$_4$; LTB$_4$, leukotriene B$_4$; LTC$_4$, leukotriene C$_4$; LXA$_4$, 5(S),6(R),15(S)-trihydroxy-7,9,13-*trans*-11-*cis*-eicosatetraenoic acid; LXB$_4$, 5(S),14(R),15(S)-trihydroxy-6,10,12-*trans*-eicosatetraenoic acid; DiPGE$_2$, 16,16-dimethyl prostaglandin E$_2$; 15-HPETE, 15-hydroperoxy-eicosatetraenoic acid; 15-HETE, 15-hydroxy eicosatetraenoic acid; 5-HETE, 5-hydroxy eicosatetraenoic acid.

# Selective association and transport of *Campylobacter jejuni* through M cells of rabbit Peyer's patches

RICHARD L. WALKER,[1] ELSA A. SCHMAUDER-CHOCK, AND JOE L. PARKER
*Armed Forces Radiobiology Research Institute, Bethesda, MD 20814-5145, U.S.A.*

AND

DONALD BURR
*Naval Medical Research Institute, Bethesda, MD 20814-5055, U.S.A.*

Received March 16, 1988

Accepted June 7, 1988

WALKER, R. L., SCHMAUDER-CHOCK, E. A., PARKER, J. L., and BURR, D. 1988. Selective association and transport of *Campylobacter jejuni* through M cells of rabbit Peyer's patches. Can. J. Microbiol. **34**: 1142–1147.

M cells in the Peyer's patches may facilitate transport of pathogens such as *Campylobacter jejuni* from the intestine. We evaluated this hypothesis by using electron microscopy to examine Peyer's patches in ligated adult rabbit ileal loops inoculated with 5-mL suspensions of $10^9$ cfu mL$^{-1}$ of *Campylobacter jejuni*. Peyer's patches taken at intervals from 15 min to 2 h after inoculation of loops in anaesthetized rabbits provided evidence that *Campylobacter jejuni* selectively adhered to M cells as opposed to absorptive epithelial cells and was transported, apparently intact, into the M cell follicle. Although intercellular organisms were seen within the follicle, many others were phagocytosed by lymphoid cells. The proximity of the lymphatic and blood circulatory systems to the M cell follicle makes this a probable route for systemic spread of *Campylobacter jejuni*.

WALKER, R. L., SCHMAUDER-CHOCK, E. A., PARKER, J. L., et BURR, D. 1988. Selective association and transport of *Campylobacter jejuni* through M cells of rabbit Peyer's patches. Can. J. Microbiol. **34**: 1142–1147.

On croit que les cellules M présentes dans les plaques de Peyer pourraient faciliter la migration de pathogènes comme *Campylobacter jejuni* à partir de l'intestin. Nous avons évalué cette hypothèse en examinant par microscopie électronique les plaques de Peyer chez le lapin adulte par la méthode des anses iléales ligaturées inoculées avec 5 mL d'une suspension contenant $10^9$ cfu mL$^{-1}$. Les plaques de Peyer prélevées entre 15 min et 2 h suivant l'inoculation des anses chez le lapin anesthésié montrent avec évidence que *Campylobacter jejuni* adhère sélectivement aux cellules M plutôt qu'aux cellules épithéliales absorbantes et qu'il est transporté apparemment intact à l'intérieur du follicule de la cellule M. Même si des bactéries se retrouvent dans le follicule plusieurs autres sont phagocytées par les cellules lymphoïdes. Le follicule M étant à proximité des systèmes circulatoires sanguin et lymphatique, il devient la voie probable de dissémination systémique de *Campylobacter jejuni*.

[Traduit par la revue]

## Introduction

M cells are important antigen-sampling structures found in the epithelial layer over lymphoid follicles of the gastrointestinal mucosa (Sneller and Strober 1986). They were originally termed M cells or Microfold cells due to their surface structure. Since the surfaces of these cells have subsequently been found to be variable, the term Microfold has been dropped, but the designation M retained. Since their initial description (Owen and Jones 1974), these cells have been shown to interact with a number of pathogens. For example, *Vibrio cholerae* attaches to and is taken up by M cells (Owen et al. 1986). In contrast, strain RDEC-1 *Escherichia coli*, which causes diarrhea in rabbits, attaches to but is not transported through the M cell to the subepithelial lymphoid tissue (Inman and Cantey 1983). *Salmonella typhi* GIFU 10007 adheres to M cell surfaces and destroys them, thereby permitting entry to deeper tissues and to the general circulation (Kohbata et al. 1986).

*Campylobacter jejuni* is now recognized as a major enteric pathogen that, among other virulence characteristics, can be invasive and has been found in blood cultures from infected humans and animals (Blaser et al. 1984; Drake et al. 1981; Longfield et al. 1979; Spelman et al. 1986). This may be a phenomenon associated with movement of the organisms through the mucosa and proliferation in the lamina propria and mesenteric lymph nodes (Butzler and Skirrow 1979; Skirrow 1977; Youssef et al. 1985). It is possible that M cells could be important in this process associated with pathogenesis as well as being key cells for presentation of foreign antigen to the mucosal immune system.

We examined Peyer's patches (PP) in ligated rabbit ileal loops because knowledge of M cell – *Campylobacter* interactions could contribute to understanding the pathogenesis of the disease as well as to the development of oral vaccines to this organism. Moreover, if *Campylobacter* does attach to and is translocated by M cells, its unique spiral morphology could provide an excellent model for the study of M cell function under a variety of experimental conditions.

## Materials and methods

### *Cultivation of* Campylobacter

*Campylobacter jejuni* strain HC, Penner serotype 27 (Walker et al. 1986), was isolated from the blood of an enteritis patient from Bethesda, Maryland. Frozen stocks of the organism were thawed, inoculated in trypicase soy blood agar plates, and incubated at 42°C in plastic bags with an atmosphere of 85% $N_2$, 10% $CO_2$, and 5% $O_2$. After 18 h the cells were suspended in brucella broth supplemented with 0.04% cysteine and 0.25% serine to a concentration having an OD at 625 nm of 0.05. Six millilitres of the resulting suspension was overlaid in 25 cm$^2$ T flasks containing 4 mL of brucella blood agar. After 18 h incubation at 37°C, the fluid portion of the biphasic culture system was collected and screened for contamination by examining the culture under dark-field microscopy. It was then pooled and used directly for rabbit challenges.

[1]Author to whom all correspondence should be addressed.

Printed in Canada / Imprimé au Canada


FIG. 1. Light micrograph of a follicle dome and overhanging adjacent villus after 15 min incubation. Villus on upper left has mature lymphocytes between absorptive epithelial cells. Absorptive cells (A), on follicle at lower right, protrude above level of M cells (M). Bacteria in lumen (arrows) are associated only with M cells.

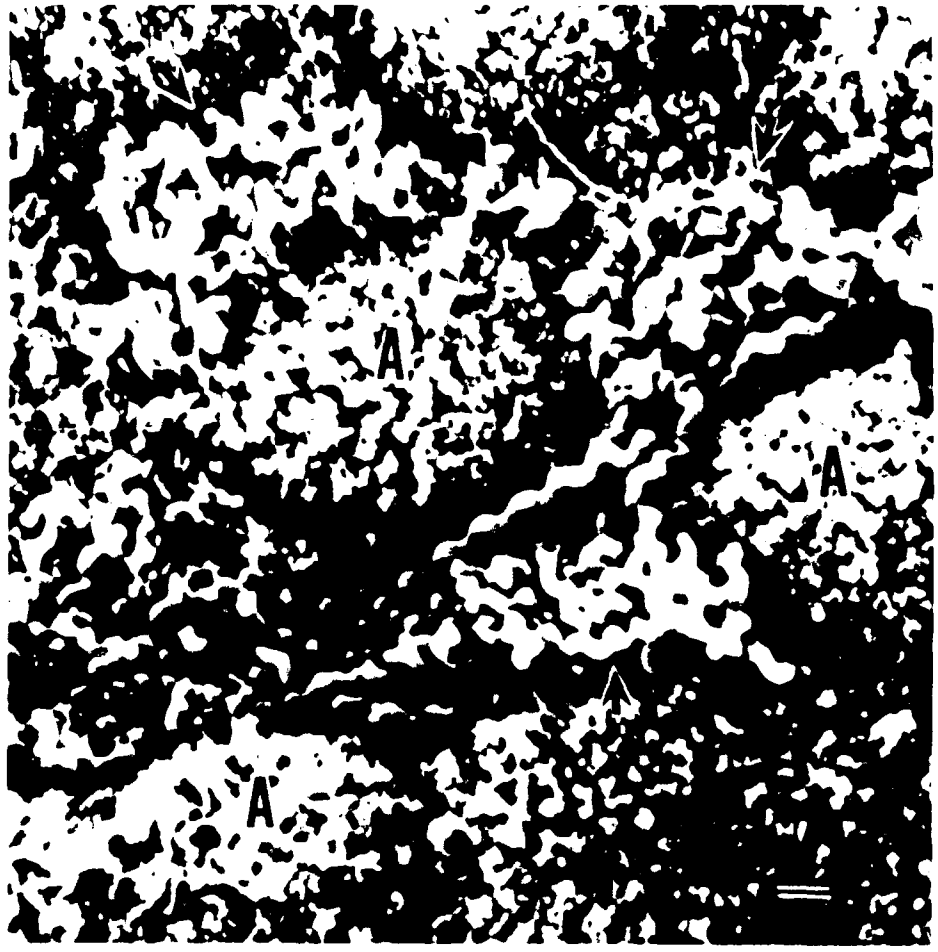


FIG. 2. Scanning electron micrograph of surface of Peyer's patch follicle after 15 min incubation with *Campylobacter*. Absorptive cells (A) protrude into lumen of gut and remain uncovered by bacteria. Bacteria with characteristic spiral shape (arrows) adhere to regions between absorptive cells. Bar = 1 μm.


FIG. 3. After 15 min incubation, *Campylobacter* (arrows) are associated with luminal surface of the M cells (M), which are separated from underlying lymphoid cells by a small space (arrowheads) and connected to each other by a membrane junction (asterisk). Bar = 3 μm.


FIG. 4. Endocytosis of bacteria by M cells (M) seen after 120 min incubation. Inset is enlargement of bacteria being endocytosed from intestinal lumen (arrow). Bar = 2 μm.

*Rabbit surgery*

Female New Zealand white rabbits, weighing 1.5–2.0 kg, were anaesthetized with 70 mg/kg ketamine and 0.4 mg/kg acepromaine. All animals were fasted for at least 18 h prior to surgery. The small intestine was drawn out aseptically through a midventral laparotomy and kept moist with saline. Loops measuring 5 cm were made using string ligatures and inoculated with 5-mL suspensions of approximately $10^9$ cfu/mL. Control loops were inoculated with sterile culture broth. The intestine was returned into the abdominal cavity and the abdominal wall closed with sutures. At predetermined times (15 min to 2 h after inoculation of loops), the animals were euthanatized (T-61 Euthanasia solution, American Hoechst Corporation, Animal Health Division, Somerville, NJ 08876), and the loops were removed to a petri dish, drained, and inverted over a glass rod.

*Sample preparation and examination*

Intestinal loops were fixed in a 4°C solution containing 2% paraformaldehyde, 2.5% glutaraldehyde, 1.5% acrolein (molecular weight, 56.06), 4 mM calcium chloride (reagent grade), and 100 mM sodium cacodylate. This fixative was made in a final volume of 100 mL of distilled water at pH 7.3. After initial fixation, PP were dissected and trimmed, and continued to fix in fresh fixative at room temperature for a total of 2 h. Specimens for transmission and scanning electron microscopy (TEM and SEM, respectively) were washed in 100 mM sodium cacodylate, postfixed 1 h in 1% osmium tetroxide, and dehydrated in an ethanol series. Specimens for TEM were embedded in Epon 812. Thick sections were stained with 1% methylene blue and 1% Azure II in 1% sodium borate (reagent grade) solution. Thin sections were stained with 1% uranylacetate and Reynold's lead


[illegible] M cells, P and bacteria beneath M cells. M after 120 min inoculation. Photographed [illegible] Note [illegible] Bar [illegible]

[illegible] SEM [illegible] SEM [illegible] P < 0.001 [illegible] SEM

## Results and discussion

[illegible] bits undergoing the removable intestinal tie adult rabbit diarrhea (RITARD) procedure (Caldwell et al. 1985; in our laboratories unpublished data).

However, when PP were examined, noticeably different associations between *Campylobacter* and host were found. The epithelium of the PP is heavily populated with M cells only over the lymphoid follicle, while the villus epithelium on the opposite side is composed entirely of absorptive cells (Fig. 1). This specimen was fixed 15 min after inoculation of *Campylobacter* into the intestinal loop, and the bacteria were seen selectively associated with M cells. No bacteria were

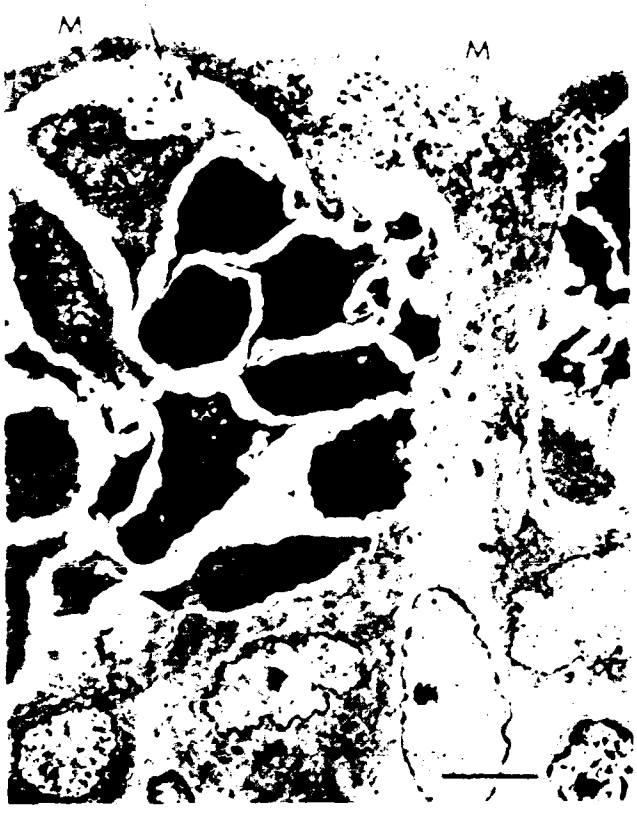


FIG. 6. *Campylobacter* (arrow) after transversing M cells (M) are clustered in intercellular space. Note space separating lymphoid cells filling M cell pocket, compared with Fig. 4. Bar = 5 μm.

seen in loops inoculated with sterile broth.

The specificity of the attachment of *Campylobacter* to M cells after a 15-min incubation was also observed using SEM (Fig. 2). Numerous *Campylobacter* were seen adhering to certain areas while leaving the absorptive epithelial cells uncovered. The identification of these covered areas as M cells was determined using TEM. With TEM the bacteria were clearly observed in association with the luminal surface of the M cells, but not absorptive cells (Fig. 3).

Vacuoles containing *Campylobacter* could be seen in the M cells (Fig. 4). Bacteria were rapidly transported to lymphoid cells, presumably macrophages (Fig. 5). The relationship between M cells and lymphoid cells can also be seen in Fig. 6, where M cell processes formed a canopy over the enclosed cells. Also seen in Fig. 6, the bacteria were free in large groups between cells.

The M cell could be a means by which *Campylobacter* leave the gut, and selective association and penetration of M cells could help explain the bacteremia seen previously in rabbits challenged with the RITARD procedure (Caldwell et al. 1983). The *C. jejuni* HC strain used here was isolated from human blood, and several examples of human bacteremia have been reported (Drake et al. 1981; Longfield et al. 1979; Spelman et al. 1986). Bacteremia is seen in normal mice inoculated orally with *Campylobacter* (Blaser et al. 1984), and *C. jejuni* is associated with mesenteric lymph nodes and PP of gnotobiotic mice given oral challenges (Fauchere et al. 1985; Yousset et al. 1985). These events may not be associated with enteroinvasive properties of the organism, but may be due to an active bacterial uptake system of the host. This conclusion is consistent with the uptake of noninvasive cholera organisms by M cells (Owen et al. 1986). In contrast to a report by Owen and Jones (1974) and another by Fujimura (1986) describing the uptake of BCG by M cells, the pseudopodlike uptake of bacteria by the M cell was rarely seen in our study.

It is of interest that not only are intact bacteria taken up by the M cells, but also many organisms can be transferred simultaneously to underlying lymphoid follicles. The large numbers of organisms placed in the loops may be responsible for the dramatic uptake seen in this study. Rapid uptake of bacteria could lead to transient bacteremia by overwhelming normal clearance mechanisms. It remains to be seen whether a similar phenomenon in immunocompromised hosts could account for opportunistic infections. The proximity of the lymphatic and blood circulatory systems makes this a likely possibility.

These data indicate that, at least in ligated ileal loops, *C. jejuni* can attach to M cells and be transported through them to the underlying follicle. This process bears similarities to and differences from the events seen with other microbial pathogens (Inman and Cantey, 1983; Kohbata et al. 1986; Owen et al. 1986). It is unknown whether phenomena seen in ligated loops truly reflect those events occurring in normal *in vivo* models. Further, much work remains to discover how bacteria reach and are transported through M cells and what effect this event may have on the bacteria and the host. The data now available for *Campylobacter* and other pathogens make these questions all the more compelling.

## Acknowledgments

We extend our thanks to Ms. Beverly Geisbert for typing this manuscript and to Ms. J. Van Deusen for her editorial assistance. This study was supported by the Naval Medical Research and Development Command, Bethesda, MD, and the Armed Forces Radiobiology Research Institute, Bethesda, MD.

BLASER, M. J., DUNCAN, D. J., and SMITH, P. F. 1984. Pathogenesis of *Campylobacter* infection: clearance of bacteremia in mice. Microecology and Therapy, **14**: 103 – 108.

BUTZLER, J. P., and SKIRROW, M. B. 1979. *Campylobacter* enteritis. Clin. Gastroenterol. **8**: 737 – 765.

CALDWELL, M. B., WALKER, R. I., STEWART, S. D., and ROGERS, J. E. 1983. Simple adult rabbit model for *Campylobacter jejuni* enteritis. Infect. Immun. **42**: 1176 – 1182.

DRAKE, A. A., GILCHRIST, M. J. R., WASHINGTON, J. A., II, HUTZENGA, K. A., and VAN SCOY, R. E. 1981. Diarrhea due to *Campylobacter fetus* subspecies *jejuni*. Mayo Clin. Proc. **56**: 414 – 423.

FAUCHERE, J. L., VERON, M., LELLOUCH-TUBIANA, A., and PFISTER, A. 1985. Experimental infection of gnotobiotic mice with *Campylobacter jejuni*: colonization of intestine and spread of lymphoid and reticulo-endothelial organs. J. Med. Microbiol. **20**: 215 – 224.

FUJIMURA, Y. 1986. Functional morphology of microfold cells (M cells) in Peyer's patches: phagocytosis and transport of BCG by M cells into rabbit Peyer's patches. Gastroenterol. Jpn. **21**: 325 – 335.

INMAN, L. R., and CANTEY, J. R. 1983. Specific adherence of *Escherichia coli* (Strain RDEC-1) to membranous (M) cells of the Peyer's patch in *Escherichia coli* diarrhea in the rabbit. J. Clin. Invest. **71**: 1 – 8.

KOHBATA, S., YOKOYAMA, H., and YABUUCHI, E. 1986. Cytopathogenic effect of *Salmonella typhi* GIFU 10007 on M cells of murine ileal Peyer's patches in ligated ileal loops: an ultrastructural study. Microbiol. Immunol. **30**: 1225–1237.

LEE, A., O'ROURKE, J. L., BARRINGTON, P. J., and TRUST, T. J. 1986. Mucus colonization as a determinant of pathogenicity in intestinal infection by *Campylobacter jejuni*: a mouse cecal model. Infect. Immun. **51**: 536–546.

LONGFIELD, R., O'DONNELL, J., VEDL, W., LISSNER, C., and BURNS, T. 1979. Acute colitis and bacteremia due to *Campylobacter fetus*. Dig. Dis. Sci. **24**: 950–953.

OWEN, R. L., and JONES, A. L. 1974. Epithelial cell specialization within human Peyer's patches: an ultrastructural study of intestinal lymphoid follicles. Gastroenterology, **66**: 189–203.

OWEN, R. L., PIERCE, N. F., APPLEL, R. F., and CRAY, W. C., JR. 1986. M cell transport of *Vibrio cholerae* from the intestinal lumen into Peyer's patches: a mechanism for antigen sampling and for microbial transepithelial migration. J. Infect. Dis. **153**: 1108–1118.

SKIRROW, M. B. 1977. *Campylobacter* enteritis: a "new" disease. Br. Med. J. **2**: 9–11.

SNELLER, M. C., and STROBER, W. 1986. M cells and host defense. J. Infect. Dis. **154**: 737–741.

SPELMAN, D. W., DAVIDSON, N., BUCKMASTER, D., SPICER, W. J., and RYAN, P. 1986. *Campylobacter bacteraemia*: a report of 10 cases. Med. J. Aust. **145**: 503–505.

WALKER, R. I., CALDWELL, M. B., LEE, E. C., GUERRY, P., TRUST, T. J., and RUIZ-PALACIOS, G. M. 1986. Pathophysiology of *Campylobacter* enteritis. Microbiol. Rev. **50**: 81–94.

YOUSSEF, M., ANDREMONT, A., and FANCREDE, C. 1985. Factors influencing translocation of *Campylobacter jejuni* to mesenteric lymph nodes in gnotobiotic mice. *In* *Campylobacter* III. *Edited by* A. D. Pearson, M. B. Skirrow, H. Lior, and B. Rowe. Public Health Laboratory Service, London.

END

FILMED

10-89

DTIC